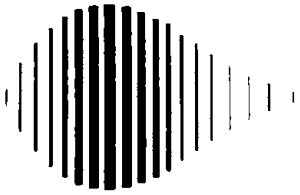

NATIONAL CENTER FOR EARTHQUAKE
ENGINEERING RESEARCH

State University of New York at Buffalo

Longitudinal Permanent Ground Deformation Effects on Buried Continuous Pipelines

by

M. J. O'Rourke and C. Nordberg
Department of Civil Engineering
Rensselaer Polytechnic Institute
Troy, New York 12180-3590

Technical Report NCEER-92-0014

June 15, 1992

This research was conducted at Rensselaer Polytechnic Institute and was partially supported by the National Science Foundation under Grant No. BCS 90-25010 and the New York State Science and Technology Foundation under Grant No. NEC-91029.

NOTICE

This report was prepared by Rensselaer Polytechnic Institute as a result of research sponsored by the National Center for Earthquake Engineering Research (NCEER) through grants from the National Science Foundation, the New York State Science and Technology Foundation, and other sponsors. Neither NCEER, associates of NCEER, its sponsors, Rensselaer Polytechnic Institute, nor any person acting on their behalf:

a. makes any warranty, express or implied, with respect to the use of any information, apparatus, method, or process disclosed in this report or that such use may not infringe upon privately owned rights; or

b. assumes any liabilities of whatsoever kind with respect to the use of, or the damage resulting from the use of, any information, apparatus, method or process disclosed in this report.

Any opinions, findings, and conclusions or recommendations expressed in this publication are those of the author(s) and do not necessarily refect the views of NCEER, the National Science Foundation, the New York State Science and Technology Foundation, or other sponsors.

50272-101

REPORT DOCUMENTATION PAGE	1. REPORT NO. NCEER-92-0014	2.	PB93-116671

4. Title and Subtitle
Longitudinal Permanent Ground Deformation Effects on Buried Continuous Pipelines

5. Report Date
June 15, 1992

6.

7. Author(s)
M. J. O'Rourke and C. Nordberg

8. Performing Organization Rept. No.

9. Performing Organization Name and Address
Department of Civil Engineering
Rensselaer Polytechnic Institute
Troy, New York 12180-3590

10. Project/Task/Work Unit No.

11. Contract(C) or Grant(G) No.
(C) BCS 90-25010
(G) NEC-91029

12. Sponsoring Organization Name and Address
National Center for Earthquake Engineering Research
State University of New York at Buffalo
Red Jack Quadrangle
Buffalo, New York 14261

13. Type of Report & Period Covered
Technical Report

14.

15. Supplementary Notes
This research was conducted at Rensselaer Polytechnic Institute and was partially supported by the National Science Foundation under Grant No. BCS 90-25010 and the New York State Science and Technology Foundation under Grant No. NEC-91029.

16. Abstract (Limit: 200 words)
The response of buried steel pipelines to permanent ground displacement is investigated. Specifically, pipeline response to four different idealized patterns of longitudinal permanent ground deformation, wherein the non-recoverable soil movement is parallel to the pipeline axis, is considered. The pipe material is assumed to be linear elastic while the force-deformation relationship of the soil-pipeline interface is taken to be elasto-plastic (elastric spring-slider) or rigid-plastic (rigid spring-slider). The four patterns of longitudinal permanent ground deformation investigated are idealizations of patterns observed in past earthquakes. They are: a) uniform ground strain (Ramp), and b) symmetric uniform ground strain (Ridge). For the first two patterns, the exact response is determined and compared with a simplified model which neglects the elastic portion of the force-deformation relationship at soil-pipeline interaction. It is found that the simplified models predict maximum pipeline strains within 5 percent of the exact values. For the third and fourth patterns of longitudinal permanent ground deformation, results are presented for the simplified interface model (rigid spring-slider) only.

17. Document Analysis a. Descriptors

b. Identifiers/Open-Ended Terms
BURIED PIPELINES. PERMANENT GROUND DEFORMATION. STEEL PIPELINES. SOIL PIPELINE INTERACTION. UNIFORM GROUND STRAIN. EARTHQUAKE ENGINEERING.

c. COSATI Field/Group

18. Availability Statement
Release Unlimited

19. Security Class (This Report)
Unclassified

20. Security Class (This Page)
Unclassified

21. No. of Pages
175

22. Price

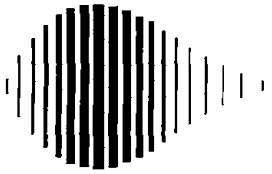

Longitudinal Permanent Ground Deformation Effects on Buried Continuous Pipelines

by

M.J. O'Rourke[1] and C. Nordberg[2]

June 15, 1992

Technical Report NCEER-92-0014

NCEER Project Number 90-3003

NSF Master Contract Number BCS 90-25010
and
NYSSTF Grant Number NEC-91029

1 Professor, Department of Civil Engineering, Rensselaer Polytechnic Institute
2 Graduate Research Assistant, Department of Civil Engineering, Rensselaer Polytechnic Institute

NATIONAL CENTER FOR EARTHQUAKE ENGINEERING RESEARCH
State University of New York at Buffalo
Red Jacket Quadrangle, Buffalo, NY 14261

PREFACE

The National Center for Earthquake Engineering Research (NCEER) was established to expand and disseminate knowledge about earthquakes, improve earthquake-resistant design, and implement seismic hazard mitigation procedures to minimize loss of lives and property. The emphasis is on structures in the eastern and central United States and lifelines throughout the country that are found in zones of low, moderate, and high seismicity.

NCEER's research and implementation plan in years six through ten (1991-1996) comprises four interlocked elements, as shown in the figure below. Element I, Basic Research, is carried out to support projects in the Applied Research area. Element II, Applied Research, is the major focus of work for years six through ten. Element III, Demonstration Projects, have been planned to support Applied Research projects, and will be either case studies or regional studies. Element IV, Implementation, will result from activity in the four Applied Research projects, and from Demonstration Projects.

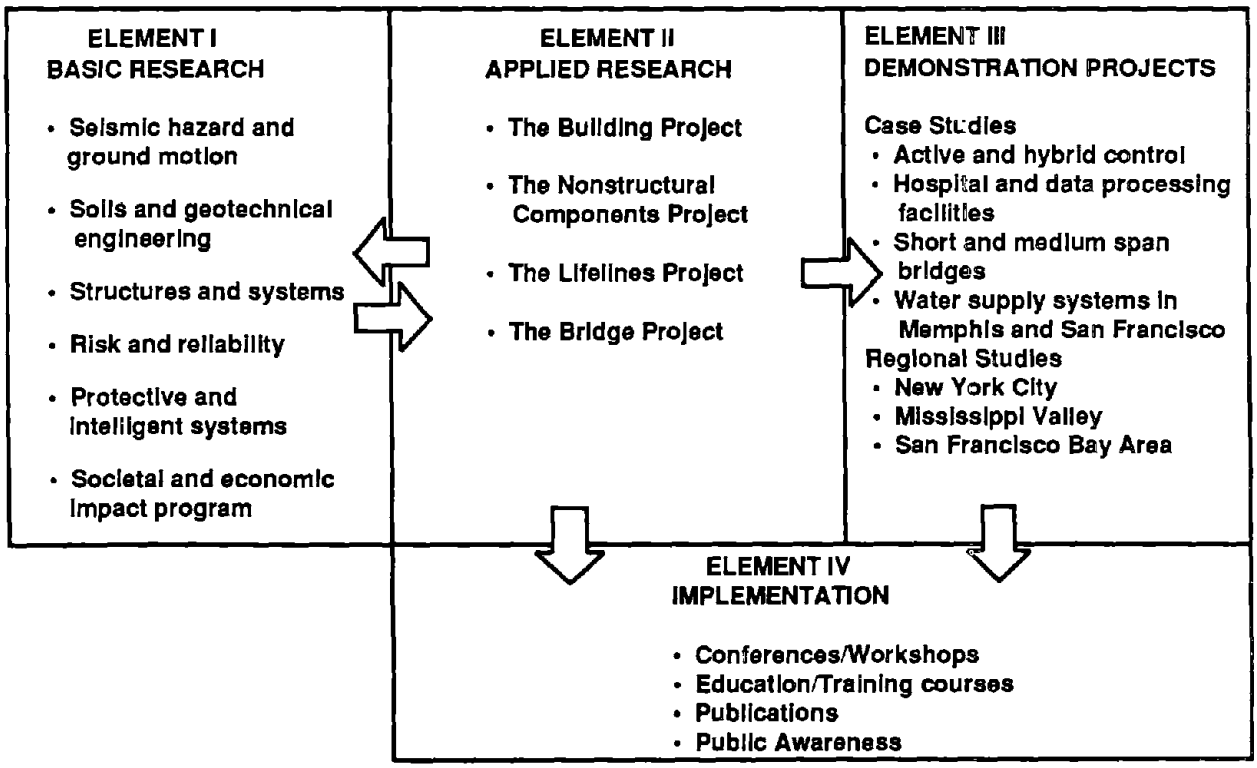

Research tasks in the **Lifeline Project** evaluate seismic performance of lifeline systems, and recommend and implement measures for mitigating the societal risk arising from their failures caused by earthquakes. Water delivery, crude oil transmission, gas pipelines, electric power and telecommunications systems are being studied. Regardless of the specific systems to be considered, research tasks focus on (1) seismic vulnerability and strengthening; (2) repair and restoration; (3) risk and reliability; (4) disaster planning; and (5) dissemination of research products.

The end products of the **Lifeline Project** will include technical reports, computer codes and manuals, design and retrofit guidelines, and recommended procedures for repair and restoration of seismically damaged systems.

The **soils and geotechnical engineering program** constitutes one of the important areas of research in Element I, **Lifelines Project**. Major tasks are described as follows:

1. Perform site response studies for code development.
2. Develop a better understanding of large lateral and vertical permanent ground deformations associated with liquefaction, and develop corresponding simplified engineering methods.
3. Continue U.S. - Japan cooperative research in liquefaction, large ground deformation, and effects on buried pipelines.
4. Perform soil-structure interaction studies on soil-pile-structure interaction and bridge foundations and abutments, with the main focus on large deformations and the effect of ground failure on structures.
5. Study small earth dams and embankments.

This report describes the development of analytical models for the behavior of continuous pipelines subjected to permanent ground deformation. Buried steel pipelines were subjected to four idealized patterns of longitudinal permanent ground deformation and their response was determined. The pipe strains induced by these four patterns were then compared. Recommendations are provided for the design of new pipelines which must cross areas which will likely be affected by permanent ground deformation. These recommendations include increasing the pipe wall thickness, using the smallest allowable soil cover over the top of the pipe, and backfilling the pipelines trench with lighter weight soils with a low angle of shearing resistance.

ABSTRACT

The response of buried steel pipelines to permanent ground displacement is investigated. Specifically, pipeline response to four different idealized patterns of longitudinal permanent ground deformation, wherein the non–recoverable soil movement is parallel to the pipeline axis, is considered. The pipe material is assumed to be linear elastic while the force–deformation relationship of the soil–pipeline interface is taken to be elasto–plastic (elastic spring–slider) or rigid–plastic (rigid spring–slider).

The four patterns of longitudinal permanent ground deformation investigated are idealizations of patterns observed in past earthquakes. They are; (a) uniform ground strain (Ramp), (b) rigid block movement, (c) uniform ground strain with a free face (Ramp/Step) and (d) symmetric uniform ground strain (Ridge). For the first two patterns, the exact response is determined and compared with a simplified model which neglects the elastic portion of the force–deformation relationship at soil–pipeline interaction. It is found that the simplified models predict maximum pipeline strains within 5 percent of the exact values. For the third and fourth patterns of longitudinal permanent ground deformation, results are presented for the simplified interface model (rigid spring–slider) only.

TABLE OF CONTENTS

TABLE OF CONTENTS (Cont'd)

LIST OF ILLUSTRATIONS

LIST OF ILLUSTRATIONS (Cont'd)

LIST OF ILLUSTRATIONS (Cont'd)

LIST OF TABLES

LIST OF TABLES (Cont'd)

SECTION I
INTRODUCTION

The integrity of buried pipelines is a major concern for designers, owners, and users. The public depends on pipelines to supply gas, oil and water, and for waste removal. Thus pipelines are the veins and arteries of society. The failure of a pipeline can lead to economic losses, ecological damage and possible loss of life.

Observed seismic damage to buried welded steel pipelines has been attributed to both wave propagation and permanent ground deformation (PGD). Seismic wave propagation damage results from axial and bending strains induced in a pipeline due to transient earthquake waves travelling along the ground surface. These strains can lead to pinhole leaks in areas previously weakened by corrosion. If the induced pipeline strains are large enough, they can cause local buckling and subsequent tearing of the pipe wall. For example, O'Rourke and Ayala [1] attribute the failure of a 42 in. diameter, x–42 grade, welded steel water pipeline in Mexico City to seismic wave propagation caused by the 1985 Michoacan earthquake.

Permanent ground deformation refers to nonrecoverable soil movement due to landslides, surface faulting, settlement, or liquefaction induced lateral spreading. Herein we restrict our attention to landslides and liquefaction induced lateral spreading. The response of a buried pipeline to this type of PGD is a function of the pipeline orientation with respect to the direction of ground movement. In general, a pipeline would be exposed to some combination of transverse PGD and longitudinal PGD. For transverse PGD the soil movement is perpendicular to the pipeline axis, while for longitudinal PGD the soil movement is parallel to the pipeline axis. This type of movement can result in pipeline failure. For example O'Rourke and Tawfik [2] describe damage to five steel pipelines near the Upper Van Norman Reservoir due to transverse PGD resulting from the 1971 San Fernando earthquake.

In this report, the response of linear elastic steel pipe to various idealized patterns of longitudinal PGD is determined. In section 2, existing information on the magnitude and spatial extent of liquefaction induced lateral spreading is briefly presented In addition, observed PGD patterns are reviewed and the four idealized patterns of longitudinal PGD considered herein are identified. A model for the force deformation relationship at the soil pipe interface is presented in Section 3. In Section 4, the axial strain in a pipeline

subjected to a uniform ground strain (Ramp) pattern of longitudinal PGD is presented. The pipe strain is evaluated using an elastic spring–slider developed in Section 3 to model the soil–pipe interface as well as a simplified model in which the spring portion of the spring–slider is assumed rigid. In Section 5, pipeline axial strain is evaluated for a rigid block pattern of longitudinal PGD. Again, both the complete soil pipeline interfaces model (elastic spring–slider) as well as a simplified model (rigid spring–slider) are used. In Section 6 pipeline axial strain resulting from uniform ground strain with a free face (Ramp/Step) longitudinal PGD patterns is presented. In this section, results are presented only for the simplified interface model (rigid spring–slider). A symmetric uniform strain (Ridge) PGD pattern is investigated in Section 7 using the simplified interface model. Section 8 presents a comparison between the pipeline strains induced by the four idealized PGD patterns. A summary and the recommendations from the study are presented in Section 9.

SECTION 2
PERMANENT GROUND DISPLACEMENT

The strain induced in a buried pipeline is a function of the PGD magnitude, the spatial extent of the PGD zone and the pattern of ground movements along the pipeline route. In this section, existing techniques for estimation of the magnitude of PGD are reviewed. Information on the spatial extent of longitudinal PGD zones is also presented. In addition, observed patterns of PGD are reviewed. Finally, four idealizations of observed PGD patterns are identified. The response of a buried pipeline subjected to these idealized patterns is determined in Section 4 through 7.

2.1 PGD Magnitude

Modeling PGD due to liquefaction induced lateral spreading is an area of ongoing research. In his state of the art report, Finn [3] summarizes some of the more important contributions. He cites work by Hamada, Yasuda, Isoyama and Emoto [4] which suggests PGD induced by liquefaction of sandy soil is closely related to the geometrical configuration of estimated liquefiable layers. They have proposed a regression formula to predict the magnitude of horizontal PGD δ, in meters, as a function of the thickness of the liquefied layer h, in meters, and the slope θ_g, in percent, of the lower boundary of the liquefied layer or the ground surface, whichever is larger

$$\delta = 0.75 \sqrt[2]{h} \cdot \sqrt[3]{\theta_g} \tag{2.1}$$

Youd and Perkins [5] introduce the concept of a Liquefaction Severity Index (LSI) which is defined as the amount of PGD, in inches, associated with lateral spreads on gently sloping ground and poor soil conditions. LSI is arbitrarily truncated at 100. They present an empirical relationship for LSI as a function of the earthquake magnitude M_w and distance R to the site, in kilometers, for Western U.S. Earthquakes

$$\log \text{LSI} = -3.49 - 1.86 \log R + 0.98 M_w \tag{2.2}$$

Figure 2–1 shows a comparison between measured LSI and values predicted by eqn. (2.2). This relationship is not directly applicable to the Eastern U.S. since seismic wave

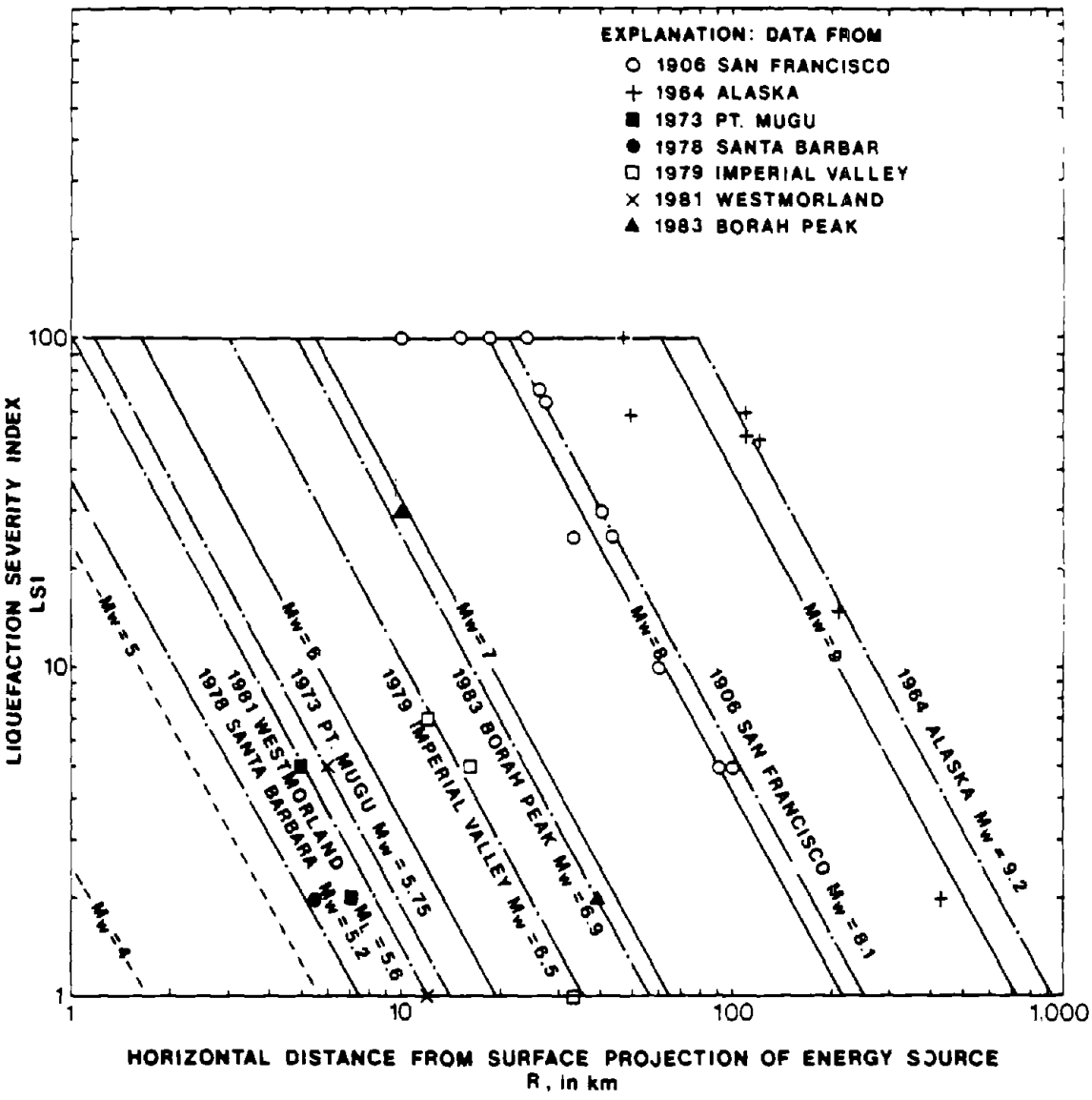

FIGURE 2-1 LSI from Several Western U.S. Earthquakes and Values Predicted by Equation 2-2 (after Youd and Perkins, 1987).

attenuation characteristics in the Western U.S. are significantly different than those in the Eastern U.S..

More recently Baziar [6] has developed an analytical relation for the magnitude of PGD, δ, for Western U.S. earthquakes based upon the Newton Sliding Block model. His relationship is

$$\delta = 2 \frac{V_{max}^2}{A_{max}} \cdot F \tag{2.3}$$

where V_{max} = peak ground velocity, A_{max} = peak ground acceleration and F is a shape factor which is a function of the ratio of the yield acceleration to the peak ground acceleration. Figure 2–2 shows a comparison between the Youd and Perkins empirical relationship for LSI = δ given by eqn. (2.2) and the Baziar analytical relationship given by eqn. 2.3.

Finally, Towhata et al. [7] use a variational principle to develop an analytical relation for the magnitude of liquefaction induced PGD. Figure 2–3 shows measured horizontal PGD magnitudes in Noshiro City caused by the 1983 Nihonkai–Chubu earthquake as well as the PGD calculated by the Towaha et al. procedure.

All four methods for estimating the magnitude of PGD are the result of recent research. The authors are not in a position to recommend any particular method as being the best.

2.2 Spatial Extent of PGD Zones

As will be shown later, the length L of the lateral spread zone (i.e. spatial dimension in the direction of ground movement) is a key parameter in determining the response of buried pipeline to longitudinal PGD. Using case history data from the 1964 Niigata Earthquake and the 1983 Nihonkai Chubu Earthquake, Suzuki and Masuda [8] present empirical information on the magnitude and extent of the lateral spread zone for longitudinal PGD. Figure 2–4 shows the PGD patterns observed by Suzuki and Masuda. The upper figure shows a region of tensile ground strain while the lower figure is compressive. Figure 2–5 shows a plot of observed values of δ and L. There are a total of 290 data points in this figure. The 133 data points with positive values of δ correspond to tensile deformations as shown in Figure 2–4a. The remaining 157 data points below the $\delta = 0$ line are compressive

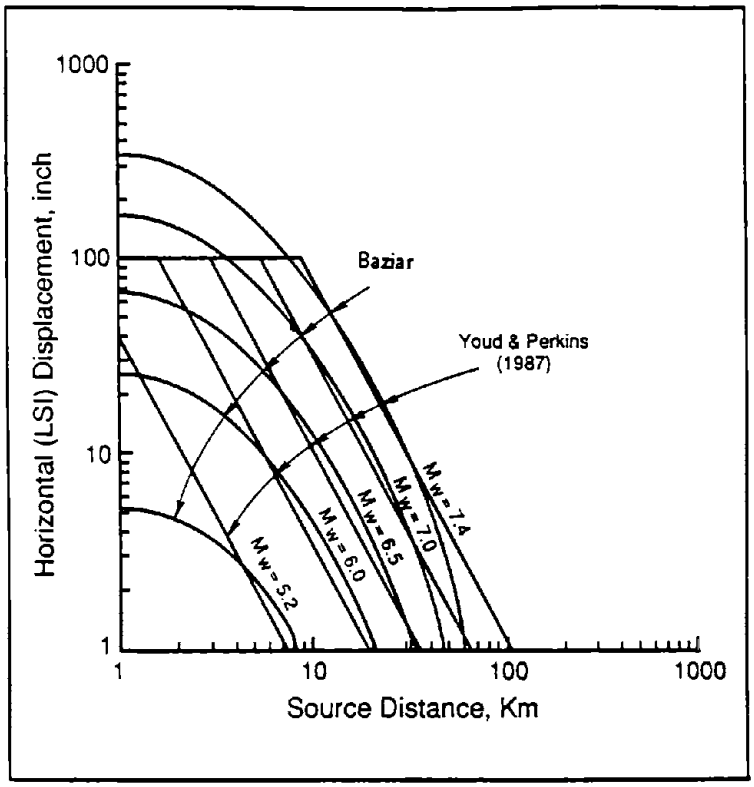

FIGURE 2-2 Comparision of Empirical LSI relationship from Youd and Perkins (1987) given by Equation 2.2 with Baziar (1991) analytical relationship given by Equation 2.3 (modified after Baziar, 1991).

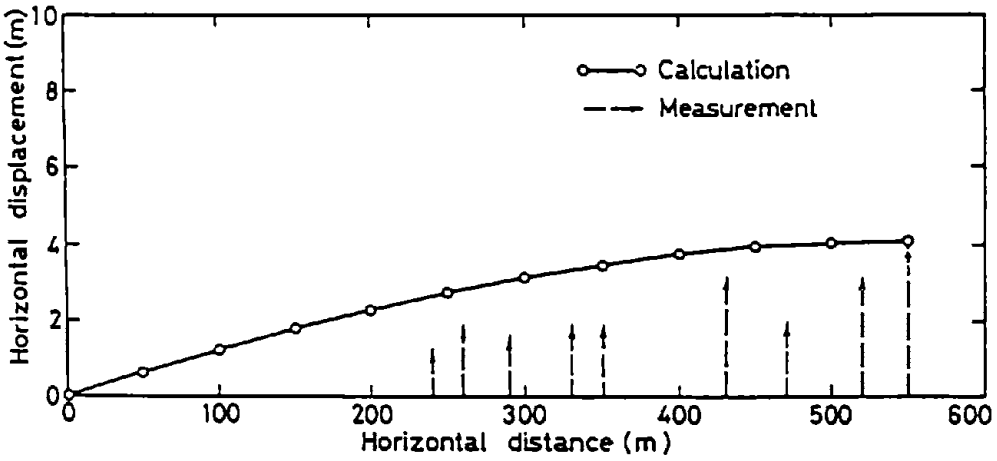

FIGURE 2-3 Measured and Calculated Horizontal Ground Movements in Noshiro City resulting from the 1983 Nihonkai-Chubu Earthquake (after Towhata et al., 1991).

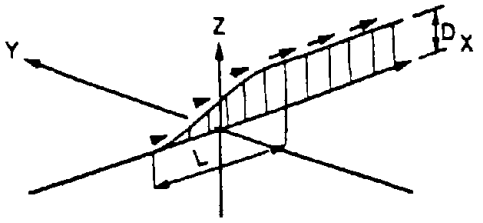

(a) Tensile Ground Strain

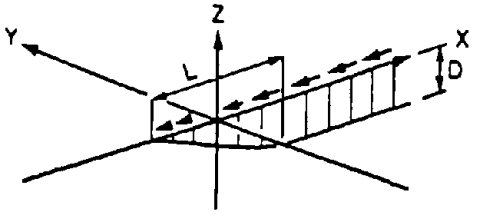

(b) Compressive Ground Strain

FIGURE 2-4 Longitudinal Permanent Ground Deformation Patterns observed by Suzuki and Masuda (1991).

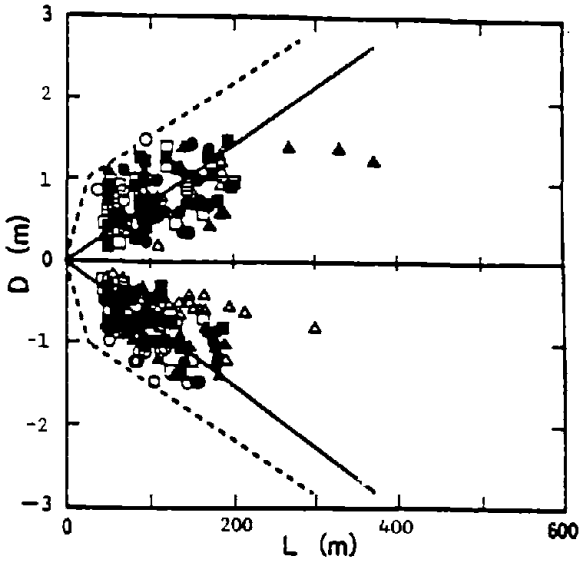

FIGURE 2-5 Empirical Data on the Magnitude $\delta = D$ for Longitudinal PGD (after Suzuki and Masuda, 1991).

deformation as shown in Figure 2–4b. Note in Figure 2–5 that L $\leq$ 400 m. and $\delta \leq$ 1.5 m. The average ground strain, $\alpha = \delta/L$, for both tensile and compressive deformations generally falls in the range $0.002 \leq \alpha \leq 0.03$ with typical values being 0.007 or 0.008.

2.3 Observed PGD Patterns

As will be shown later, the pattern of ground deformation (i.e. the distribution of PGD along the pipeline axis) influences the strain induced in a buried pipeline by longitudinal PGD. Towhata et al. [7] observed that vertical soil movement occasionally accompany liquefaction induced lateral spreading. In general, subsidence tends to occur in the upper portion of the slope and heaving at the lower portion. Herein, these possible vertical soil movements are neglected and buried pipe response to the horizontal component of PGD will be determined.

Hamada et al. [9] have studied PGD which resulted from liquefaction during the 1964 Niigata Earthquake and the 1983 Nihonkai–Chubu Earthquake. Figure 2–6 shows PGD observed along six section lines in Niigata City as a result of the 1964 earthquake. In this figure as well as in Figures 2–7, 2–8 and 2–9, a vertical line with an open circle indicates permanent movement to the right while a solid circle indicates movement to the left. In general, at the bank of a river the PGD is towards the river. For example Figure 2–6(c) shows PGD to the left near the right abutment of the Bandai Bridge, and PGD to the right near the left abutment. The same pattern is evident at the left bank of the Shinano River in Figure 2–6(a), the left abutment of the Showa Bridge in Figure 2–6(b), and the left abutment of the Yachiyo Bridge in figure 2–6(f). At some distance away from a river, Hamada et al. [9] note that the direction of PGD appears to be controlled by the slope of the ground surface or the slope of the bottom of the liquefied layer. For example the PGD between the Echigo line and the Niigata–Kotsu line in Figure 2–6(a) is away from the Shinano River because the lower boundary face of the liquefied layer falls away from the river at that location. Figure 2–7 shows PGD observed along twenty–seven section lines in Noshiro City as a result of the 1983 Nihonkai–Chubu Earthquake.

As shown in Figure 2–6 and 2–7, the observed patterns of longitudinal PGD can be quite complex. However for some of these case histories, the observed patterns can be idealized. For example in Figure 2–6(e), there is a fairly linear variation of PGD with distance from the right, resulting in a displacement of roughly 3.5 m. about 350 m. to the left of the point of zero PGD. This corresponds to an average ground strain $\alpha = \delta/L$ of roughly 0.01 over

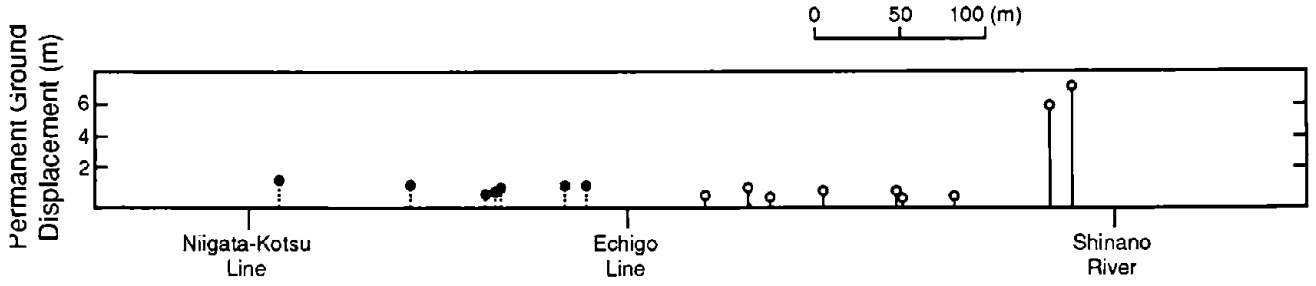

(a)

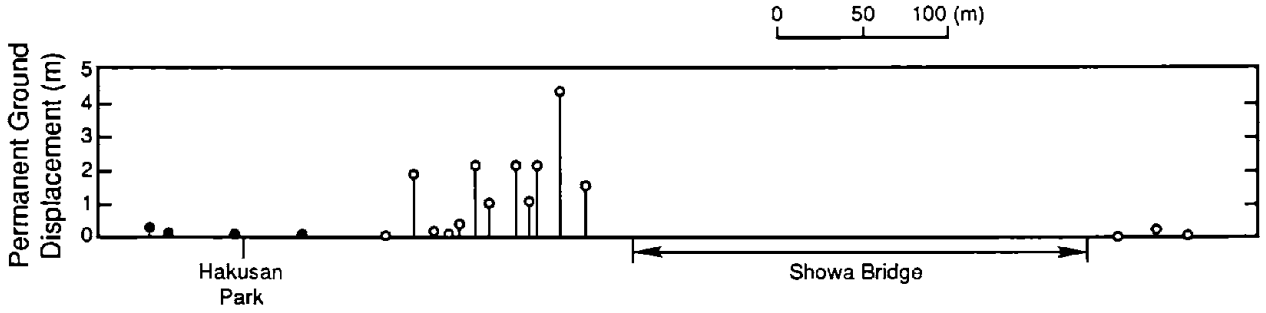

(b)

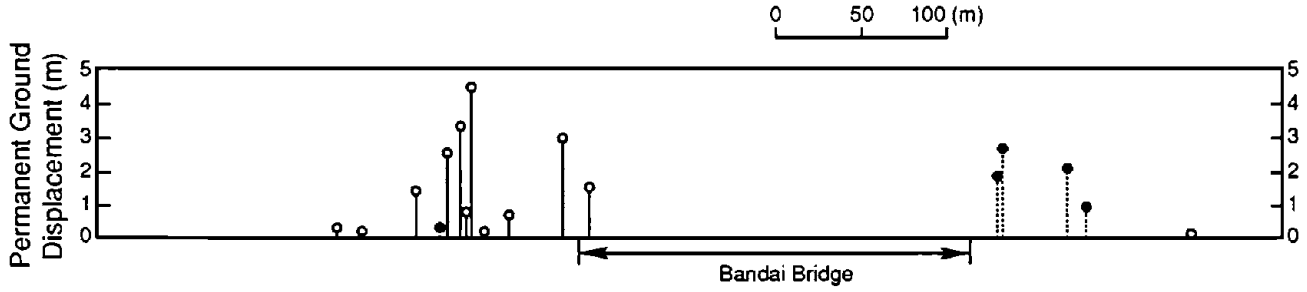

(c)

FIGURE 2-6 PGD patterns observed in Niigata City after the 1964 Niigata Earthquake, solid circle indicates movement to the left, open circle indicates movement to the right (after Hamada et al. 1986).

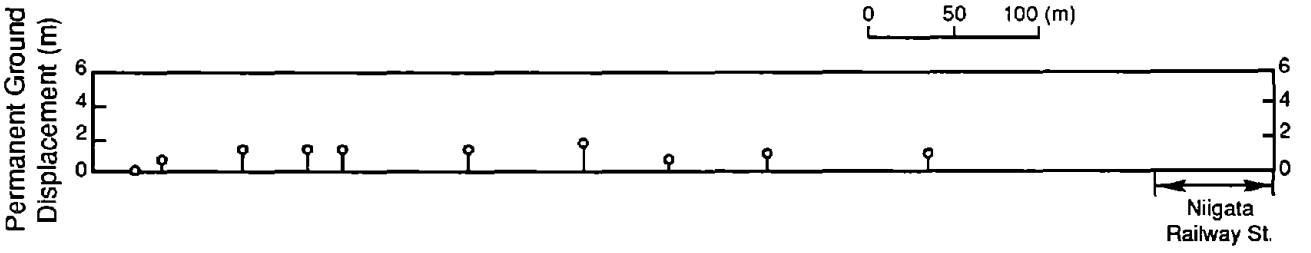

(d)

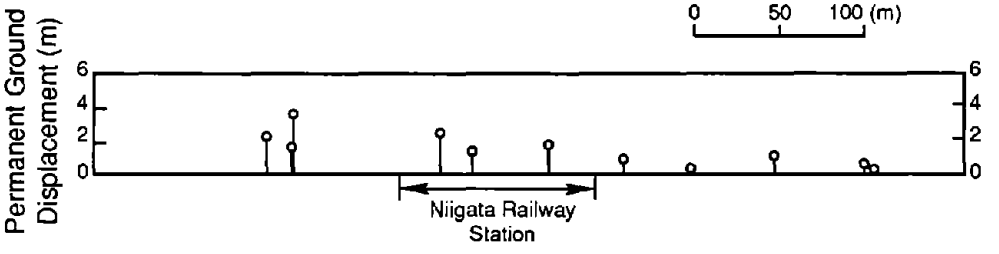

(e)

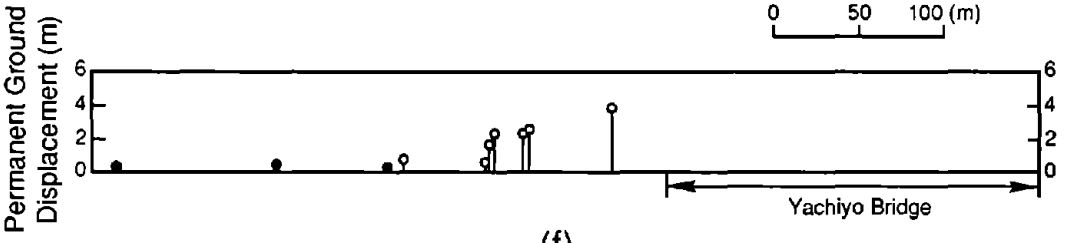

(f)

FIGURE 2-6 (continued)

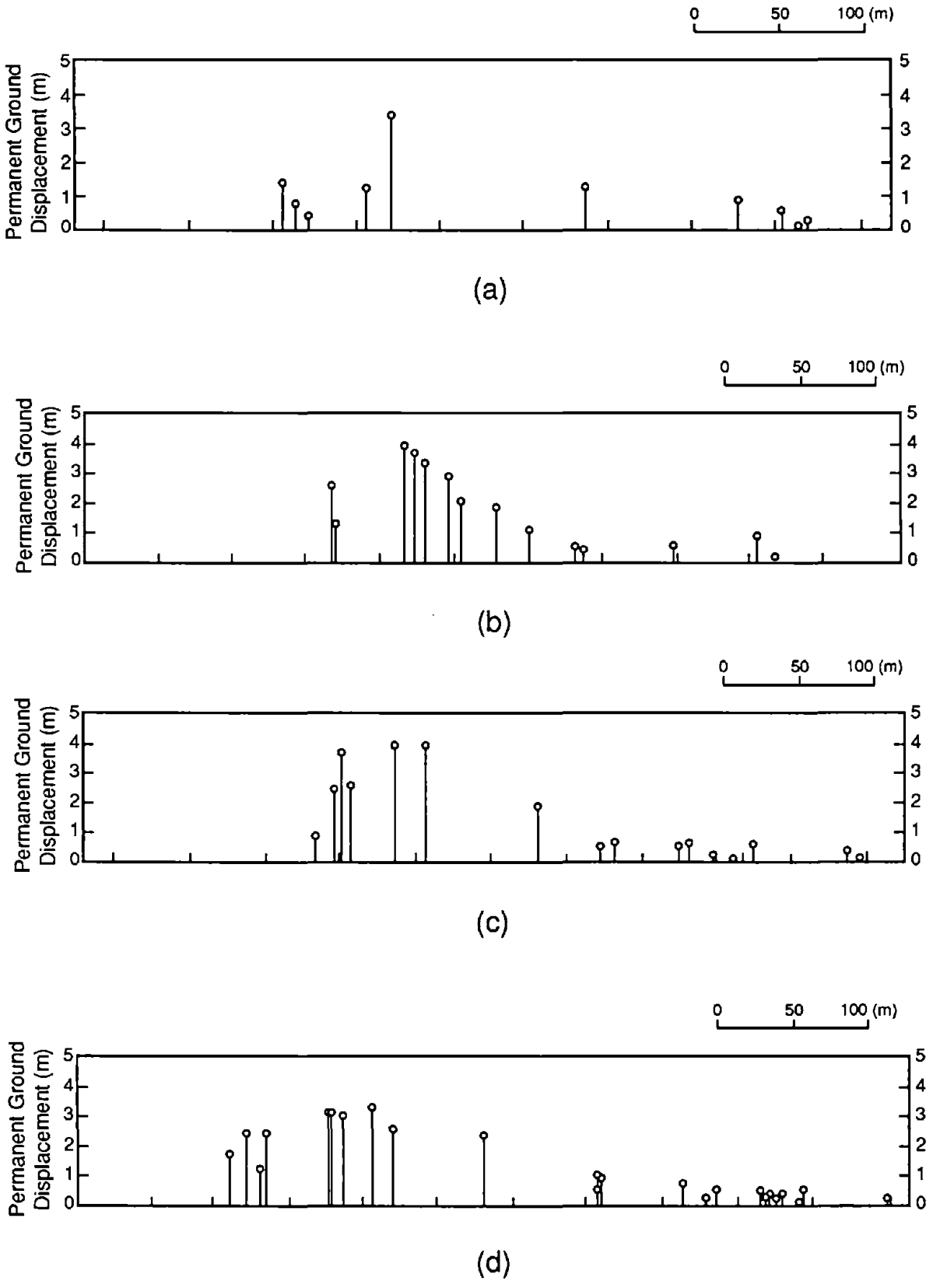

FIGURE 2-7 PGD patterns observed in Noshiro City after the 1983 Nihonkai-Chubu Earthquake (after Hamada et al., 1986).

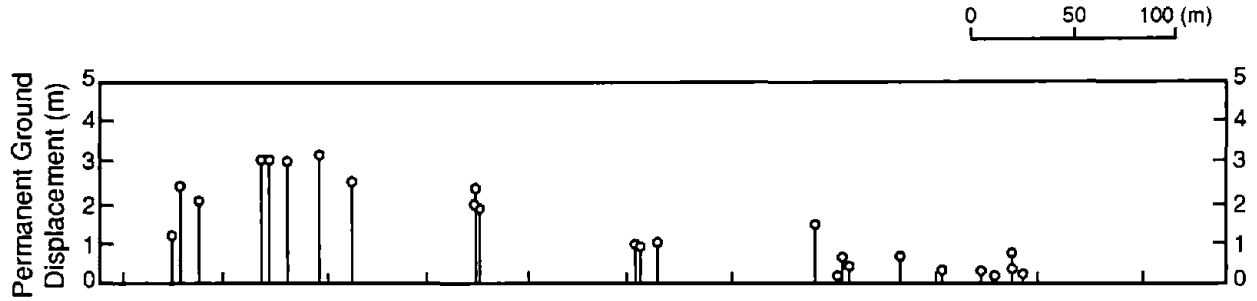

(e)

(f)

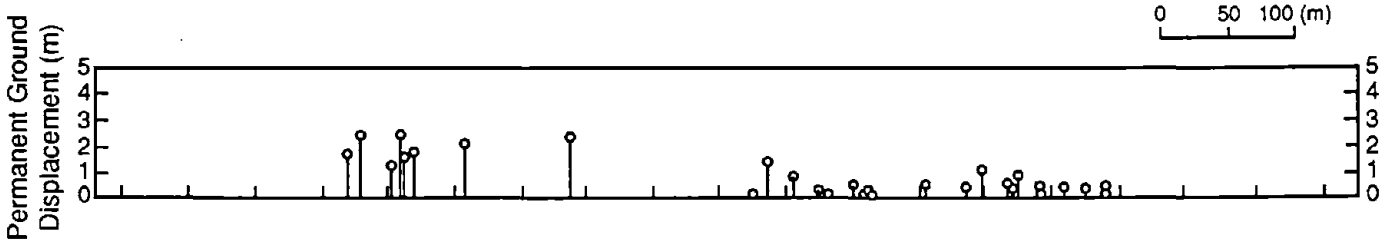

(g)

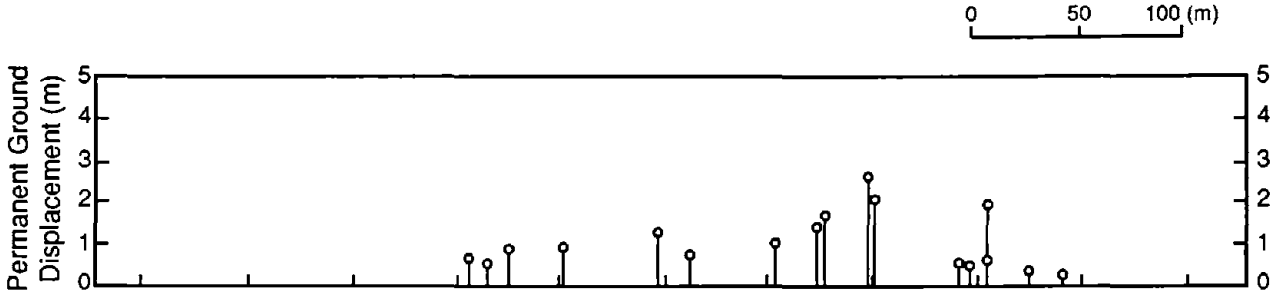

(h)

FIGURE 2-7 (continued).

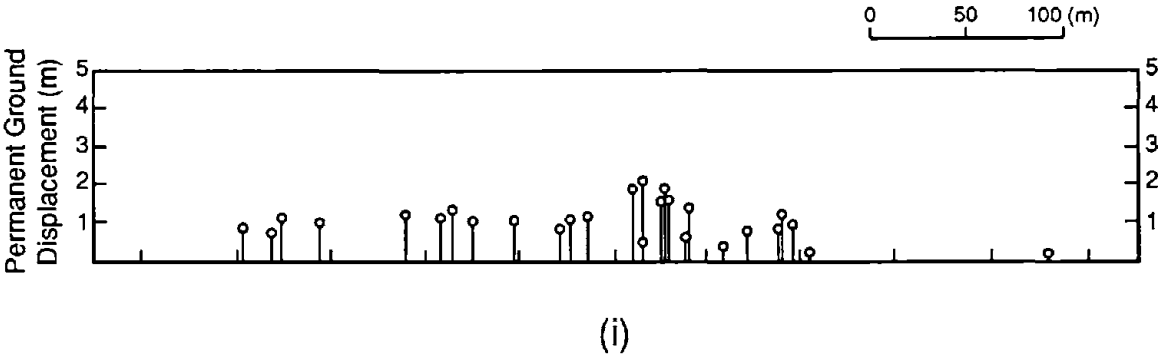

(i)

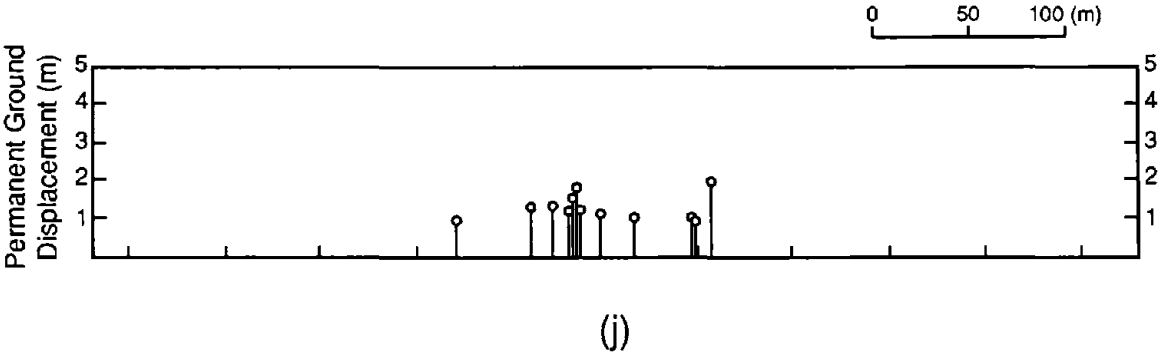

(j)

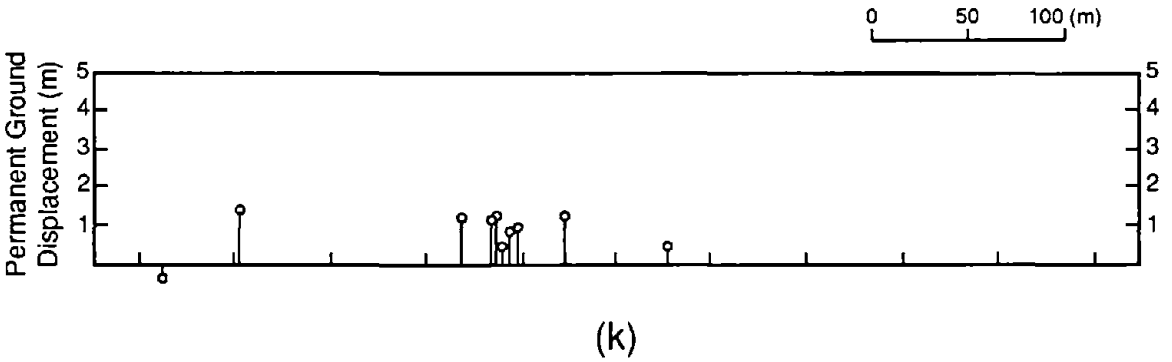

(k)

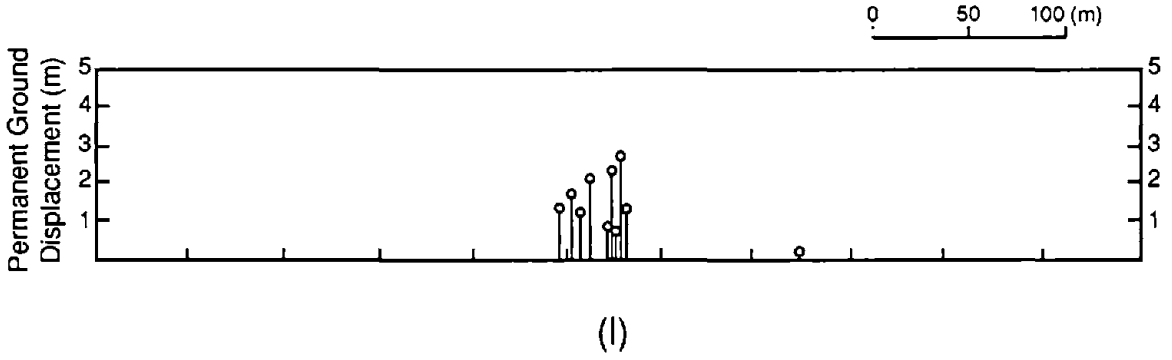

(l)

FIGURE 2-7 (continued)

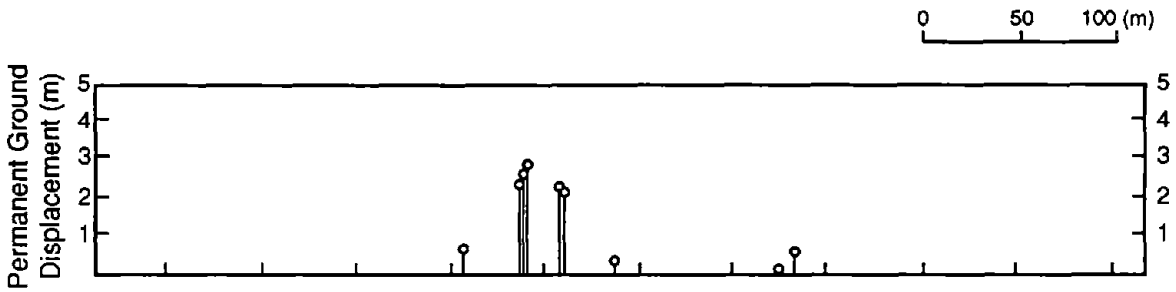

(m)

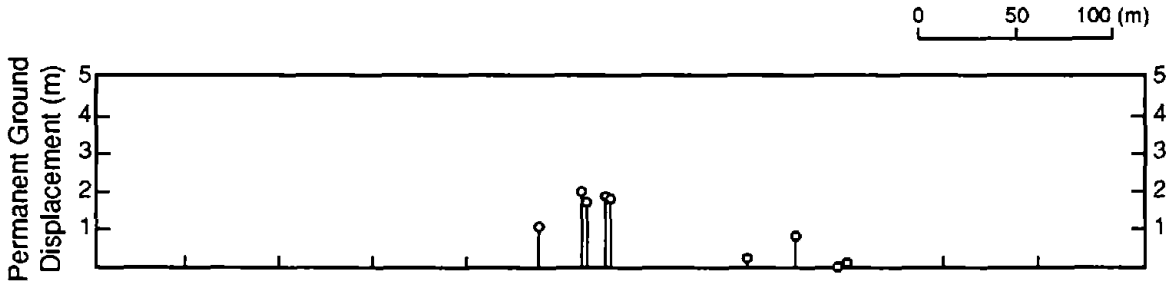

(n)

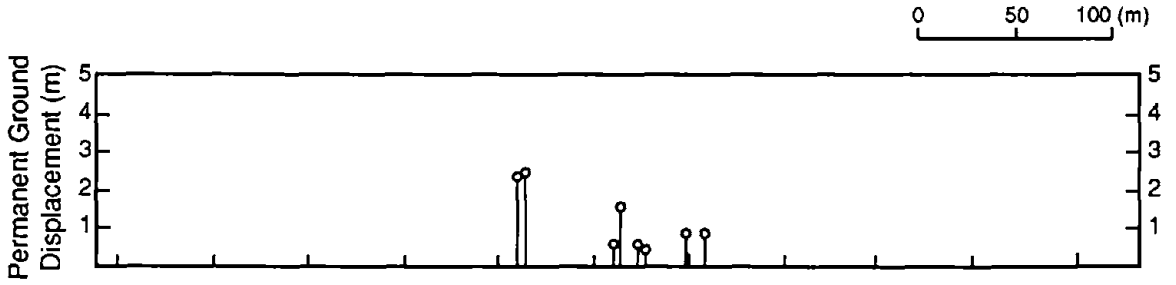

(o)

(p)

FIGURE 2-7 (continued)

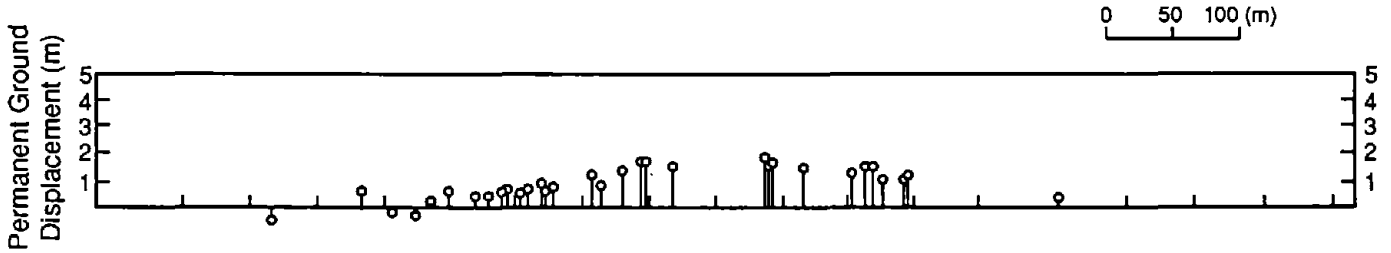

(q)

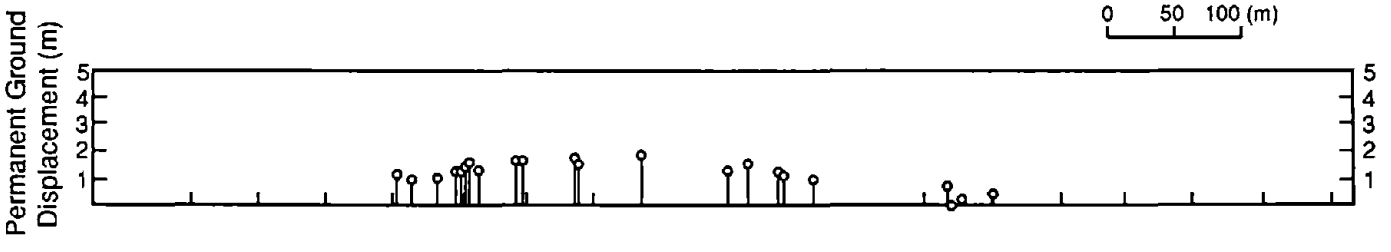

(r)

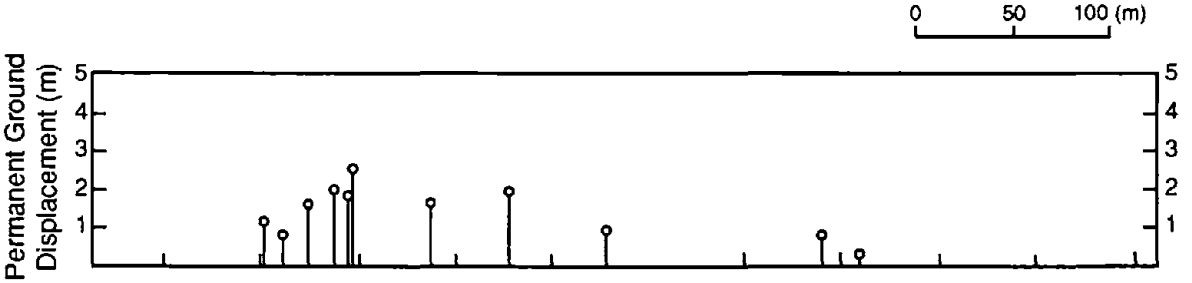

(s)

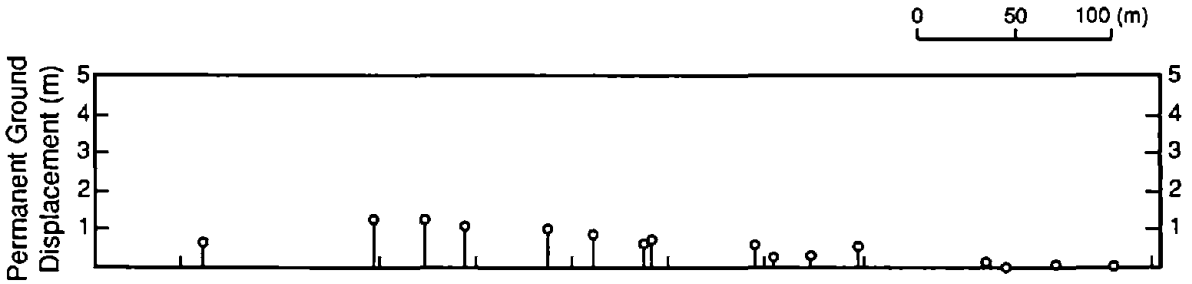

(t)

FIGURE 2-7 (continued)

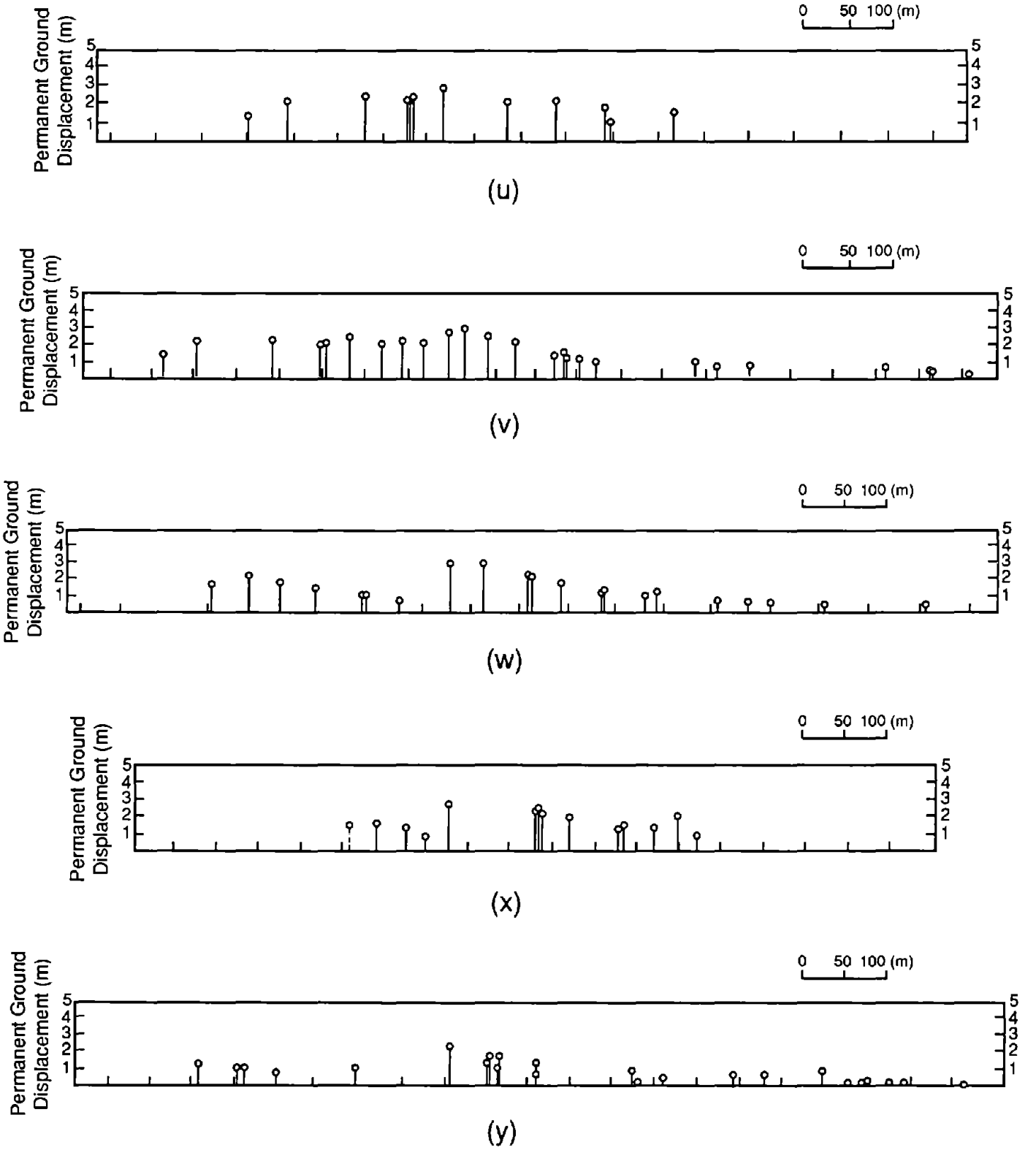

FIGURE 2-7 (continued)

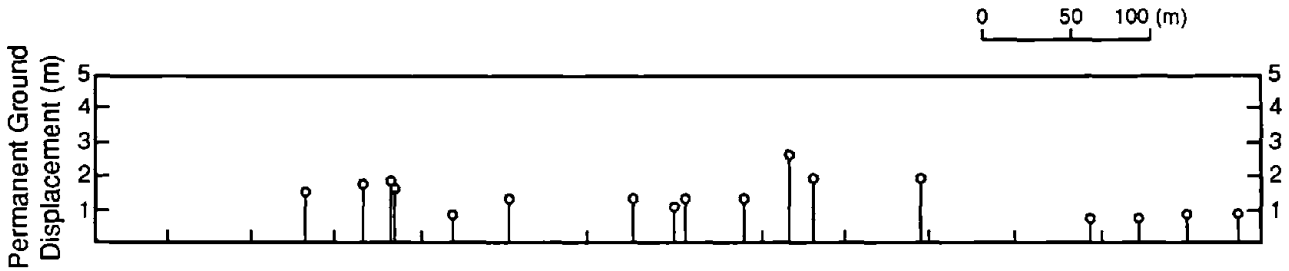

(z)

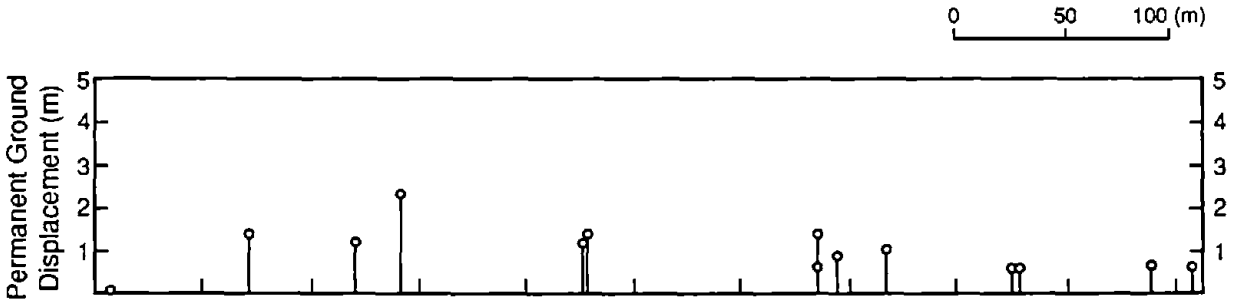

(aa)

FIGURE 2-7 (continued)

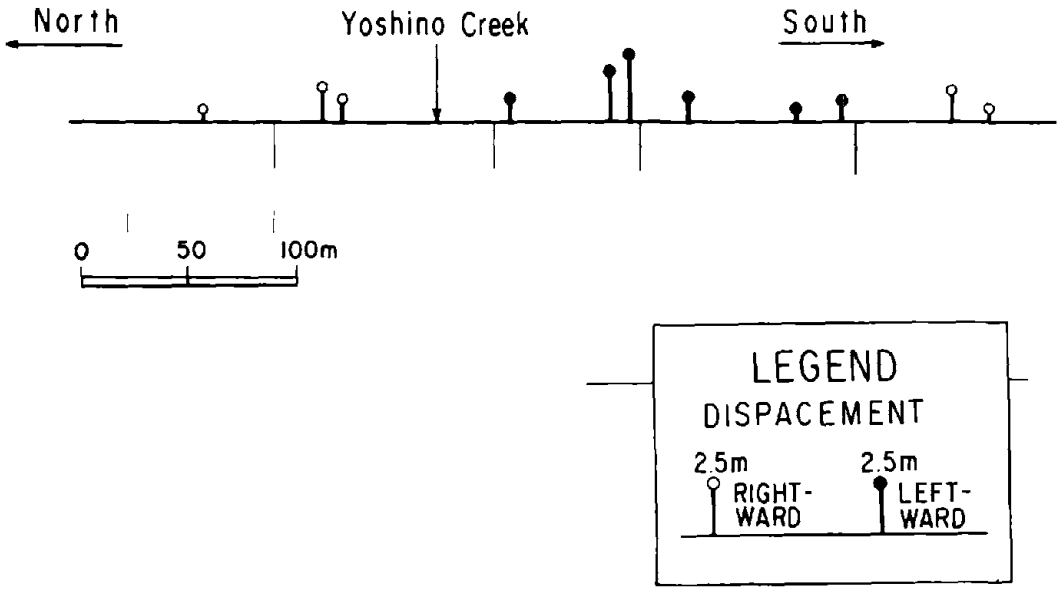

FIGURE 2-8 PGD pattern observed near the Yoshino Creek in Fukui City after the 1948 Fukui Earthquake (after Hamada, Wakamatsu and Yasuda, 1989).

the length L of 350 m. A somewhat similar pattern can be observed at the far left hand side of Figure 2–6(d) when a displacement of roughly 2.0 m. occurs about 60 m to the right of the zero PGD point. This corresponds to an average ground strain of roughly 0.033 over a distance of 60 m.

Other examples of fairly linear variation of PGD with distance were observed in Noshiro City. In Figure 2–7(a), the maximum PGD is roughly 3.5 m, while about 250 m. to the right the PGD is zero. This results in an average ground strain of 0.014. In the center of Figure 2–7(b), the maximum PGD is roughly 4 m. but about 140 m. to the right it's zero, resulting in a ground strain of about 0.029. Finally, towards the center of Figure 2–7(s), the maximum PGD is roughly 2.5 m and there is no PGD about 280 m. to the right, leading to an average ground strain of 0.009.

Some of the other case histories for Noshiro City show relatively uniform PGD over various distances. For example the observed PGD in Figure 2–7(j) has a relatively constant value of roughly 1.5 m. over a distance of roughly 130 m. Similarly in Figure 2–7(u), the observed PGD is almost a constant value of 2 m. over a distance of roughly 500 m.

Hamada, Wakamatsu and Yasuda [10] have investigated observed PGD due to liquefaction occasioned by the 1948 Fukui Earthquake. Figure 2–8 shows PGD near the Yoshino Creek in the Western part of Morita–cho. The PGD in Figure 2–8 follows the trend noted previously, that is, at each side of the creek the ground movement was towards the creek. The maximum PGD was about 3 m. and occurred about 85 m. to the right of the creek. The ground movement on either side of this maximum PGD point decrease in roughly a linear fashion, being about zero immediately to the right of the creek and about zero roughly 190 m. to the right of the creek. The corresponding ground strain on either side of the point of maximum PGD is roughly 0.035. The ground deformation is tensile to the right of the point of maximum PGD,and compressive to the left.

On the left hand side of Figure 2–8 the maximum PGD was about 2 m in a direction towards the creek and occurred about 60 m to the left of the creek. The PGD on either side of this local maximum decrease in roughly a linear fashion, being about zero immediately to the left of the creek and about zero roughly 120 m to the left of the creek. The corresponding ground strain on either side of this local maximum PGD is roughly 0.033, being tensile to the left and compressive to the right.

A final example of observed PGD is the area between the Ohgata Elementary School and the Tsusen River in Niigata City which was investigated by Yasuda et al. [11]. Figure 2–9 shows PGD that resulted from the 1964 Niigata Earthquake. In the center of this figure, the PGD was towards the river, as one might expect based on the trend previously noted herein. The maximum PGD is roughly 7.5 m and occurs roughly 210 m to the left of the Ohgata School. Between the school and the point of maximum PGD, there is a fairly linear variation of PGD with distance from the point of zero PGD at the school. This corresponds to an average tensile ground strain of roughly 0.036.

There are only two data points in Figure 2–9 between the maximum PGD location in the center of the figure and the Tsusen River on the left. Figure 2–10 shows the idealized horizontal soil displacement within 210 m of the Ohgata school and three possible soil displacement patterns over the 180 m distance to the right of the river.

2.4 Idealized PGD Patterns

In subsequent sections, the axial strain in a buried pipeline subject to four idealized patterns of longitudinal PGD will be determined. These four idealized patterns are based upon the observed PGD patterns mentioned above. They are: (a) Ramp PGD, (b) Rigid Block PGD, (c) Ramp/Step PGD and (d) Ridge PGD.

2.4.1 Ramp PGD

The first idealized longitudinal PGD pattern considered herein is Ramp PGD. This corresponds to uniform ground strain α over a length L as shown in Figure 2–11. The ground strains on either side of the transition zone are zero. The soil displacement to the left of the transition zone is zero while the soil displacement to the right of the transition zone have a constant value of $\delta = \alpha L$.

The Ramp PGD pattern approximates the patterns quantified by Suzuki and Masuda [8] and shown in Figure 2–4. It also approximates the PGD pattern shown on the far left hand side of Figure 2–6(d) and towards the center of Figure 2–7(q). The Ramp pattern would be an appropriate model for the PGD shown in Figure 2–6(e) if the soil displacements on the left hand side of the figure have a constant value of about 3.5 m.

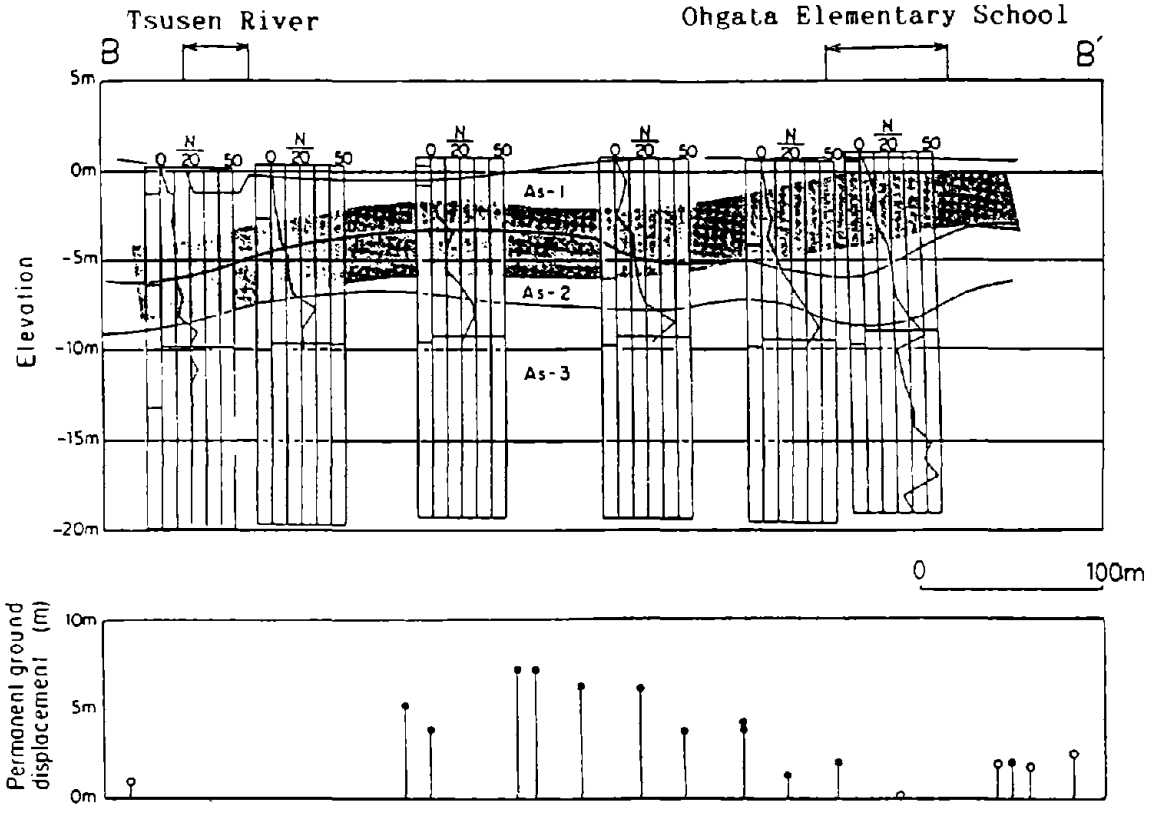

FIGURE 2-9 Permanent Ground Deformation Between the Ohgata Elementary School and the Tsusen River in Niigata City as Result of the 1964 Niigata Earthquake (after Yasuda et al. [10]).

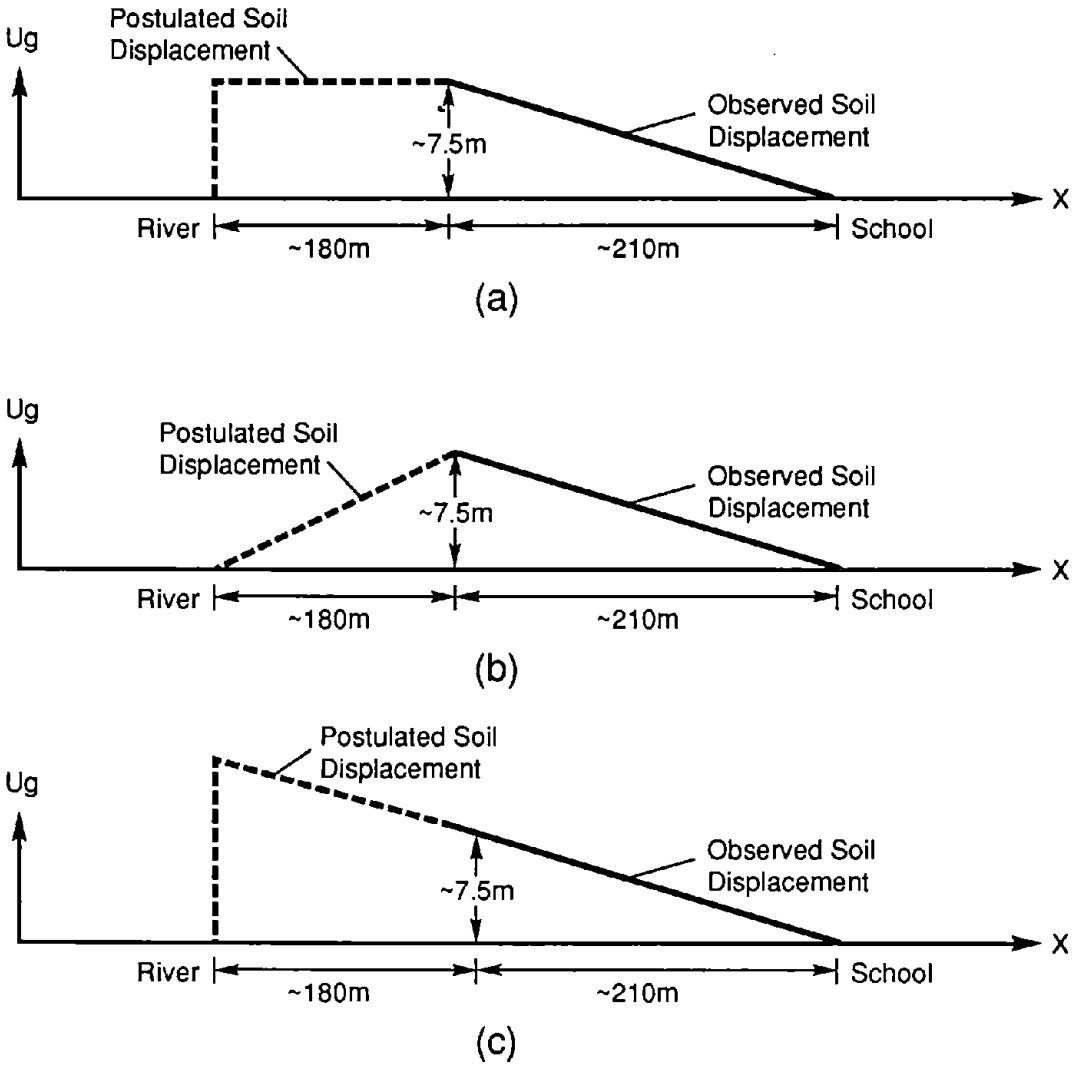

FIGURE 2-10 Idealized and Postulated Soil Displacement Patterns between the Ohgata School and the Tsusen River, (a) Combination Ramp and Ridge Block, (b) Ridge, (c) Ramp/Step.

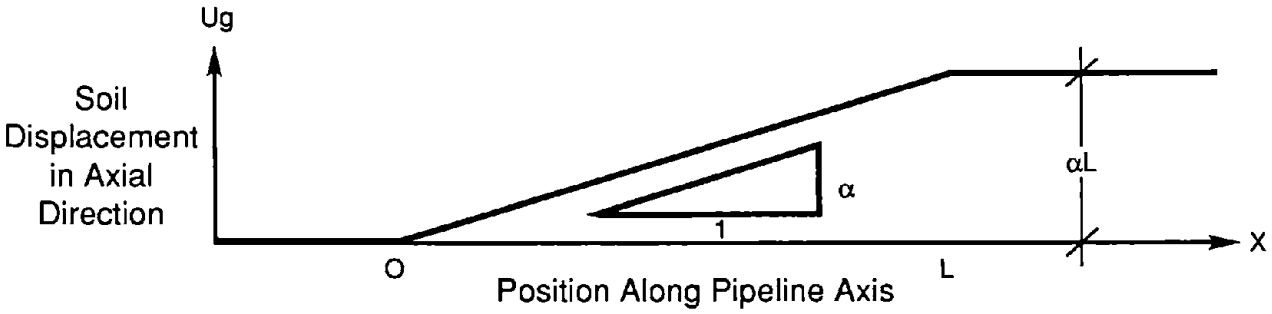

FIGURE 2-11 Idealized Ramp pattern of Longitudinal PGD.

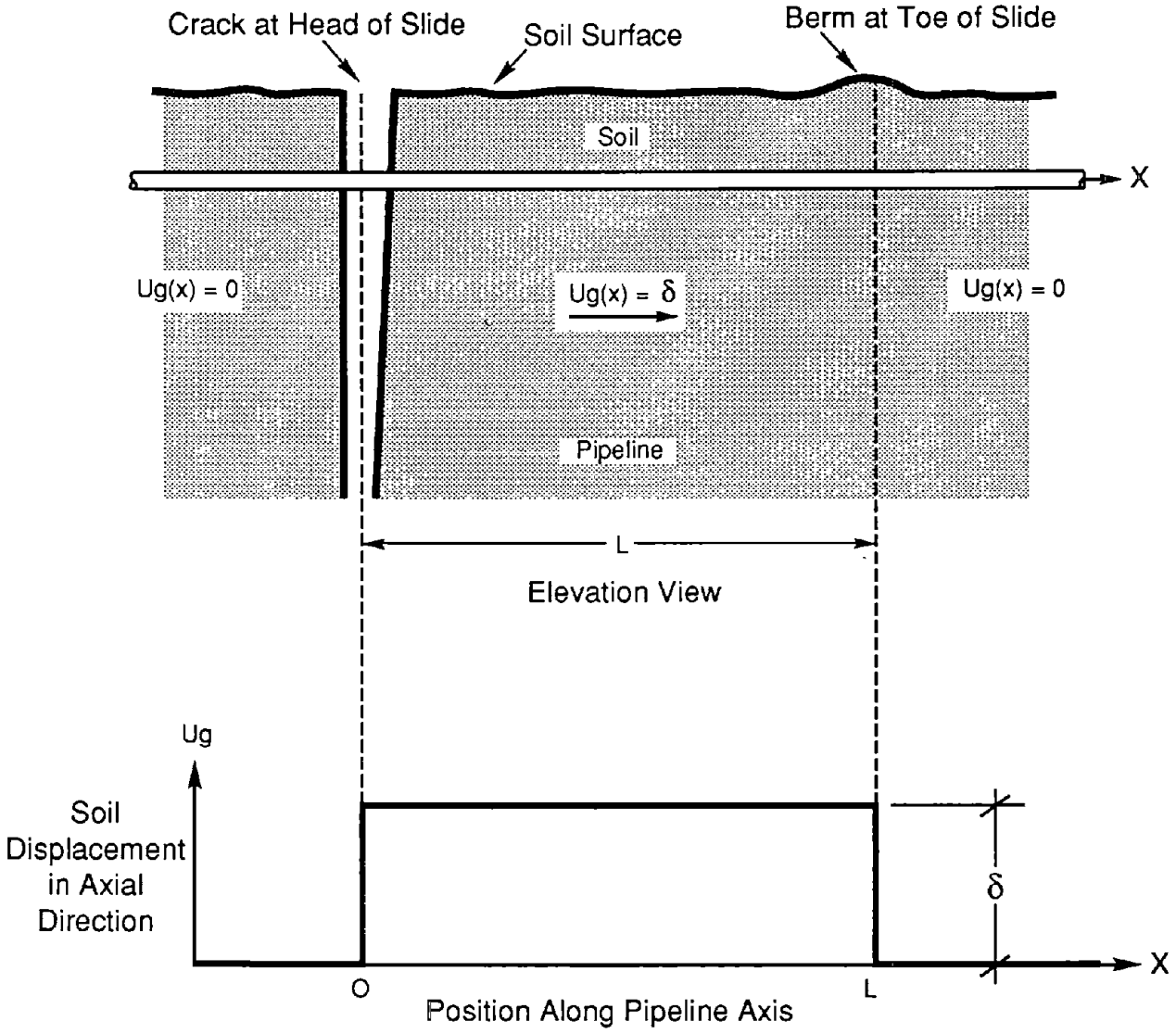

FIGURE 2-12 Idealized Rigid Block pattern of Longitudinal PGD.

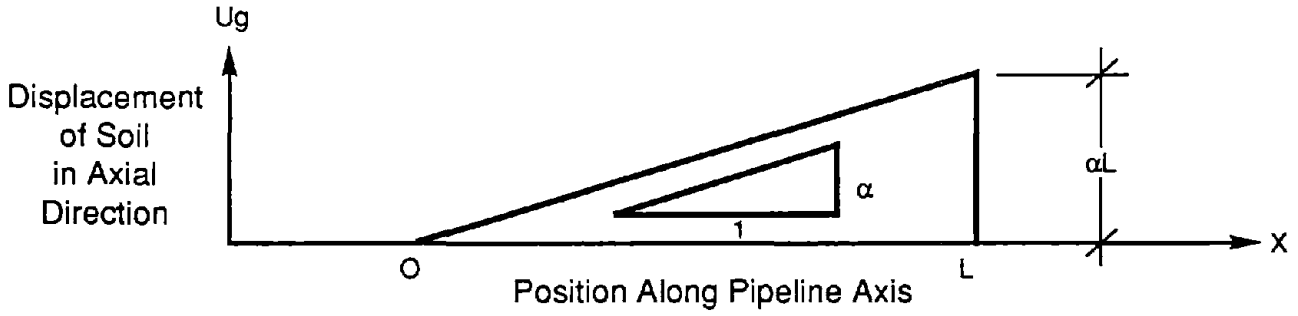

FIGURE 2-13 Idealized Ramp/Step pattern of Longitudinal PGD.

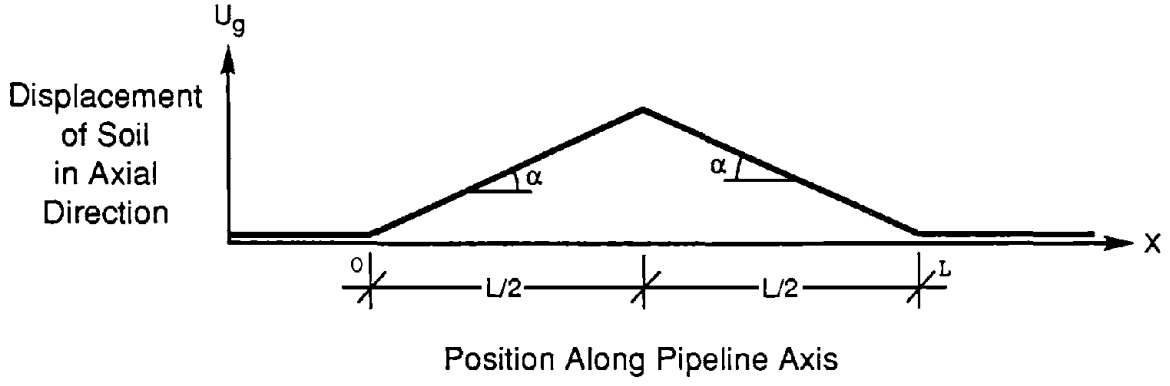

FIGURE 2-14 Idealized Ridge pattern of Longitudinal PGD.

Establishing a coordinate system with an origin at the boundary between the stable soil region (zero PGD) and the transition zone, the assumed horizontal soil displacement, $u_g(x)$, for Ramp PGD become

$$u_g(x) = \begin{cases} 0 & x < 0 \\ \alpha x & 0 < x < L \\ \alpha L & x > L \end{cases} \tag{2.4}$$

Axial pipeline strain induced by Ramp PGD is determined in Section 4.

2.4.2 Rigid Block PGD

The second idealized longitudinal PGD pattern considered herein is Rigid Block PGD. This corresponds to a mass of soil having length L, moving as a rigid body down a slight incline as shown in Figure 2–12. The soil displacement and soil strain at either side of the landslide or lateral spread zone are zero, while the displacement of the soil within lateral spread zone is a constant value δ. A ground crack or gap occurs at the head of the slide and a compression mound or berm at the toe.

The idealized Rigid Block pattern would be an appropriate model for the PGD in Figures 2–7(j) and 2–7(u) if the ground displacements on the left and right sides of these figures were zero. Establishing a coordinate system with an origin at the head of the lateral spread zone, the assumed horizontal ground displacements for Rigid Block PGD are given by

$$u_g(x) = \begin{cases} 0 & x < 0 \\ \delta & 0 < x < L \\ 0 & x > L \end{cases} \tag{2.5}$$

Axial pipeline strain induced by Rigid Block PGD is determined in Section 5.

2.4.3 Ramp/Step PGD

The third idealized PGD pattern considered herein is Ramp/Step PGD shown in Figure 2–13. This pattern could result from lateral spreading near a free face such as a

river. Soil displacement and soil strain are both zero on either side of the lateral spread zone, while the soil strain within the zone has a constant value of α.

The Ramp/Step PGD pattern would be an appropriate model for the ground movements on the right hand side of Figure 2–6(c) if the ground displacements under the BandaiBridge were zero, for the ground displacements in Figure 2–7(c) and Figure 2–7(o) if the ground displacements to the left were zero, and for the postulated pattern shown in Figure 2–10(c). Establishing a coordinate system with an origin at the beginning of the ramp, the assumed horizontal ground displacements for Ramp/Step PGD are given by

$$u_g(x) = \begin{cases} 0 & x < 0 \\ \alpha\, x & 0 < x < L \\ 0 & x > L \end{cases} \tag{2.6}$$

2.4.4 Ridge PGD

The fourth idealized pattern considered herein is Ridge PGD as shown in Figure 2–14. Soil displacement and soil strain are zero outside the zone of lateral spreading. Within the lateral spread zone, there is uniform tensile ground strain, α, to the left of the ridge (i.e. the point of maximum ground movement) and uniform compressive ground strain, α, to the right of the ridge.

The Ridge PGD pattern might be an appropriate model for the observed ground movement to the left of the Bandai Bridge in Figure 2–6(c), for the pattern in Figure 2–7(b), for the south side of the Yoshino Creek in Figure 2–8 and the postulated pattern shown in Figure 2–10(b). Establishing a coordinate system with an origin at the left side of the lateral spread zone, the assumed horizontal ground displacements for Ridge PGD are

$$u_g(x) = \begin{cases} 0 & x < 0 \\ \alpha\, x & 0 < x < L/2 \\ \alpha(L-x) & L/2 < x < L \\ 0 & x > L \end{cases} \tag{2.7}$$

Pipeline axial strain induced by Ridge PGD is determined in Section 7.

SECTION 3
SOIL – PIPELINE INTERACTION

The stress and strain in a buried pipeline subject to pseudo–static PGD are due to forces at the soil–pipeline interface. For longitudinal PGD, the key relationship is that between the force at the soil–pipeline interface and the relative displacement between the pipe and surrounding soil (i.e. direction of force and displacement parallel to the pipeline axis). The American Society of Civil Engineers Committee on Gas and Liquid Fuel Lifelines [12] suggests the use of elasto–plastic or hyperbolic models for this relationship. For simplicity, the elasto–plastic model (i.e. elastic spring–slider model) shown in Figure 3–1 is adopted herein.

Tests performed by Colton et al. [13] on a full–scale pipe placed in a trench and backfilled with cohesionless soil, indicate that the axial force/displacement relationship is linear at small displacements. The soil force reaches a "plateau" when slippage of the pipe with respect to the soil occurs. In the plateau or plastic region, the force per unit length exerted on the pipe is a constant value f_m. This is illustrated in Figure 3–2, which shows the relationship between the axial force per unit length at the soil/pipeline interface, and the relative axial displacement between the soil and pipeline.

The elasto–plastic model shown in Figure 3–2 is fully defined by two parameters. These are the maximum axial force per unit length at the soil/pipeline interface, f_m, and the axial stiffness of the soil spring, k. The relative displacement at which slippage occurs, D_s, is simply the ratio f_m/k. Characteristics of these spring–sliders are determined in this section after review and synthesis of the existing literature.

3.1 Maximum Axial Force Per Unit Length

For the case where the pipeline trench is backfilled with cohesionless soil, the ultimate force per unit length at the soil/pipeline interface, f_m, is simply the product of the coefficient of friction and the average of the vertical and horizontal forces on the pipeline, that is:

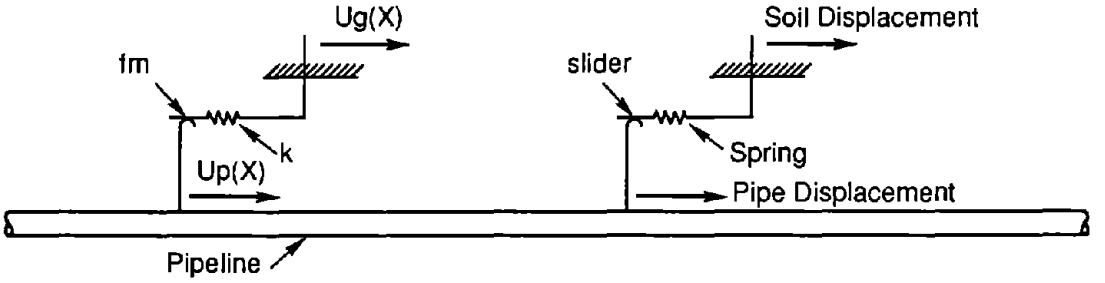

FIGURE 3-1 Spring/Slider Model for Axial Soil-Pipeline Interface Forces.

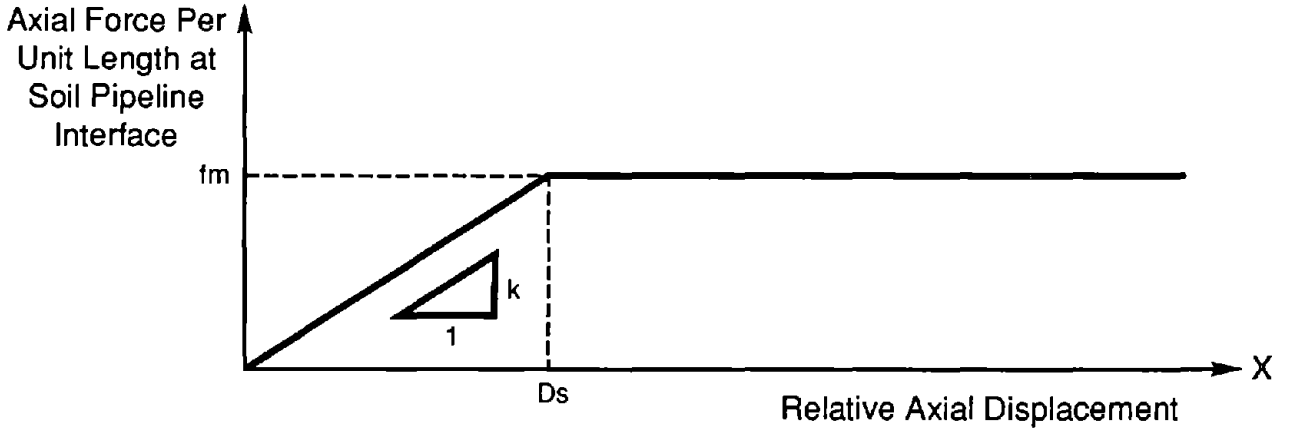

FIGURE 3-2 Assumed Axial Force vs. Relative Displacement Relation for Elastic Spring/Slider Model of the Soil-Pipeline Interface.

$$f_m = \mu \cdot \gamma H \cdot \frac{(1 + K_0)}{2} \cdot \pi\phi \tag{3.1}$$

where μ is the coefficient of friction at or near the soil/pipeline interface, γ is the unit weight of the soil, H is the depth to the pipe centerline, K_0 is the coefficient of lateral earth pressure and ϕ is the outside diameter of the pipe.

Experimental studies have shown that the coefficient of friction, μ, between the soil and the pipeline depends mainly on the nature of the pipe surface, the angularity of the soil grains and the relative roughness of the pipe surface with respect to the soil grains. Results obtained by Kulhawy and Peterson [14] show that for rough concrete pipe surfaces, slippage occurs in the soil near the interface and that $\mu \simeq \tan\theta$ where θ is the angle of shearing resistance of the soil. For the case of a concrete pipe with smooth surfaces, slippage occurs at the interface for $\mu/\tan\theta$ ranging from 0.8 to 1.0, with a mean value of 0.9 ($\mu \simeq 0.9 \tan\theta$). Colton et al. [13] noticed that for pipes wrapped with plastic covering, slippage happens in the soil near the pipe rather than at the interface. The reason is that the soil grains become partially embedded in the plastic cover at the interface. Brumund and Leonards [15] also observed that $\tan\theta$ is an upper bound for μ, regardless of the rate at which slippage is initiated. Two types of surfaces were studied: Mortar/Sand and Polished Steel/Sand. The result for the first surface was similar to Kulhawy and Peterson's result for concrete surfaces. For the Polished Steel surface, the mean value of μ is equal to 0.5 $\tan\theta$. Based on these experimental results, the coefficient of friction for normal (i.e. unpolished) steel pipe is taken to be that for concrete pipe with smooth surface, that is

$$\mu = 0.9 \tan\theta \tag{3.2}$$

The magnitude of K_0 for normally consolidated cohesionless soil has been reported to range from 0.35 to 0.47 (Perloff and Baron [16]). However, because of the backfilling and compaction of the soil around the pipeline, one expects K_0 to be somewhat larger. O'Rourke et al. [17] recommend $K_0 = 1.0$, as a conservative estimate for most conditions of pipeline burial.

3.2 Axial Stiffness

The technical literature contains a number of relations for the initial axial stiffness, k. For the plane strain case, Novak et al. [18] presented the initial axial stiffness as a function of frequency with values ranging from about 1.50 to 2.75 times the dynamic soil shear modulus, G ($1.50\ G \leq k \leq 2.75\ G$). O'Leary and Datta [19] calculated k at low frequency to be about two times G. In their comparison of the observed behavior of a tunnel with a multiple mass–spring model, Shibata et al. [20] have used $k = G$. In a Japanese design procedure for buried pipelines, Kuboto Ltd [21] suggests a value of $k = 3.0\ G$. Based upon an analytical study of piles, O'Rourke and Wang [22] use $k = 2.0\ G$. These analytical results suggest $1.0G \leq k \leq 3.0\ G$.

Colton et al. [13] performed full–scale experiments which studied axial soil–pipe interaction for buried pipeline. ElHmadi and O'Rourke [23] used the Colton results to back calculate the equivalent value for k. They found that $1.57G \leq k \leq 1.70\ G$ when G is evaluated for the expected level of soil strain. Based upon the analytical and experimental values mentioned above, the initial spring stiffness k is taken herein as twice the soil shear modulus, or

$$k = 2.0\ G \tag{3.3}$$

The procedure used to evaluate G for the appropriate level of soil strain follows that in ElHmadi and O'Rourke [24].

3.3 Relative Axial Displacement for Slippage

As noted previously, the relative axial displacement for slippage at or near the soil–pipe interface, D_s, is simply f_m/k as shown in Figure 3–2. Table 3.1 lists D_s for various values of the pipe diameter, ϕ, and burial depth to the top of the pipe, $C = H - \phi/2$, evaluated for a soil unit weight of 100 pcf. Table 3.I(a) is for a coefficient of friction $\mu = 0.45$ which corresponds to an angle of shearing resistance of $\theta = 27°$. Tables 3.I(b) and 3.I(c) are for coefficients of friction of 0.60 and 0.75 respectively, which correspond to $\theta = 34°$ and $40°$.

As shown in Table 3–I the D_s values are increasing functions of μ, ϕ and C. However, for what is felt to be a reasonable range of parameters, all D_s values are less than 0.075 inches. Note in this regard that Holloway [25] infers values in the 0.01 to 0.04 in. range for the

relative displacement at slippage based upon tests of soil/pile interaction.

The small values for D_s suggests a simplified model for soil–pipe interaction. This simplified model, shown in Figure 3–3, assumes that the soil spring is rigid ($k = \infty$ and $D_s = 0$). That is, the spring portion of the spring slider is neglected.

In the next two sections, the response of buried pipelines subject to two idealized patterns of longitudinal PGD will be evaluated using both the elastic spring/slider model in Figure 3–2 and the rigid spring/slider model in Figure 3–3. In subsequent sections, the rigid spring/slider model is used to evaluate response for two additional PGD patterns.

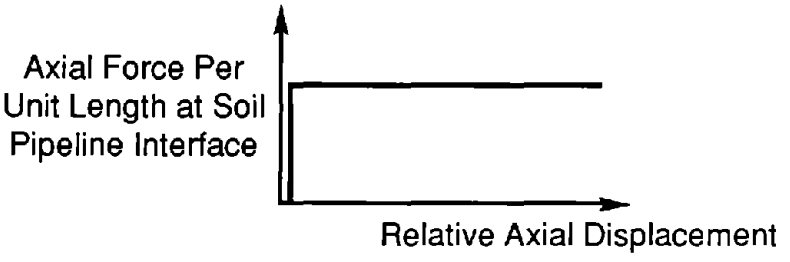

FIGURE 3-3 Assumed Axial Force vs. Relative Displacement Relation for Rigid Spring/Slider Model of the Soil-Pipeline Interface.

Pipe Diameter ϕ (in)	Burial Depth to Top of Pipe, C (ft)		
	3 (.91 m)	6 (1.83 m)	9 (2.74 m)
12 (30.5 cm)	.004	.007	.010
30 (76.2 cm)	.011	.018	.026
48 (122 cm)	.020	.032	.044

(a) Coefficient of Friction $\mu = 0.45$.

Pipe Diameter ϕ (in)	Burial Depth to Top of Pipe, C (ft)		
	3 (.91 m)	6 (1.83 m)	9 (2.74 m)
12 (30.5 cm)	.005	.009	.013
30 (76.2 cm)	.014	.024	.034
48 (122 cm)	.027	.043	.059

(b) Coefficient of Friction $\mu = 0.60$.

Pipe Diameter ϕ (in)	Burial Depth to Top of Pipe, C (ft)		
	3 (.91 m)	6 (1.83 m)	9 (2.74 m)
12 (30.5 cm)	.006	.011	.016
30 (76.2 cm)	.018	.030	.043
48 (122 cm)	.033	.054	.074

(c) Coefficient of Friction $\mu = 0.75$.

Table 3–I Relative Axial Displacement, D_s, in inches, for Slippage at the Soil/Pipe Interface evaluated for Unit Weight of Soil $\gamma = 100$ pcf (1610 kg/m^3).

SECTION 4
RAMP PGD

The axial strain induced in a continuous steel pipeline due to a Ramp pattern of longitudinal PGD is determined in this section. As mentioned previously, pipe response to the horizontal component of PGD parallel to the pipe axis will be determined and any vertical component (i.e. subsidence and heaving) is neglected. Initially the soil–pipeline interface is modeled by the elastic spring–slider model shown in Figure 3–2. In addition, the pipeline strain is also determined using a simplified rigid spring–slider model for the soil–pipeline interface as shown in Figure 3–3. For the Ramp pattern considered in this section as well as the other longitudinal PGD patterns investigated in Sections 5, 6 and 7, the burial depth to the pipeline centerline, H, is assumed to be constant in and around the PGD zone.

As noted previously the idealized Ramp pattern shown in Figure 2–11 approximates the PGD patterns quantified by Suzuki and Masuda [8] and shown in Figure 2–4. It may also be appropriate for the observed PGD patterns shown in Figure 2–6(d), 2–6(e) and 2–7(q). Results are presented herein for Ramp PGD with tensile ground strain α. However the results are also applicable with a change in sign, to situations with a compressive ground strain of magnitude α.

As shown in Figure 4–1, a coordinate system is established with $x = 0$ at the head of the transition zone, and the assumed ground movement is given as a function of the axial coordinate x by Equation 2.4. The length of the transition zone is L. Since the distribution of pipe strain is symmetric about the center of the transition zone, only the area $x \leq L/2$ is considered.

4.1 Elastic Spring/Slider Model

The solution using the elastic spring/slider model is obtained by dividing the pipeline into three regions (Region I, II and III) as shown in Figure 4–1. Differential equations governing the pipe response in each region are derived. The solution for the pipeline as a whole is then obtained by enforcing equilibrium and continuity at the boundaries between regions.

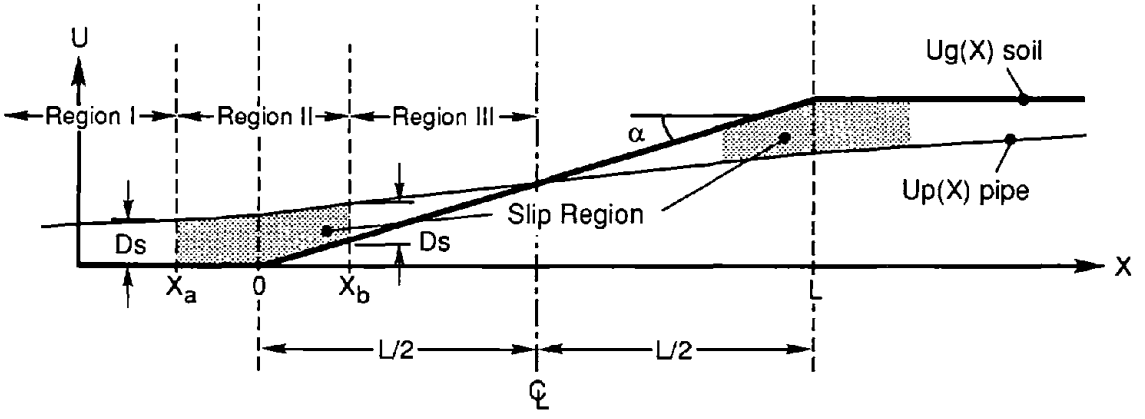

FIGURE 4-1 Model of Pipeline Subjected to a Ramp pattern of Longitudinal PGD.

In Region I ($x \leq x_a$) the displacement of the soil is zero and the relative displacement between the pipe and soil is small enough so that the soil–pipeline interface behaves as a linear spring. That is, the interface force is less than f_m given by Equation 3.1. Region II ($x_a \leq x \leq x_b$) is a slip region where the relative displacements between the pipe and soil are large and the soil–pipeline interface force is a constant equal to f_m. In Region III ($x_b \leq x \leq L/2$) the soil displacement is a linear function of the coordinate x, but the relative displacements between the pipe and soil are small and hence the soil–pipeline interface is again modeled as a linear spring. The values for x_a and x_b are not known a priori, but are calculated as part of the solution.

4.1.1 Region I ($x \leq x_a$)

Figure 4–2(a) shows the forces acting on a differential length of pipe in Region I. Since the ground displacement, u_g, equals zero, the soil–pipeline interface force is simply the pipe displacement, $u_p(x)$, times the spring constant, k given in equation 3.3. Summing forces we obtain:

$$A(\sigma + d\sigma) = k u_p(x)\, dx + A\sigma \tag{4.1}$$

where A is the cross sectional area of the pipeline and σ is the induced stress in the pipeline. Assuming a linear elastic pipe material ($\sigma = E\epsilon$) and noting $\epsilon = du_p/dx$, we obtain:

$$\frac{d^2u_p(x)}{dx^2} - \frac{k}{EA} u_p(x) = 0 \tag{4.2}$$

where E is Young's modulus for the pipe. Thus the differential equation governing the displacement of the pipe in Region I becomes:

$$\frac{d^2u_p(x)}{dx^2} - \beta^2 u_p(x) = 0 \tag{4.3}$$

where $\beta^2 = k/EA$.

At $x = -\infty$ the displacement of the pipeline is zero. We define F_a as the force in the pipe at x_a. Thus, the boundary conditions for Region I are

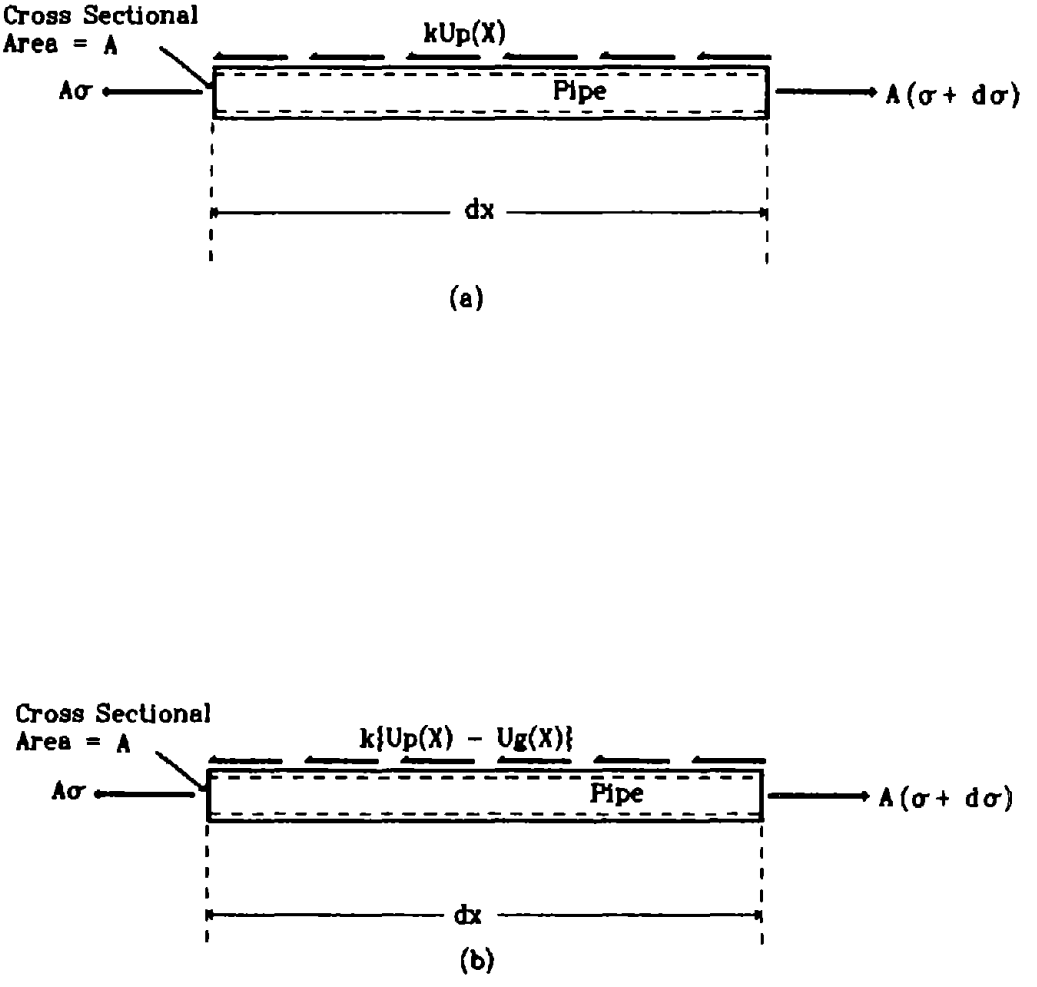

FIGURE 4-2 Forces Acting on a Differential Length of Pipe in Region I (a) and Region III (b) for a Ramp pattern of Longitudinal PGD.

$$u_p(-\infty) = 0 \tag{4.4}$$

$$\frac{du_p(x_a)}{dx} = \frac{F_a}{EA} \tag{4.5}$$

The solution of the differential equation given by equation (4.3) subject to the boundary conditions in equations (4.4) and (4.5) is:

$$u_p(x) = \frac{F_a}{EA\beta} e^{\beta(x-x_a)} \tag{4.6}$$

Since $x = x_a$ is the boundary between the linear spring (Region I) and the "plastic" slider (Region II), the relative displacement between the pipe and the soil equals D_s at x_a (i.e. $u_g(x_a) - u_p(x_a) = D_s$ which is a property of the soil–pipeline interface as discussed in Section 3). However, since the soil displacement in Region I is zero:

$$u_p(x_a) = \frac{F_a}{EA\beta} = D_s \tag{4.7}$$

and

$$u_p(x) = D_s e^{\beta(x-x_a)} \qquad -\infty \le x \le x_a \tag{4.8}$$

Note that, based on Equation 4.7, the soil–pipe system in Region I can be treated as an equivalent linear spring with spring constant $K_a = EA\beta$. That is, as shown in Figure 4–3, the displacement of this equivalent spring is taken as the relative displacement between the pipeline and soil at $x = x_a$ (i.e. D_s) and the force in this equivalent spring is taken as the force in the pipe at $x = x_a$ (i.e. F_a).

4.1.2 Region II ($x_a \le x \le x_b$)

The displacement of the pipeline in Region II can be determined from the known displacement at $x = x_a$ and the distribution of forces on the pipe as shown in Figure 4–4. Note that the displacement of the pipe at $x = x_a$ is equal to D_s. The force in the pipe in Region II is the sum of the force at $x = x_a$ (i.e. K_aD_s) and a contribution due to the

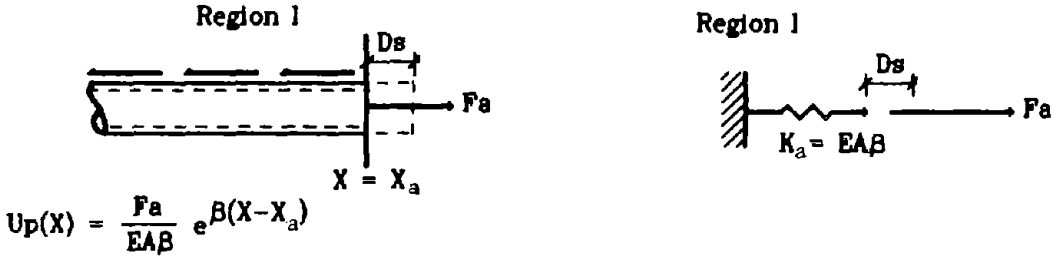

FIGURE 4-3 Equivalent Spring for the Soil-Pipe System in Region I.

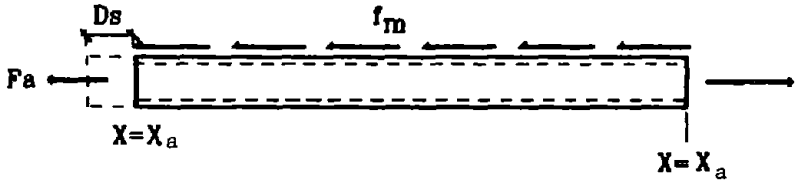

FIGURE 4-4 Forces Acting on Pipe in Region II.

soil–pipeline interaction force f_m:

$$f(x) = K_a D_s + f_m(x - x_a) \tag{4.9}$$

The displacement of the pipe in Region II then becomes:

$$u_p(x) = D_s + \int_{x_a}^{x} \frac{f(x)}{EA}\, dx \tag{4.10}$$

or

$$u_p(x) = D_s + \frac{K_a D_s\,(x - x_a)}{EA} + \frac{f_m(x - x_a)^2}{2EA} \qquad x_a \le x \le x_b \tag{4.11}$$

4.1.3 Region III ($x_b \le x \le L/2$)

Figure 4–2(b) shows the forces acting on a differential length of pipe in Region III. Equating these forces we obtain:

$$A\sigma + d\sigma) = k(u_p(x) - u_g(x))dx + A\sigma \tag{4.12}$$

Again for a linear elastic pipe material and noting $\epsilon = du_p/dx$, the differential equation governing the pipe displacement, u_p, in Region III becomes:

$$\frac{d^2u_p(x)}{dx^2} - \beta^2 u_p(x) = -\beta^2 u_g(x) \tag{4.13}$$

At the boundary between Region II and III (i.e. $x = x_b$) the displacement of the pipeline is equal to the ground displacement plus the relative displacement at which the soil spring becomes plastic (i.e. relative displacement = D_s).

$$u_p(x_b) = D_s + u_g(x_b) \tag{4.14}$$

Noting that $u_g(x) = \alpha x$ in Region III this boundary condition becomes:

$$u_p(x_b) = D_s + \alpha x_b \tag{4.15}$$

At the center of the transition zone, the displacement of the pipe by symmetry, equals the displacement of the soil; as shown in Figure 4–1:

$$u_p(L/2) = u_g(L/2) = \alpha L/2 \tag{4.16}$$

The solution to the differential equation given in equation (4.13) subject to the boundary conditions given in equations (4.15) and (4.16) is:

$$u_p(x) = -\frac{D_s e^{\beta(x-x_b)}}{e^{\beta(L-2x_b)} - 1} + \frac{D_s e^{-\beta(x+x_b)}}{e^{-2\beta x_b} - e^{-\beta L}} + \alpha x \qquad x_b \le x \le L/2 \tag{4.17}$$

which is the pipe displacement in Region III.

4.1.4 Continuity

Continuity of the pipe requires that the pipe displacement immediately to the left of $x = x_b$ (i.e. equation (4.11) evaluated at $x = x_b$) must match the displacement immediately to the right (i.e. equation (4.17) evaluated at $x = x_b$). That is:

$$D_s + \frac{K_a D_s (x_b - x_a)}{EA} + \frac{f_m (x_b - x_a)^2}{2EA} = D_s + \alpha x_b \tag{4.18}$$

Rearranging the terms yields the following:

$$\frac{f_m (x_b - x_a)^2}{2EA} + \frac{K_a D_s}{EA}(x_b - x_a) - \alpha x_b = 0 \tag{4.19}$$

This can be viewed as a quadratic equation in terms of the quantity $x_b - x_a$. Since we are interested in the solution with $x_b > x_a$, the quadratic equation results in the following transcendental equation:

$$x_b - x_a = \frac{-K_a D_s/EA + \sqrt{(K_a D_s/EA)^2 + 2f_m \alpha x_b/EA}}{f_m/EA} \tag{4.20}$$

4.1.5 Equilibrium

A second relation for the quantity $x_b - x_a$ can be derived by enforcing equilibrium. The force in the pipe immediately to the left of $x = x_b$ must equal the force in the pipe immediately to the right of $x = x_b$. The force in the pipe immediately to the left is given by Equation 4.9 evaluated for $x = x_b$. The force immediately to the right is simply the pipe axial rigidity EA times the pipe strain in Region III evaluated for $x = x_b$. Thus:

$$K_a D_s + f_m(x_b - x_a) = EA \frac{du_p}{dx}(x_b) \tag{4.21}$$

where $u_p(x_b)$ is given by equation 4.17. Hence

$$\frac{K_a D_s}{EA} + \frac{f_m(x_b - x_a)}{EA} = -\beta D_s \left[\frac{e^{-\beta L} + e^{-2\beta x_b}}{e^{-2\beta x_b} - e^{-\beta L}} \right] + \alpha \tag{4.22}$$

Equation (4.22) can be simplified and rearranged to yield a second expression for $x_a - x_b$:

$$x_a - x_b = -\frac{K_a D_s}{f_m} \left[\frac{e^{-\beta L} + e^{-2\beta x_b}}{e^{-2\beta x_b} - e^{-\beta L}} + 1 \right] + EA\alpha/f_m \tag{4.23}$$

The right hand side of equations 4.20 and 4.23 can be set equal to each other. This results in an equation which is solely a function the unknown x_b. Herein, the Newton–Raphson Method is applied to the resulting equation to determine x_b.

4.1.6 Maximum Pipe Strain

The maximum strain, ϵ, in the pipe occurs at $x = L/2$. Knowing the value of x_b, ϵ can be determined by evaluating the derivative of equation (4.17) for $x = L/2$:

$$\frac{du_p(L/2)}{dx} = \epsilon = \alpha - \frac{2\beta D_s e^{-\beta(L/2+x_b)}}{e^{-\beta 2x_b} - e^{-\beta L}} \tag{4.24}$$

Tables 4–Ia through 4–XXVIIa present the maximum pipe strain, ϵ, for a Ramp pattern of longitudinal PGD evaluated using equation 4.24. In these tables the unit weight of soil, γ, is taken as 100 pcf and the coefficient of friction of the soil pipe interface, μ, is taken as 0.75. Results are presented for pipe diameters, ϕ, of 12, 30 and 48 inches, pipe wall thickness, t, of 1/4, 1/2, and 3/4 inch, and soil cover C over the top of the pipe of 3, 6, and 9 feet. The range of values for the ground strain, α, and the length of the PGD zone, L, are based on the work by Suzuki and Masuda [8].

For fixed ground strain, α, the maximum stress in the pipe increases with the length of the transition zone, L. For fixed L, the maximum pipe strain increases with increasing soil strain, α. For fixed α and L the pipe strain is an increasing function of the cover over top of pipe C = H – $\phi/2$, and a decreasing function of the wall thickness, t. It also appears to be an increasing function of pipe diameter, ϕ.

4.2 Rigid Spring/Slider Model

The results presented in table 4–Ia through 4–XXVIIa cover what is felt to be a reasonable range for the parameters of interest. However, for situations not covered by these tables, or for hand calculation, a simplified approach is useful. This simplified approach uses the rigid spring/slider model for the soil pipe interface shown in Figure 3–3. Figure 4–5 shows the two possible configurations of such a simplified model. It is assumed that slip occurs between the soil and pipeline over a length L_e on either side of the center of the transition zone, x = L/2. Beyond L_e the relative displacement between the soil and pipe is assumed to be zero.

In Figure 4–5(a) the slip region extends all the way to the center of the transition zone and the resulting pipe strain is less than the ground strain α. In Figure 4–5(b), the slip region exists over a limited length near the ends of the transition zone, and the pipe strain towards the center of the zone is equal to the ground strain α. That is the maximum pipe strain for the Ramp pattern is always less than or equal to α. For the configuration in Figure 4.5(a), the maximum pipe strain ($\epsilon < \alpha$) can be determined by noting that the displacement of the pipeline at the center of the transition zone is equal to the displacement of the soil (i.e. $u_p(L/2) = u_g(L/2)$). Hence, the stretching of the pipe along

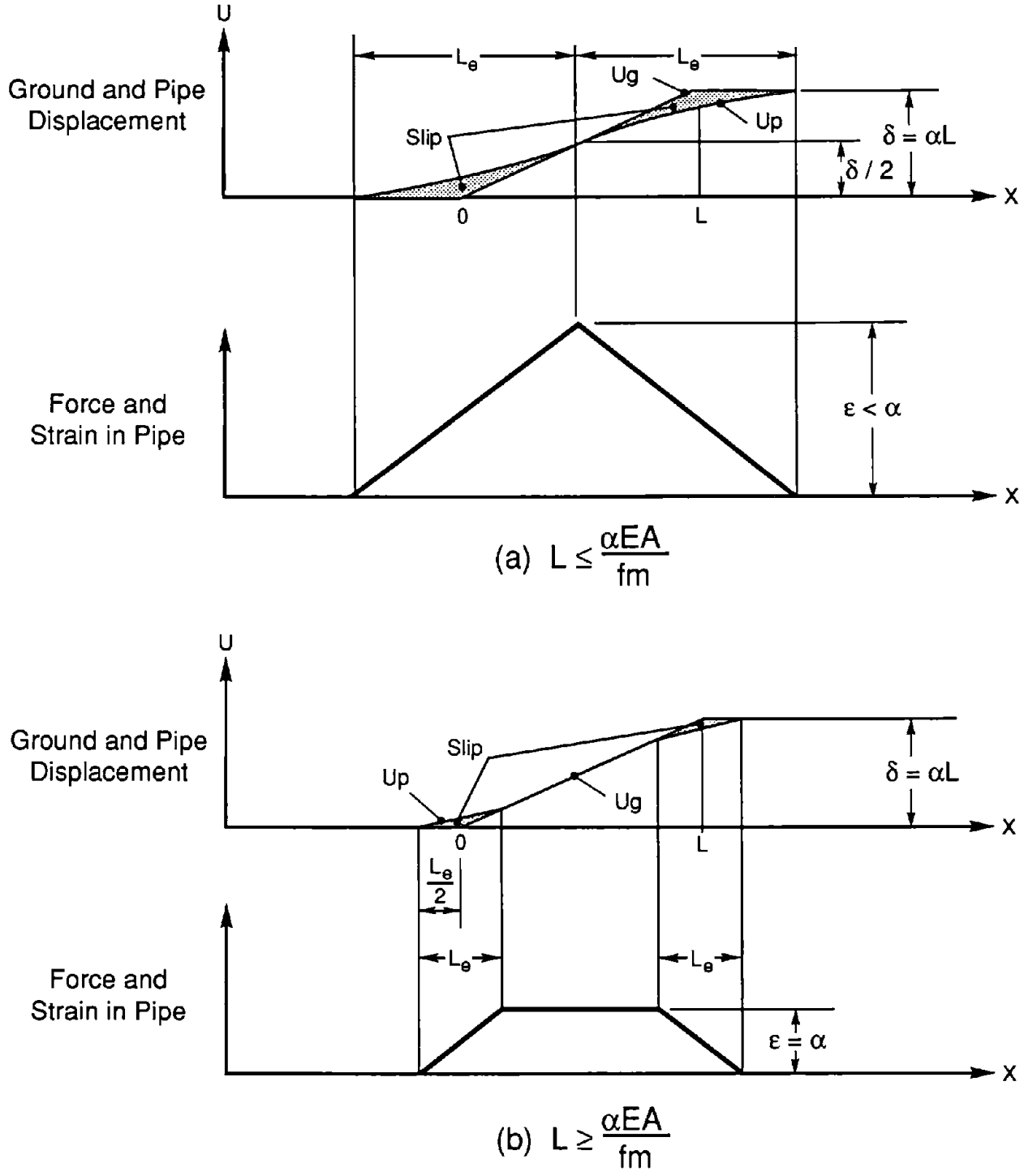

FIGURE 4-5 Simplified Model of Buried Pipe Subjected to a Ramp pattern of Longitudinal PGD.

the length L_e is due to the constant force per unit length, f_m, at the soil pipe interface and results in a pipe displacement of $\alpha L/2$ at $x = L/2$. The displacement can be calculated by integration of the pipe strain over the slip length L_e.

$$u_p(L/2) = \alpha L/2 = \int_0^{L_e} \frac{f_m s}{EA}\, ds = \frac{f_m L_e^2}{2EA} \tag{4.25}$$

Equation (4.25) can be solved for L_e. The maximum force in the pipe is equal to f_m time L_e since it is assumed that the pipe is not stressed beyond L_e. The maximum pipe strain, ϵ_a, is then $f_m L_e/EA$.

$$\epsilon = \sqrt{\frac{\alpha L f_m}{EA}} \leq \alpha \tag{4.26}$$

Note for $L \leq \alpha EA/f_m$, which corresponds to Figure 4–5(a), the maximum pipe strain is a function of the length of the transient spread zone, but is less than the ground strain, α. For $L \geq \alpha EA/f_m$, which corresponds to Figure 4–5(b) the maximum pipe strain is independent of the length, L, and is equal to the ground strain, α. That is if the length of the transient zone is large enough the maximum pipe strain and the ground strain are identical.

Tables 4–Ib through 4–XXVIIb present results from equation 4.26 for the maximum pipe strain using the simplified model. Results are given for the same range of parameters used with the elastic spring/slider model which were presented in Tables 4–Ia through 4–XXVIIa. Note that equation (4.26) explains the influence of various parameters on the maximum pipe strain which were observed previously in relation to the complete interface model. That is the pipe strain is always an increasing function of the ground strain α. For situations where $L \leq \alpha EA/f_m$, ϵ is an increasing function of the length L, and cover over the top of the pipe, C, or the burial depth, H. It is a decreasing function of the wall thickness, t. Since f_m and A are proportional to the pipe diameter, ϕ, the maximum pipe strain using the simplified soil pipe interface model is not directly a function of the pipe diameter. However, since table 4–I through 4–XXVII are presented in terms of cover over top of pipe C, a larger pipe diameter results in a larger burial depth, $H = C + \phi/2$, and pipe strain is a function of burial depth.

4.3 Comparison of Models

Tables 4–Ic through 4–XXVIIc list the percent difference in the maximum pipe strain due to Ramp PGD evaluated using the complete elastic spring/slider model and the simplified rigid spring/slider model. Note that both models give very similar results, and the simplified model is always conservative predicting maximum pipe strain slightly higher than the complete model. In the cases examined, which represent what is felt to be typical pipeline conditions, the error between the models does not exceed 4 percent.

α	L(m) 25	50	100	150	200
0.0025	0.0007745	0.0010961	0.0015505	0.0018989	0.0021919
0.0033	0.0008948	0.0012661	0.0017910	0.0021936	0.0025328
0.0050	0.0010964	0.0015511	0.0021939	0.0026872	0.0031029
0.0100	0.0015512	0.0021940	0.0031028	0.0037996	0.0043864
0.0200	0.0021942	0.0031032	0.0043542	0.0053236	0.0061355

TABLE 4–Ia Maximum Pipe Strain for a Ramp pattern of Longitudinal PGD using the Complete Soil–Pipeline Interface Model.
ϕ = 12 in (30.5 cm), t = 0.25 in (6.4 mm), C = 3 ft (0.91 m)

α	L(m) 25	50	100	150	200
0.0025	0.0007759	0.0010973	0.0015518	0.0019005	0.0021945
0.0033	0.0008959	0.0012670	0.0017918	0.0021945	0.0025340
0.0050	0.0010973	0.0015518	0.0021945	0.0026877	0.0031035
0.0100	0.0015518	0.0021945	0.0031035	0.0038010	0.0043891
0.0200	0.0021945	0.0031035	0.0043891	0.0053755	0.0062071

TABLE 4–Ib Maximum Pipe Strain for a Ramp pattern of Longitudinal PGD using the Simplified Model.
ϕ = 12 in (30.5 cm), t = 0.25 in (6.4 mm), C = 3 ft (0.91 m)

α	L(m) 25	50	100	150	200
0.0025	0.174	0.107	0.079	0.083	0.122
0.0033	0.124	0.073	0.049	0.044	0.047
0.0050	0.077	0.043	0.027	0.022	0.022
0.0100	0.039	0.025	0.025	0.037	0.061
0.0200	0.017	0.010	0.800	0.974	1.167

TABLE 4–Ic Percent Difference in Maximum Pipe Strain Between the Complete and Simplified Models.
ϕ = 12 in (30.5 cm), t = 0.25 in (6.4 mm), C = 3 ft (0.91 m)

α	L(m) 25	50	100	150	200
0.0025	0.0008503	0.0012049	0.0017051	0.0020866	0.0023932
0.0033	0.0009834	0.0013929	0.0019712	0.0024143	0.0027866
0.0050	0.0012062	0.0017076	0.0024161	0.0029595	0.0034175
0.0100	0.0017081	0.0024168	0.0034187	0.0041872	0.0048348
0.0200	0.0024170	0.0034190	0.0048358	0.0059228	0.0068392

TABLE 4–IIa Maximum Pipe Strain for a Ramp pattern of Longitudinal PGD Using the Complete Soil–Pipeline Interface Model.
ϕ = 30 in (76.2 cm), t = 0.25 in (6.4 mm), C = 3 ft (0.91 m)

α	L(m) 25	50	100	150	200
0.0025	0.0008550	0.0012091	0.0017100	0.0020943	0.0024183
0.0033	0.0009873	0.0013962	0.0019745	0.0024183	0.0027924
0.0050	0.0012091	0.0017100	0.0024183	0.0029618	0.0034199
0.0100	0.0017100	0.0024183	0.0034199	0.0041886	0.0048365
0.0200	0.0024183	0.0034199	0.0048365	0.0059235	0.0068399

TABLE 4–IIb Maximum Pipe Strain for a Ramp pattern of Longitudinal PGD Using the Simplified Model.
ϕ = 30 in (76.2 cm), t = 0.25 in (6.4 mm), C = 3 ft (0.91 m)

α	L(m) 25	50	100	150	200
0.0025	0.556	0.353	0.287	0.368	1.045
0.0033	0.390	0.235	0.167	0.165	0.208
0.0050	0.241	0.138	0.088	0.074	0.072
0.0100	0.110	0.061	0.036	0.031	0.035
0.0200	0.052	0.028	0.015	0.012	0.010

TABLE 4–IIc Percent Difference in Maximum Pipe Strain Between the Complete and Simplified Models.
ϕ = 30 in (76.2 cm), t = 0.25 in (6.4 mm), C = 3 ft (0.91 m)

	L(m)				
α	25	50	100	150	200
0.0025	0.0009173	0.0013021	0.0018426	0.0022462	0.0024753
0.0033	0.0010627	0.0015073	0.0021340	0.0026126	0.0030089
0.0050	0.0013054	0.0018497	0.0026183	0.0032073	0.0037033
0.0100	0.0018508	0.0026199	0.0037069	0.0045407	0.0052436
0.0200	0.0026204	0.0037075	0.0052444	0.0064236	0.0074175

TABLE 4–IIIa Maximum Pipe Strain for a Ramp pattern of Longitudinal PGD Using the Complete Soil–Pipeline Interface Model.
ϕ = 48 in (122 cm), t = 0.25 in (6.4 mm), C = 3 ft (0.91 m)

	L(m)				
a	25	50	100	150	200
0.0025	0.0009274	0.0013115	0.0018547	0.0022716	0.0025000
0.0033	0.0010708	0.0015144	0.0021416	0.0026230	0.0030287
0.0050	0.0013115	0.0018547	0.0026230	0.0032125	0.0037094
0.0100	0.0018547	0.0026230	0.0037094	0.0045431	0.0052459
0.0200	0.0026230	0.0037094	0.0052459	0.0064249	0.0074189

TABLE 4–IIIb Maximum Pipe Strain for a Ramp pattern of Longitudinal PGD Using the Simplified Model.
ϕ = 48 in (122 cm), t = 0.25 in (6.4 mm), C = 3 ft (0.91 m)

	L(m)				
α	25	50	100	150	200
0.0025	1.100	0.722	0.656	1.128	0.999
0.0033	0.763	0.472	0.359	0.398	0.660
0.0050	0.467	0.273	0.180	0.160	0.165
0.0100	0.211	0.117	0.070	0.052	0.045
0.0200	0.099	0.053	0.029	0.022	0.018

TABLE 4–IIIc Percent Difference in Maximum Pipe Strain Between the Complete and Simplified Models.
ϕ = 48 in (122 cm), t = 0.25 in (6.4 mm), C = 3 ft (0.91 m)

α	L(m) 25	50	100	150	200
0.0025	0.0010533	0.0014912	0.0021072	0.0024860	0.0025000
0.0033	0.0012177	0.0017237	0.0024381	0.0029827	0.0033242
0.0050	0.0014929	0.0021127	0.0029886	0.0036602	0.0042256
0.0100	0.0021131	0.0029892	0.0042284	0.0051790	0.0059802
0.0200	0.0029896	0.0042286	0.0059804	0.0073241	0.0084563

TABLE 4–IVa Maximum Pipe Strain for a Ramp pattern of Longitudinal PGD Using the Complete Soil–Pipeline Interface Model.
ϕ = 12 in (30.5 cm), t = 0.25 in (6.4 mm), C = 6 ft (1.82 m)

α	L(m) 25	50	100	150	200
0.0025	0.0010574	0.0014953	0.0021147	0.0025000	0.0025000
0.0033	0.0012209	0.0017267	0.0024419	0.0029906	0.0033333
0.0050	0.0014953	0.0021147	0.0029906	0.0036628	0.0042294
0.0100	0.0021147	0.0029906	0.0042294	0.0051800	0.0059813
0.0200	0.0029906	0.0042294	0.0059813	0.0073256	0.0084588

TABLE 4–IVb Maximum Pipe Strain for a Ramp pattern of Longitudinal PGD Using the Simplified Model.
ϕ = 12 in (30.5 cm), t = 0.25 in (6.4 mm), C = 6 ft (1.82 m)

α	L(m) 25	50	100	150	200
0.0025	0.387	0.277	0.355	0.565	0.001
0.0033	0.264	0.173	0.156	0.265	0.276
0.0050	0.159	0.097	0.070	0.069	0.090
0.0100	0.074	0.048	0.024	0.019	0.018
0.0200	0.034	0.020	0.015	0.019	0.030

TABLE 4–IVc Percent Difference in Maximum Pipe Strain Between the Complete and Simplified Models.
ϕ = 12 in (30.5 cm), t = 0.25 in (6.4 mm), C = 6 ft (1.82 m)

α	L(m) 25	50	100	150	200
0.0025	0.0011042	0.0015661	0.0022043	0.0024874	0.0024998
0.0033	0.0012797	0.0018142	0.0025658	0.0031208	0.0033268
0.0050	0.0015721	0.0022271	0.0031518	0.0038596	0.0044510
0.0100	0.0022289	0.0031549	0.0044636	0.0054675	0.0063136
0.0200	0.0031556	0.0044645	0.0063152	0.0077350	0.0089318

TABLE 4–Va Maximum Pipe Strain for a Ramp pattern of Longitudinal PGD Using the Complete Soil–Pipeline Interface Model.
ϕ = 30 in (76.2 cm), t = 0.25 in (6.4 mm), C = 6 ft (1.83 m)

α	L(m) 25	50	100	150	200
0.0025	0.0011167	0.0015792	0.0022334	0.0025000	0.0025000
0.0033	0.0012894	0.0018235	0.0025789	0.0031585	0.0033333
0.0050	0.0015792	0.0022334	0.0031585	0.0038683	0.0044668
0.0100	0.0022334	0.0031585	0.0044668	0.0054706	0.0063170
0.0200	0.0031585	0.0044668	0.0063170	0.0077367	0.0089335

TABLE 4–Vb Maximum Pipe Strain for a Ramp pattern of Longitudinal PGD Using the Simplified Model.
ϕ = 30 in (76.2 cm), t = 0.25 in (6.4 mm), C = 6 ft (1.83 m)

α	L(m) 25	50	100	150	200
0.0025	1.130	0.840	1.320	0.507	0.009
0.0033	0.764	0.515	0.508	1.207	0.196
0.0050	0.456	0.281	0.211	0.227	0.354
0.0100	0.200	0.114	0.070	0.057	0.053
0.0200	0.092	0.050	0.029	0.022	0.019

TABLE 4–Vc Percent Difference in Maximum Pipe Strain Between the Complete and Simplified Models.
ϕ = 30 in (76.2 cm), t = 0.25 in (6.4 mm), C = 6 ft (1.83 m)

α	L(m) 25	50	100	150	200
0.0025	0.0011490	0.0016326	0.0022763	0.0024873	0.0024995
0.0033	0.0013358	0.0018972	0.0026806	0.0032081	0.0033275
0.0050	0.0016453	0.0023340	0.0033044	0.0040441	0.0046472
0.0100	0.0023377	0.0033110	0.0046861	0.0057405	0.0066289
0.0200	0.0033124	0.0046879	0.0066322	0.0081238	0.0093812

TABLE 4–VIa Maximum Pipe Strain for a Ramp pattern of Longitudinal PGD Using the Complete Soil–Pipeline Interface Model.
ϕ = 48 in (122 cm), t = 0.25 in (6.4 mm), C = 6 ft (1.83 m)

α	L(m) 25	50	100	150	200
0.0025	0.0011730	0.0016589	0.0023461	0.0025000	0.0025000
0.0033	0.0013545	0.0019155	0.0027090	0.0033178	0.0033333
0.0050	0.0016589	0.0023461	0.0033178	0.0040635	0.0046921
0.0100	0.0023461	0.0033178	0.0046921	0.0057466	0.0066357
0.0200	0.0033178	0.0046921	0.0066357	0.0081270	0.0093842

TABLE 4–VIb Maximum Pipe Strain for a Ramp pattern of Longitudinal PGD Using the Simplified Model.
ϕ = 48 in (122 cm), t = 0.25 in (6.4 mm), C = 6 ft (1.83 m)

α	L(m) 25	50	100	150	200
0.0025	2.090	1.613	3.066	0.510	0.021
0.0033	1.400	0.967	1.060	3.421	0.177
0.0050	0.827	0.518	0.406	0.480	0.967
0.0100	0.360	0.206	0.129	0.107	0.102
0.0200	0.165	0.090	0.051	0.039	0.033

TABLE 4–VIc Percent Difference in Maximum Pipe Strain Between the Complete and Simplified Models.
ϕ = 48 in (122 cm), t = 0.25 in (6.4 mm), C = 6 ft (1.83 m)

	L(m)				
α	25	50	100	150	200
0.0025	0.0012698	0.0017973	0.0024580	0.0024999	0.0025000
0.0033	0.0014696	0.0020806	0.0029370	0.0033290	0.0033333
0.0050	0.0018032	0.0025523	0.0036102	0.0044178	0.0049753
0.0100	0.0025538	0.0036132	0.0051110	0.0062600	0.0072283
0.0200	0.0036137	0.0051117	0.0072299	0.0088549	0.0102246

TABLE 4–VIIa Maximum Pipe Strain for a Ramp pattern of Longitudinal PGD Using the Complete Soil–Pipeline Interface Model.
ϕ = 12 in (30.5 cm), t = 0.25 in (6.4 mm), C = 9 ft (2.74 m)

	L(m)				
α	25	50	100	150	200
0.0025	0.0012783	0.0018078	0.0025000	0.0025000	0.0025000
0.0033	0.0014760	0.0020874	0.0029521	0.0033333	0.0033333
0.0050	0.0018078	0.0025566	0.0036155	0.0044281	0.0050000
0.0100	0.0025566	0.0036155	0.0051131	0.0062623	0.0072310
0.0200	0.0036155	0.0051131	0.0072310	0.0088562	0.0102262

TABLE 4–VIIb Maximum Pipe Strain for a Ramp pattern of Longitudinal PGD Using the Simplified Model.
ϕ = 12 in (30.5 cm), t = 0.25 in (6.4 mm), C = 9 ft (2.74 m)

	L(m)				
α	25	50	100	150	200
0.0025	0.668	0.583	1.708	0.003	0.000
0.0033	0.439	0.326	0.514	0.132	0.000
0.0050	0.255	0.167	0.147	0.233	0.496
0.0100	0.110	0.064	0.042	0.036	0.038
0.0200	0.050	0.027	0.016	0.014	0.016

TABLE 4–VIIc Percent Difference in Maximum Pipe Strain Between the Complete and Simplified Models.
ϕ = 12 in (30.5 cm), t = 0.25 in (6.4 mm), C = 9 ft (2.74 m)

α	L(m) 25	50	100	150	200
0.0025	0.0013032	0.0018462	0.0024489	0.0024991	0.0025000
0.0033	0.0015146	0.0021481	0.0030144	0.0033232	0.0033332
0.0050	0.0018646	0.0026432	0.0037392	0.0045615	0.0049792
0.0100	0.0026476	0.0037489	0.0053049	0.0064980	0.0075028
0.0200	0.0037504	0.0053071	0.0075077	0.0091960	0.0106191

TABLE 4–VIIIa Maximum Pipe Strain for a Ramp pattern of Longitudinal PGD Using the Complete Soil–Pipeline Interface Model.
ϕ = 30 in (76.2 cm), t = 0.25 in (6.4 mm), C = 9 ft (2.74 m)

α	L(m) 25	50	100	150	200
0.0025	0.0013278	0.0018778	0.0025000	0.0025000	0.0025000
0.0033	0.0015332	0.0021683	0.0030664	0.0033333	0.0033333
0.0050	0.0018778	0.0026556	0.0037555	0.0045996	0.0050000
0.0100	0.0026556	0.0037555	0.0053111	0.0065048	0.0075110
0.0200	0.0037555	0.0053111	0.0075110	0.0091991	0.0106222

TABLE 4–VIIIb Maximum Pipe Strain for a Ramp pattern of Longitudinal PGD Using the Simplified Model.
ϕ = 30 in (76.2 cm), t = 0.25 in (6.4 mm), C = 9 ft (2.74 m)

α	L(m) 25	50	100	150	200
0.0025	1.883	1.711	2.087	0.038	0.001
0.0033	1.228	0.937	1.724	0.303	0.006
0.0050	0.707	0.469	0.437	0.834	0.418
0.0100	0.300	0.176	0.117	0.105	0.110
0.0200	0.135	0.075	0.044	0.034	0.029

TABLE 4–VIIIc Percent Difference in Maximum Pipe Strain for Uniform Strain PGD Between the Complete and Simplified Models.
ϕ = 30 in (76.2 cm), t = 0.25 in (6.4 mm), C = 9 ft (2.74 m)

α	L(m) 25	50	100	150	200
0.0025	0.0013306	0.0018854	0.0024424	0.0024975	0.0024999
0.0033	0.0015543	0.0022084	0.0030681	0.0033193	0.0033327
0.0050	0.0019213	0.0027281	0.0038584	0.0046754	0.0049807
0.0100	0.0027367	0.0038785	0.0054905	0.0067256	0.0077646
0.0200	0.0038814	0.0054948	0.0077750	0.0095240	0.0109982

TABLE 4–IXa Maximum Pipe Strain for a Ramp pattern of Longitudinal PGD Using the Complete Soil–Pipeline Interface Model.
ϕ = 48 in (122 cm), t = 0.25 in (6.4 mm), C = 9 ft (2.74 m)

α	L(m) 25	50	100	150	200
0.0025	0.0013755	0.0019452	0.0025000	0.0025000	0.0025000
0.0033	0.0015883	0.0022462	0.0031766	0.0033333	0.0033333
0.0050	0.0019452	0.0027510	0.0038905	0.0047649	0.0050000
0.0100	0.0027510	0.0038905	0.0055020	0.0067385	0.0077810
0.0200	0.0038905	0.0055020	0.0077810	0.0095297	0.0110040

TABLE 4–IXb Maximum Pipe Strain for a Ramp pattern of Longitudinal PGD Using the Simplified Model.
ϕ = 48 in (122 cm), t = 0.25 in (6.4 mm), C = 9 ft (2.74 m)

α	L(m) 25	50	100	150	200
0.0025	3.375	3.174	2.358	0.098	0.004
0.0033	2.185	1.712	3.535	0.422	0.018
0.0050	1.246	0.839	0.833	1.913	0.387
0.0100	0.523	0.309	0.210	0.192	0.211
0.0200	0.235	0.130	0.077	0.060	0.052

TABLE 4–IXc Percent Difference in Maximum Pipe Strain Between the Complete and Simplified Models.
ϕ = 48 in (122 cm), t = 0.25 in (6.4 mm), C = 9 ft (2.74 m)

α	L(m) 25	50	100	150	200
0.0025	0.0005478	0.0007752	0.0010967	0.0013433	0.0015512
0.0033	0.0006328	0.0008954	0.0012665	0.0015512	0.0017914
0.0050	0.0007753	0.0010967	0.0015511	0.0018995	0.0021942
0.0100	0.0010969	0.0015514	0.0021942	0.0026873	0.0031029
0.0200	0.0015515	0.0021810	0.0030834	0.0037739	0.0043543

TABLE 4–Xa Maximum Pipe Strain for a Ramp pattern of Longitudinal PGD Using the Complete Soil–Pipeline Interface Model.
ϕ = 12 in (30.5 cm), t = 0.50 in (12.7 mm), C = 3 ft (0.91 m)

α	L(m) 25	50	100	150	200
0.0025	0.0005486	0.0007759	0.0010973	0.0013439	0.0015518
0.0033	0.0006335	0.0008959	0.0012670	0.0015518	0.0017918
0.0050	0.0007759	0.0010973	0.0015518	0.0019005	0.0021945
0.0100	0.0010973	0.0015518	0.0021945	0.0026877	0.0031035
0.0200	0.0015518	0.0021945	0.0031035	0.0038010	0.0043891

TABLE 4–Xb Maximum Pipe Strain for a Ramp pattern of Longitudinal PGD Using the Simplified Model.
ϕ = 12 in (30.5 cm), t = 0.50 in (12.7 mm), C = 3 ft (0.91 m)

α	L(m) 25	50	100	150	200
0.0025	0.154	0.087	0.053	0.044	0.040
0.0033	0.111	0.062	0.039	0.037	0.024
0.0050	0.077	0.047	0.042	0.055	0.013
0.0100	0.036	0.021	0.015	0.016	0.019
0.0200	0.017	0.621	0.655	0.721	0.798

TABLE 4–Xc Percent Difference in Maximum Pipe Strain Between the Complete and Simplified Models.
ϕ = 12 in (30.5 cm), t = 0.50 in (12.7 mm), C = 3 ft (0.91 m)

α	L(m) 25	50	100	150	200
0.0025	0.0006017	0.0008526	0.0012070	0.0014787	0.0017075
0.0033	0.0006957	0.0009853	0.0013945	0.0017084	0.0019729
0.0050	0.0008531	0.0012077	0.0017088	0.0020932	0.0024172
0.0100	0.0012079	0.0017090	0.0024175	0.0029611	0.0034193
0.0200	0.0017091	0.0024176	0.0034795	0.0041881	0.0048202

TABLE 4–XIa Maximum Pipe Strain for a Ramp pattern of Longitudinal PGD Using the Complete Soil–Pipeline Interface Model.
ϕ = 30 in (76.2 cm), t = 0.50 in (12.7 mm), C = 3 ft (0.91 m)

α	L(m) 25	50	100	150	200
0.0025	0.0006046	0.0008550	0.0012091	0.0014809	0.0017100
0.0033	0.0006981	0.0009873	0.0013962	0.0017100	0.0019745
0.0050	0.0008550	0.0012091	0.0017100	0.0020943	0.0024183
0.0100	0.0012091	0.0017100	0.0024183	0.0029618	0.0034199
0.0200	0.0017100	0.0024183	0.0034199	0.0041886	0.0048365

TABLE 4–XIb Maximum Pipe Strain for a Ramp pattern of Longitudinal PGD Using the Simplified Model.
ϕ = 30 in (76.2 cm), t = 0.50 in (12.7 mm), C = 3 ft (0.91 m)

α	L(m) 25	50	100	150	200
0.0025	0.483	0.277	0.176	0.149	0.144
0.0033	0.347	0.194	0.118	0.093	0.084
0.0050	0.220	0.121	0.071	0.052	0.044
0.0100	0.104	0.055	0.031	0.023	0.019
0.0200	0.050	0.026	0.014	0.010	0.339

TABLE 4–XIc Percent Difference in Maximum Pipe Strain Between the Complete and Simplified Models.
ϕ = 30 in (76.2 cm), t = 0.50 in (12.7 mm), C = 3 ft (0.91 m)

α	L(m) 25	50	100	150	200
0.0025	0.0006496	0.0009223	0.0013068	0.0016011	0.0018486
0.0033	0.0007521	0.0010668	0.0015108	0.0018511	0.0021378
0.0050	0.0009235	0.0013084	0.0018522	0.0022692	0.0026206
0.0100	0.0013089	0.0018528	0.0026214	0.0032111	0.0037081
0.0200	0.0018530	0.0026217	0.0037085	0.0045423	0.0052452

TABLE 4–XIIa Maximum Pipe Strain for a Ramp pattern of Longitudinal PGD Using the Complete Soil–Pipeline Interface Model.
ϕ = 48 in (122 cm), t = 0.50 in (12.7 mm), C = 3 ft (0.91 m)

α	L(m) 25	50	100	150	200
0.0025	0.0006557	0.0009274	0.0013115	0.0016062	0.0018541
0.0033	0.0007572	0.0010708	0.0015114	0.0018547	0.0021416
0.0050	0.0009274	0.0013115	0.0018547	0.0022716	0.0026230
0.0100	0.0013115	0.0018547	0.0026230	0.0032125	0.0037094
0.0200	0.0018547	0.0026230	0.0037094	0.0045431	0.0052459

TABLE 4–XIIb Maximum Pipe Strain for a Ramp pattern of Longitudinal PGD Using the Simplified Model.
ϕ = 48 in (122 cm), t = 0.50 in (12.7 mm), C = 3 ft (0.91 m)

α	L(m) 25	50	100	150	200
0.0025	0.939	0.547	0.361	0.319	0.330
0.0033	0.670	0.380	0.236	0.193	0.180
0.0050	0.423	0.233	0.136	0.105	0.090
0.0100	0.198	0.105	0.058	0.043	0.036
0.0200	0.095	0.049	0.026	0.019	0.015

TABLE 4–XIIc Percent Difference in Maximum Pipe Strain Between the Complete and Simplified Models.
ϕ = 48 in (122 cm), t = 0.50 in (12.7 mm), C = 3 ft (0.91 m)

α	L(m) 25	50	100	150	200
0.0025	0.0007453	0.0010553	0.0014933	0.0018289	0.0021109
0.0033	0.0008614	0.0012193	0.0017252	0.0021131	0.0024400
0.0050	0.0010559	0.0014941	0.0021137	0.0025890	0.0029896
0.0100	0.0014943	0.0021139	0.0029898	0.0036616	0.0042276
0.0200	0.0021140	0.0029901	0.0042290	0.0051795	0.0059807

TABLE 4–XIIIa Maximum Pipe Strain for a Ramp pattern of Longitudinal PGD Using the Complete Soil–Pipeline Interface Model.
ϕ = 12 in (30.5 cm), t = 0.50 in (12.7 mm), C = 6 ft (1.83 m)

α	L(m) 25	50	100	150	200
0.0025	0.0007477	0.0010574	0.0014953	0.0018314	0.0021147
0.0033	0.0008633	0.0012209	0.0017267	0.0021147	0.0024419
0.0050	0.0010574	0.0014953	0.0021147	0.0025900	0.0029906
0.0100	0.0014953	0.0021147	0.0029906	0.0036628	0.0042294
0.0200	0.0021147	0.0029906	0.0042294	0.0051800	0.0059813

TABLE 4–XIIIb Maximum Pipe Strain for a Ramp pattern of Longitudinal PGD Using the Simplified Model.
ϕ = 12 in (30.5 cm), t = 0.50 in (12.7 mm), C = 6 ft (1.83 m)

α	L(m) 25	50	100	150	200
0.0025	0.319	0.193	0.139	0.138	0.179
0.0033	0.226	0.132	0.087	0.076	0.078
0.0050	0.141	0.079	0.048	0.039	0.035
0.0100	0.068	0.039	0.028	0.032	0.044
0.0200	0.032	0.017	0.011	0.010	0.010

TABLE 4–XIIIc Percent Difference in Maximum Pipe Strain Between the Complete and Simplified Models.
ϕ = 12 in (30.5 cm), t = 0.50 in (12.7 mm), C = 6 ft (1.83 m)

α	L(m) 25	50	100	150	200
0.0025	0.0007825	0.0011104	0.0015726	0.0019255	0.0022181
0.0033	0.0009059	0.0012845	0.0018189	0.0022281	0.0025723
0.0050	0.0011122	0.0015757	0.0022302	0.0027322	0.0031552
0.0100	0.0015763	0.0022311	0.0031567	0.0038667	0.0044651
0.0200	0.0022314	0.0031570	0.0044656	0.0054697	0.0063160

TABLE 4–XIVa Maximum Pipe Strain for a Ramp pattern of PGD using the Complete Soil–Pipeline Interface Model.
ϕ = 30 in (76.2 cm), t = 0.50 in (12.7 mm), C = 6 ft (1.83 m)

α	L(m) 25	50	100	150	200
0.0025	0.0007896	0.0011167	0.0015792	0.0019342	0.0022334
0.0033	0.0009118	0.0012894	0.0018235	0.0022334	0.0025789
0.0050	0.0011167	0.0015792	0.0022334	0.0027353	0.0031585
0.0100	0.0015792	0.0022334	0.0031585	0.0038683	0.0044668
0.0200	0.0022334	0.0031585	0.0044668	0.0054706	0.0063170

TABLE 4–XIVb Maximum Pipe Strain for a Ramp pattern of Longitudinal PGD using the Simplified Model.
ϕ = 30 in (76.2 cm), t = 0.50 in (12.7 mm), C = 6 ft (1.83 m)

α	L(m) 25	50	100	150	200
0.0025	0.916	0.563	0.421	0.453	0.690
0.0033	0.646	0.381	0.257	0.235	0.256
0.0050	0.402	0.228	0.140	0.114	0.105
0.0100	0.185	0.100	0.057	0.043	0.037
0.0200	0.087	0.046	0.025	0.018	0.014

TABLE 4–XIVc Percent Difference in Maximum Pipe Strain Between the Complete and Simplified Models.
ϕ = 30 in (76.2 cm), t = 0.50 in (12.7 mm), C = 6 ft (1.83 m)

α	L(m) 25	50	100	150	200
0.0025	0.0008159	0.0011610	0.0016456	0.0020127	0.0023056
0.0033	0.0009467	0.0013451	0.0019063	0.0023353	0.0026945
0.0050	0.0011646	0.0016521	0.0023400	0.0028672	0.0033111
0.0100	0.0016535	0.0023419	0.0033144	0.0040604	0.0046891
0.0200	0.0023424	0.0033151	0.0046900	0.0057448	0.0066339

TABLE 4–XVa Maximum Pipe Strain for a Ramp pattern of Longitudinal PGD Using the Complete Soil–Pipeline Interface Model.
ϕ = 48 in (122 cm), t = 0.50 in (12.7 mm), C = 6 ft (1.83 m)

α	L(m) 25	50	100	150	200
0.0025	0.0008295	0.0011730	0.0016589	0.0020317	0.0023461
0.0033	0.0009578	0.0013545	0.0019155	0.0023461	0.0027090
0.0050	0.0011730	0.0016589	0.0023461	0.0028733	0.0033178
0.0100	0.0016589	0.0023461	0.0033178	0.0040635	0.0046921
0.0200	0.0023461	0.0033178	0.0046921	0.0057466	0.0066357

TABLE 4–XVb Maximum Pipe Strain for a Ramp pattern of Longitudinal PGD Using the Simplified Model.
ϕ = 48 in (122 cm), t = 0.50 in (12.7 mm), C = 6 ft (1.83 m)

α	L(m) 25	50	100	150	200
0.0025	1.667	1.039	0.810	0.946	1.755
0.0033	1.168	0.696	0.483	0.460	0.539
0.0050	0.722	0.412	0.259	0.215	0.203
0.0100	0.330	0.179	0.103	0.077	0.065
0.0200	0.156	0.082	0.045	0.032	0.026

TABLE 4–XVc Percent Difference in Maximum Pipe Strain Between the Complete and Simplified Models.
ϕ = 48 in (122 cm), t = 0.50 in (12.7 mm), C = 6 ft (1.83 m)

	L(m)				
α	25	50	100	150	200
0.0025	0.0008993	0.0012740	0.0018025	0.0022039	0.0024761
0.0033	0.0010400	0.0014728	0.0020840	0.0025521	0.0029444
0.0050	0.0012755	0.0018055	0.0025544	0.0031289	0.0036129
0.0100	0.0018060	0.0025552	0.0036143	0.0044269	0.0051117
0.0200	0.0025554	0.0036146	0.0051124	0.0062616	0.0072304

TABLE 4–XVIa Maximum Pipe Strain for a Ramp pattern of Longitudinal PGD Using the Complete Soil–Pipeline Interface Model.
ϕ = 12 in (30.5 cm), t = 0.50 in (12.7 mm), C = 9 ft (2.74 m)

	L(m)				
α	25	50	100	150	200
0.0025	0.0009039	0.0012783	0.0018078	0.0022140	0.0025000
0.0033	0.0010437	0.0014760	0.0020874	0.0025566	0.0029521
0.0050	0.0012783	0.0018078	0.0025566	0.0031311	0.0036155
0.0100	0.0018078	0.0025566	0.0036155	0.0044281	0.0051131
0.0200	0.0025566	0.0036155	0.0051131	0.0062623	0.0072310

TABLE 4–XVIb Maximum Pipe Strain for a Ramp pattern of Longitudinal PGD Using the Simplified Model.
ϕ = 12 in (30.5 cm), t = 0.50 in (12.7 mm), C = 9 ft (2.74 m)

	L(m)				
α	25	50	100	150	200
0.0025	0.512	0.333	0.293	0.459	0.965
0.0033	0.357	0.219	0.163	0.174	0.262
0.0050	0.219	0.128	0.083	0.073	0.073
0.0100	0.099	0.055	0.032	0.027	0.028
0.0200	0.047	0.025	0.014	0.010	0.008

TABLE 4–XVIc Percent Difference in Maximum Pipe Strain Between the Complete and Simplified Models.
ϕ = 12 in (30.5 cm), t = 0.50 in (12.7 mm), C = 9 ft (2.74 m)

α	L(m) 25	50	100	150	200
0.0025	0.0009257	0.0013154	0.0018616	0.0022645	0.0024750
0.0033	0.0010735	0.0015239	0.0021581	0.0026415	0.0030381
0.0050	0.0013198	0.0018712	0.0026494	0.0032456	0.0037473
0.0100	0.0018727	0.0026516	0.0037522	0.0045964	0.0053080
0.0200	0.0026521	0.0037529	0.0053088	0.0065022	0.0075079

TABLE 4–XVIIa Maximum Pipe Strain for a Ramp pattern of PGD using the Complete Soil–Pipeline Interface Model.
ϕ = 30 in (76.2 cm), t = 0.50 in (12.7 mm), C = 9 ft (2.74 m)

α	L(m) 25	50	100	150	200
0.0025	0.0009389	0.0013278	0.0018778	0.0022998	0.0025000
0.0033	0.0010841	0.0015332	0.0021683	0.0026556	0.0030664
0.0050	0.0013278	0.0018778	0.0026556	0.0032524	0.0037555
0.0100	0.0018778	0.0026556	0.0037555	0.0045996	0.0053111
0.0200	0.0026556	0.0037555	0.0053111	0.0065048	0.0075110

TABLE 4–XVIIb Maximum Pipe Strain for a Ramp pattern of Longitudinal PGD using the Simplified Model.
ϕ = 30 in (76.2 cm), t = 0.50 in (12.7 mm), C = 9 ft (2.74 m)

α	L(m) 25	50	100	150	200
0.0025	1.423	0.939	0.868	1.556	1.010
0.0033	0.985	0.612	0.470	0.532	0.929
0.0050	0.602	0.353	0.234	0.209	0.220
0.0100	0.271	0.150	0.088	0.068	0.059
0.0200	0.129	0.071	0.044	0.039	0.042

TABLE 4–XVIIc Percent Difference in Maximum Pipe Strain Between the Complete and Simplified Models.
ϕ = 30 in (76.2 cm), t = 0.50 in (12.7 mm), C = 9 ft (2.74 m)

α	L(m) 25	50	100	150	200
0.0025	0.0009487	0.0013528	0.0019139	0.0023076	0.0024740
0.0033	0.0011040	0.0015712	0.0022270	0.0027227	0.0031113
0.0050	0.0013612	0.0019333	0.0027395	0.0033564	0.0038742
0.0100	0.0019361	0.0027438	0.0038845	0.0047592	0.0054962
0.0200	0.0027450	0.0038859	0.0054983	0.0067351	0.0077776

TABLE 4–XVIIIa Maximum Pipe Strain for a Ramp pattern of Longitudinal PGD Using the Complete Soil–Pipeline Interface Model.
ϕ = 48 in (122 cm), t = 0.50 in (12.7 mm), C = 9 ft (2.74 m)

α	L(m) 25	50	100	150	200
0.0025	0.0009726	0.0013755	0.0019452	0.0023824	0.0025000
0.0033	0.0011231	0.0015883	0.0022462	0.0027510	0.0031766
0.0050	0.0013755	0.0019452	0.0027510	0.0033693	0.0038905
0.0100	0.0019452	0.0027510	0.0038905	0.0047649	0.0055020
0.0200	0.0027510	0.0038905	0.0055020	0.0067385	0.0077810

TABLE 4–XVIIIb Maximum Pipe Strain for a Ramp pattern of Longitudinal PGD Using the Simplified Model.
ϕ = 48 in (122 cm), t = 0.50 in (12.7 mm), C = 9 ft (2.74 m)

α	L(m) 25	50	100	150	200
0.0025	2.519	1.681	1.636	3.243	1.049
0.0033	1.734	1.086	0.861	1.038	2.098
0.0050	1.052	1.620	0.419	0.384	0.420
0.0100	0.471	0.261	0.154	0.120	0.105
0.0200	0.219	0.118	0.066	0.050	0.044

TABLE 4–XVIIIc Percent Difference in Maximum Pipe Strain Between the Complete and Simplified Models.
ϕ = 48 in (122 cm), t = 0.50 in (12.7 mm), C = 9 ft (2.74 m)

α	L(m) 25	50	100	150	200
0.0025	0.0004473	0.0006330	0.0008955	0.0010969	0.0012666
0.0033	0.0005167	0.0007311	0.0010342	0.0012667	0.0014626
0.0050	0.0006330	0.0008955	0.0012666	0.0015512	0.0017911
0.0100	0.0008956	0.0012668	0.0017916	0.0021943	0.0025337
0.0200	0.0012668	0.0017806	0.0025183	0.0030834	0.0035589

TABLE 4–XIXa Maximum Pipe Strain for a Ramp pattern of Longitudinal PGD Using the Complete Soil–Pipeline Interface Model.
ϕ = 12 in (30.5 cm), t = 0.75 in (19.1 mm), C = 3 ft (0.91 m)

α	L(m) 25	50	100	150	200
0.0025	0.0004480	0.0006335	0.0008959	0.0010973	0.0012670
0.0033	0.0005173	0.0007315	0.0010345	0.0012670	0.0014630
0.0050	0.0006335	0.0008959	0.0012670	0.0015518	0.0017918
0.0100	0.0008959	0.0012670	0.0017918	0.0021945	0.0025340
0.0200	0.0012670	0.0017918	0.0025340	0.0031035	0.0035837

TABLE 4–XIXb Maximum Pipe Strain for a Ramp pattern of Longitudinal PGD Using the Simplified Model.
ϕ = 12 in (30.5 cm), t = 0.75 in (19.1 mm), C = 3 ft (0.91 m)

α	L(m) 25	50	100	150	200
0.0025	0.146	0.080	0.047	0.036	0.031
0.0033	0.107	0.058	0.034	0.027	0.026
0.0050	0.073	0.043	0.032	0.035	0.043
0.0100	0.035	0.020	0.013	0.012	0.013
0.0200	0.016	0.633	0.623	0.653	0.696

TABLE 4–XIXc Percent Difference in Maximum Pipe Strain Between the Complete and Simplified Models.
ϕ = 12 in (30.5 cm), t = 0.75 in (19.1 mm), C = 3 ft (0.91 m)

α	L(m) 25	50	100	150	200
0.0025	0.0004914	0.0006963	0.0009858	0.0012077	0.0013947
0.0033	0.0005681	0.0008046	0.0011388	0.0013951	0.0016111
0.0050	0.0006966	0.0009861	0.0013953	0.0017091	0.0019737
0.0100	0.0009863	0.0013954	0.0019739	0.0024178	0.0027919
0.0200	0.0013955	0.0019740	0.0027920	0.0034108	0.0039377

TABLE 4–XXa Maximum Pipe Strain for a Ramp pattern of PGD using the Complete Soil–Pipeline Interface Model.
ϕ = 30 in (76.2 cm), t = 0.75 in (19.1 mm), C = 3 ft (0.91 m)

α	L(m) 25	50	100	150	200
0.0025	0.0004936	0.0006981	0.0009873	0.0012091	0.0013962
0.0033	0.0005700	0.0008061	0.0011400	0.0013962	0.0016122
0.0050	0.0006981	0.0009873	0.0013962	0.0017100	0.0019745
0.0100	0.0009873	0.0013962	0.0019745	0.0024183	0.0027924
0.0200	0.0013962	0.0019745	0.0027924	0.0034199	0.0039490

TABLE 4–XXb Maximum Pipe Strain for a Ramp pattern of Longitudinal PGD Using the Simplified Model.
ϕ = 30 in (76.2 cm), t = 0.75 in (19.1 mm), C = 3 ft (0.91 m)

α	L(m) 25	50	100	150	200
0.0025	0.456	0.253	0.151	0.118	0.103
0.0033	0.331	0.180	0.104	0.079	0.067
0.0050	0.212	0.114	0.064	0.048	0.042
0.0100	0.101	0.053	0.029	0.021	0.017
0.0200	0.049	0.025	0.013	0.268	0.288

TABLE 4–XXc Percent Difference in Maximum Pipe Strain Between the Complete and Simplified Models.
ϕ = 30 in (76.2 cm), t = 0.75 in (19.1 mm), C = 3 ft (0.91 m)

α	L(m) 25	50	100	150	200
0.0025	0.0005307	0.0007535	0.0010676	0.0013083	0.0015111
0.0033	0.0006143	0.0008713	0.0012340	0.0015120	0.0017463
0.0050	0.0007541	0.0010685	0.0015125	0.0018530	0.0021400
0.0100	0.0010688	0.0015128	0.0021405	0.0026219	0.0030278
0.0200	0.0015130	0.0021406	0.0030280	0.0037088	0.0042827

TABLE 4–XXIa Maximum Pipe Strain for a Ramp pattern of Longitudinal PGD Using the Complete Soil–Pipeline Interface Model.
ϕ = 48 in (122 cm), t = 0.75 in (19.1 mm), C = 3 ft (0.91 m)

α	L(m) 25	50	100	150	200
0.0025	0.0005354	0.0007572	0.0010708	0.0013115	0.0015144
0.0033	0.0006182	0.0008743	0.0012365	0.0015144	0.0017486
0.0050	0.0007572	0.0010708	0.0015144	0.0018547	0.0021416
0.0100	0.0010708	0.0015144	0.0021416	0.0026230	0.0030287
0.0200	0.0015144	0.0021416	0.0030287	0.0037094	0.0042833

TABLE 4–XXIb Maximum Pipe Strain for a Ramp pattern of Longitudinal PGD Using the Simplified Model.
ϕ = 48 in (122 cm), t = 0.75 in (19.1 mm), C = 3 ft (0.91 m)

α	L(m) 25	50	100	150	200
0.0025	0.881	0.494	0.300	0.240	0.217
0.0033	0.636	0.350	0.205	0.157	0.135
0.0050	0.406	0.219	0.124	0.091	0.075
0.0100	0.192	0.101	0.055	0.039	0.031
0.0200	0.093	0.048	0.025	0.018	0.014

TABLE 4–XXIc Percent Difference in Maximum Pipe Strain Between the Complete and Simplified Models.
ϕ = 48 in (122 cm), t = 0.75 in (19.1 mm), C = 3 ft (0.91 m)

α	L(m) 25	50	100	150	200
0.0025	0.0006087	0.0008619	0.0012196	0.0014939	0.0017251
0.0033	0.0007034	0.0009957	0.0014088	0.0017257	0.0019927
0.0050	0.0008622	0.0012200	0.0017259	0.0021140	0.0024412
0.0100	0.0012201	0.0017260	0.0024413	0.0029900	0.0034525
0.0200	0.0017261	0.0024414	0.0034530	0.0042291	0.0048372

TABLE 4–XXIIa Maximum Pipe Strain for a Ramp pattern of Longitudinal PGD Using the Complete Soil–Pipeline Interface Model.
ϕ = 12 in (30.5 cm), t = 0.75 in (19.1 mm), C = 6 ft (1.83 m)

α	L(m) 25	50	100	150	200
0.0025	0.0006105	0.0008633	0.0012209	0.0014953	0.0017267
0.0033	0.0007049	0.0009969	0.0014098	0.0017267	0.0019938
0.0050	0.0008633	0.0012209	0.0017267	0.0021147	0.0024419
0.0100	0.0012209	0.0017267	0.0024419	0.0029906	0.0034533
0.0200	0.0017267	0.0024419	0.0034533	0.0042294	0.0048837

TABLE 4–XXIIb Maximum Pipe Strain for a Ramp pattern of Longitudinal PGD Using the Simplified Model.
ϕ = 12 in (30.5 cm), t = 0.75 in (19.1 mm), C = 6 ft (1.83 m)

α	L(m) 25	50	100	150	200
0.0025	0.296	0.170	0.109	0.092	0.090
0.0033	0.212	0.120	0.072	0.058	0.052
0.0050	0.135	0.074	0.043	0.032	0.027
0.0100	0.065	0.036	0.023	0.022	0.024
0.0200	0.031	0.017	0.010	0.008	0.961

TABLE 4–XXIIc Percent Difference in Maximum Pipe Strain Between the Complete and Simplified Models.
ϕ = 12 in (30.5 cm), t = 0.75 in (19.1 mm), C = 6 ft (1.83 m)

α	L(m) 25	50	100	150	200
0.0025	0.0006393	0.0009073	0.0012853	0.0015748	0.0018184
0.0033	0.0007400	0.0010492	0.0014858	0.0018204	0.0021023
0.0050	0.0009083	0.0012867	0.0018213	0.0022313	0.0025768
0.0100	0.0012871	0.0018218	0.0025775	0.0031573	0.0036460
0.0200	0.0018220	0.0025777	0.0036462	0.0044660	0.0051571

TABLE 4–XXIIIa Maximum Pipe Strain for a Ramp pattern of PGD using the Complete Soil–Pipeline Interface Model.
ϕ = 30 in (76.2 cm), t = 0.75 in (19.1 mm), C = 6 ft (1.83 m)

α	L(m) 25	50	100	150	200
0.0025	0.0006447	0.0009118	0.0012894	0.0015792	0.0018235
0.0033	0.0007445	0.0010528	0.0014889	0.0018235	0.0021057
0.0050	0.0009118	0.0012894	0.0018235	0.0022334	0.0025789
0.0100	0.0012894	0.0018235	0.0025789	0.0031585	0.0036471
0.0200	0.0018235	0.0025789	0.0036471	0.0044668	0.0051578

TABLE 4–XXIIIb Maximum Pipe Strain for a Ramp pattern of Longitudinal PGD Using the Simplified Model.
ϕ = 30 in (76.2 cm), t = 0.75 in (19.1 mm), C = 6 ft (1.83 m)

α	L(m) 25	50	100	150	200
0.0025	0.845	0.491	0.321	0.281	0.286
0.0033	0.604	0.342	0.211	0.171	0.158
0.0050	0.382	0.210	0.123	0.094	0.080
0.0100	0.179	0.095	0.052	0.038	0.031
0.0200	0.086	0.045	0.024	0.017	0.013

TABLE 4–XXIIIc Percent Difference in Maximum Pipe Strain Between the Complete and Simplified Models.
ϕ = 30 in (76.2 cm), t = 0.75 in (19.1 mm), C = 6 ft (1.83 m)

α	L(m) 25	50	100	150	200
0.0025	0.0006670	0.0009493	0.0013464	0.0016500	0.0019045
0.0033	0.0007736	0.0010991	0.0015580	0.0019094	0.0022052
0.0050	0.0009513	0.0013494	0.0019113	0.0023420	0.0027049
0.0100	0.0013502	0.0019123	0.0027064	0.0033156	0.0038290
0.0200	0.0019126	0.0027068	0.0038295	0.0046907	0.0054167

TABLE 4–XXIVa Maximum Pipe Strain for a Ramp pattern of Longitudinal PGD Using the Complete Soil–Pipeline Interface Model.
ϕ = 48 in (122 cm), t = 0.75 in (19.1 mm), C = 6 ft (1.83 m)

α	L(m) 25	50	100	150	200
0.0025	0.0006772	0.0009578	0.0013545	0.0016589	0.0019155
0.0033	0.0007820	0.0011059	0.0015640	0.0019155	0.0022119
0.0050	0.0009578	0.0013545	0.0019155	0.0023461	0.0027090
0.0100	0.0013545	0.0019155	0.0027090	0.0033178	0.0038311
0.0200	0.0019155	0.0027090	0.0038311	0.0046921	0.0054180

TABLE 4–XXIVb Maximum Pipe Strain for a Ramp pattern of Longitudinal PGD Using the Simplified Model.
ϕ = 48 in (122 cm), t = 0.75 in (19.1 mm), C = 6 ft (1.83 m)

α	L(m) 25	50	100	150	200
0.0025	1.529	0.895	0.599	0.541	0.579
0.0033	1.088	0.619	0.388	0.322	0.305
0.0050	0.684	0.378	0.223	0.172	0.150
0.0100	0.318	0.170	0.094	0.068	0.056
0.0200	0.152	0.079	0.042	0.030	0.024

TABLE 4–XXIVc Percent Difference in Maximum Pipe Strain Between the Complete and Simplified Models.
ϕ = 48 in (122 cm), t = 0.75 in (19.1 mm), C = 6 ft (1.83 m)

	L(m)				
α	25	50	100	150	200
0.0025	0.0007346	0.0010408	0.0014731	0.0018042	0.0020823
0.0033	0.0008494	0.0012029	0.0017022	0.0020852	0.0024077
0.0050	0.0010416	0.0014743	0.0020859	0.0025551	0.0029506
0.0100	0.0014746	0.0020863	0.0029512	0.0036147	0.0041740
0.0200	0.0020865	0.0029514	0.0041694	0.0051050	0.0058926

TABLE 4–XXVa Maximum Pipe Strain for a Ramp pattern of Longitudinal PGD Using the Complete Soil–Pipeline Interface Model.
ϕ = 12 in (30.5 cm), t = 0.75 in (19.1 mm), C = 9 ft (2.74 m)

	L(m)				
α	25	50	100	150	200
0.0025	0.0007380	0.0010437	0.0014760	0.0018078	0.0020874
0.0033	0.0008522	0.0012052	0.0017044	0.0020874	0.0024103
0.0050	0.0010437	0.0014760	0.0020874	0.0025566	0.0029521
0.0100	0.0014760	0.0020874	0.0029521	0.0036155	0.0041748
0.0200	0.0020874	0.0029521	0.0041748	0.0051131	0.0059041

TABLE 4–XXVb Maximum Pipe Strain for a Ramp pattern of Longitudinal PGD Using the Simplified Model.
ϕ = 12 in (30.5 cm), t = 0.75 in (19.1 mm), C = 9 ft (2.74 m)

	L(m)				
α	25	50	100	150	200
0.0025	0.464	0.280	0.199	0.195	0.244
0.0033	0.329	0.192	0.125	0.109	0.110
0.0050	0.206	0.116	0.072	0.056	0.050
0.0100	0.096	0.052	0.029	0.022	0.019
0.0200	0.045	0.024	0.130	0.159	0.196

TABLE 4–XXVc Percent Difference in Maximum Pipe Strain for Between the Complete and Simplified Models.
ϕ = 12 in (30.5 cm), t = 0.75 in (19.1 mm), C = 9 ft (2.74 m)

	L(m)				
α	25	50	100	150	200
0.0025	0.0007569	0.0010757	0.0015245	0.0018669	0.0021512
0.0033	0.0008772	0.0012452	0.0017642	0.0021615	0.0024955
0.0050	0.0010780	0.0015283	0.0021641	0.0026514	0.0030620
0.0100	0.0015292	0.0021652	0.0030639	0.0037533	0.0043344
0.0200	0.0021655	0.0030643	0.0043348	0.0053094	0.0061309

TABLE 4–XXVIa Maximum Pipe Strain for a Ramp pattern of PGD using the Complete Soil–Pipeline Interface Model.
ϕ = 30 in (76.2 cm), t = 0.75 in (19.1 mm), C = 9 ft (2.74 m)

	L(m)				
α	25	50	100	150	200
0.0025	0.0007666	0.0010841	0.0015332	0.0018778	0.0021683
0.0033	0.0008852	0.0012518	0.0017704	0.0021683	0.0025037
0.0050	0.0010841	0.0015332	0.0021683	0.0026556	0.0030664
0.0100	0.0015332	0.0021683	0.0030664	0.0037555	0.0043365
0.0200	0.0021683	0.0030664	0.0043365	0.0053111	0.0061327

TABLE 4–XXVIb Maximum Pipe Strain for a Ramp pattern of Longitudinal PGD Using the Simplified Model.
ϕ = 30 in (76.2 cm), t = 0.75 in (19.1 mm), C = 9 ft (2.74 m)

	L(m)				
α	25	50	100	150	200
0.0025	1.283	0.779	0.567	0.582	0.791
0.0033	0.906	0.530	0.351	0.313	0.329
0.0050	0.564	0.318	0.194	0.156	0.142
0.0100	0.260	0.140	0.079	0.059	0.048
0.0200	0.125	0.067	0.039	0.031	0.029

TABLE 4–XXVIc Percent Difference in Maximum Pipe Strain Between the Complete and Simplified Models.
ϕ = 30 in (76.2 cm), t = 0.75 in (19.1 mm), C = 9 ft (2.74 m)

α	L(m) 25	50	100	150	200
0.0025	0.0007766	0.0011078	0.0015721	0.0019240	0.0022100
0.0033	0.0009027	0.0012849	0.0018225	0.0022333	0.0025775
0.0050	0.0011122	0.0015795	0.0022385	0.0027433	0.0031684
0.0100	0.0015812	0.0022407	0.0031722	0.0038865	0.0044885
0.0200	0.0022414	0.0031730	0.0044896	0.0054995	0.0063508

TABLE 4–XXVIIa Maximum Pipe Strain for a Ramp pattern of Longitudinal PGD Using the Complete Soil–Pipeline Interface Model.
ϕ = 48 in (122 cm), t = 0.75 in (19.1 mm), C = 9 ft (2.74 m)

α	L(m) 25	50	100	150	200
0.0025	0.0007941	0.0011231	0.0015883	0.0019452	0.0022462
0.0033	0.0009170	0.0012968	0.0018340	0.0022462	0.0025937
0.0050	0.0011231	0.0015883	0.0022462	0.0027510	0.0031766
0.0100	0.0015883	0.0022462	0.0031766	0.0038905	0.0044924
0.0200	0.0022462	0.0031766	0.0044924	0.0055020	0.0063532

TABLE 4–XXVIIb Maximum Pipe Strain for a Ramp pattern of Longitudinal PGD Using the Simplified Model.
ϕ = 48 in (122 cm), t = 0.75 in (19.1 mm), C = 9 ft (2.74 m)

α	L(m) 25	50	100	150	200
0.0025	2.260	1.380	1.029	1.103	1.635
0.0033	1.587	0.932	0.629	0.575	0.627
0.0050	0.984	0.555	0.343	0.279	0.258
0.0100	0.451	0.244	0.138	0.103	0.086
0.0200	0.213	0.113	0.062	0.045	0.037

TABLE 4–XXVIIc Percent Difference in Maximum Pipe Strain Between the Complete and Simplified Models.
ϕ = 48 in (122 cm), t = 0.75 in (19.1 mm), C = 9 ft (2.74 m)

SECTION 5
RIGID BLOCK PGD

The axial strain induced in a continuous steel pipeline due to a Rigid Block pattern of longitudinal PGD is determined in this section. As mentioned previously, pipe response to the horizontal component of PGD is determined and any vertical component of ground deformation (i.e. subsidence and heaving) is neglected. It is assumed that the burial depth of the pipeline is constant in and around the PGD zone. Initially the soil–pipeline interface is modeled by the elastic spring–slide model shown in Figure 3–2. The pipeline strain is also determined using a simplified rigid spring–slider model for the soil–pipeline interface as shown in Figure 3–3.

As mentioned previously, the idealized Rigid Block pattern shown in Figure 2–12 corresponds to a mass of soil having length L, moving down a slight incline. There is little or no relative displacement within the soil block which overrides a liquefied layer. It may be an appropriate model for the observed PGD patterns shown in Figure 2–7(j) and 2–7(u).

As noted previously, a coordinate system is established with $x = 0$ at the head of the slide. The assumed ground movement is given, as a function of the axial coordinate x, in Equation 2.5. The maximum tensile strain in the pipe occurs at $x = 0$ while the maximum compressive strain occurs at $x = L$. The problem is anti–symmetric about the point $x = L/2$ where the pipe strain is zero. Results are presented herein for the region $x \leq L/2$. However because of the aforementioned anti–symmetry they apply to $x > L/2$ with a change of sign.

5.1 Elastic Spring–Slider Model

The solution for the elastic spring–slider model of the soil pipeline interface was obtained by dividing the pipeline into three regions as shown in Figure 5–1. In Region I ($x \leq x_a$) and Region III ($x_b \leq x \leq L/2$) the relative displacement between the pipe and soil are small and the soil–pipeline interaction behaves as a linear spring. Region II ($x_a \leq x \leq x_b$) is the slip region where a constant force per unit length, f_m, acts on the pipe. The values of x_a and x_b are not known a priori but are calculated as part of the solution. Note, however, that the magnitude of x_b is always greater than or equal to the magnitude of x_a. This is due to the fact that Region I is infinite in length while Region III is finite.

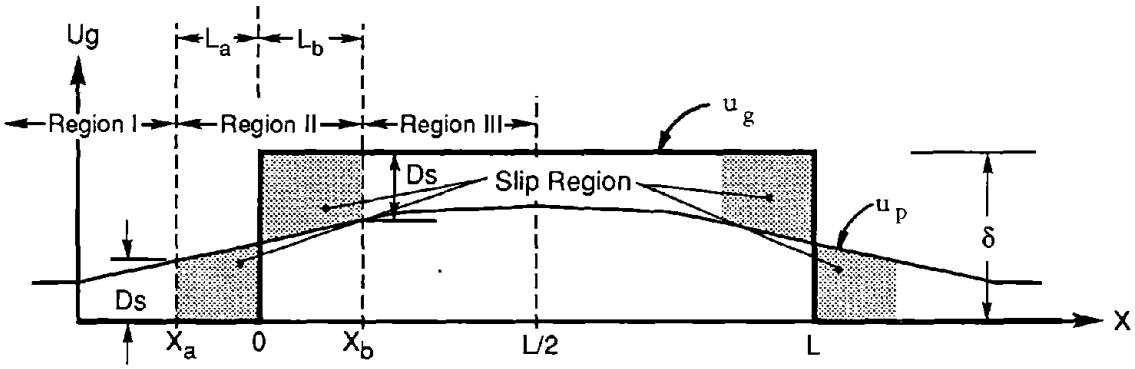

FIGURE 5-1 Model of Pipeline Subjected to Rigid Block PGD.

5.1.1 Region I ($x \leq x_a$)

As noted in the previous section, the soil–pipeline system in Region I can be represented by an equivalent linear spring with spring constant K_a as shown in Figure 4–3. The pipe displacement at $x = x_a$ is equal to D_s, and displacement of the pipe in Region I is:

$$u_p(x) = D_s e^{\beta(x-x_a)} \qquad -\infty \leq x \leq x_a \qquad (5.1)$$

as shown in Section 4.1.1.

5.1.2 Region III ($x_b \leq x \leq L/2$)

Equating the forces acting on a differential length of pipe in Region III and noting that the ground displacement, u_g, equals a constant, δ, we obtain:

$$A(\sigma + d\sigma) = k(u_p(x) - \delta)dx + A\sigma \qquad (5.2)$$

Assuming a linear elastic pipe material the differential equation for Region III becomes:

$$\frac{d^2u_p(x)}{dx^2} - \beta^2 u_p(x) = -\beta^2\delta \qquad (5.3)$$

At the boundary between Region II and III (i.e. $x = x_b$) the relative displacement between the soil and pipe equals D_s. The displacement of the pipeline is therefore equal to the ground displacement, δ, minus the relative displacement, D_s:

$$u_p(x_b) = \delta - D_s \qquad (5.4)$$

At the center of the PGD zone the strain in the pipe is zero by symmetry:

$$\frac{du_p}{dx}(L/2) = 0 \qquad (5.5)$$

The solution to the differential equation (5.3) subjected to the boundary conditions of

equations (5.4) and (5.5) is simply:

$$u_p(x) = -D_s \left[\frac{e^{\beta x}}{e^{\beta x_b} + e^{\beta(L-x_b)}} + \frac{e^{-\beta x}}{e^{-\beta x_b} + e^{-\beta(L-x_b)}} \right] + \delta \tag{5.6}$$

5.1.3 Continuity

The pipe displacements at the beginning and end of Region II are known, as well as the forces on the pipe in the region . Continuity requires that the displacement of the pipe at x_b equals the displacement at x_a plus the stretching over the length $L_a + L_b$. A relation for L_b in terms of L_a can be derived from this requirement:

$$D_s + \frac{K_a D_s (L_b + L_a)}{EA} + \frac{f_m}{2EA}(L_a^2 + 2L_a L_b - L_b^2) = \delta - D_s \tag{5.7}$$

Rearranging yields:

$$L_b^2 - (2L_a + \frac{2}{\beta})L_b - \left[\frac{4}{\beta^2} + \frac{2L_a}{\beta} - \frac{2AE\delta}{f_m} + L_a^2 \right] = 0 \tag{5.8}$$

which can be solved for L_b by noting that equation 5.8 is a quadratic equation in terms of the unknown L_b.

$$L_b = \frac{1}{\beta} + L_a \pm \sqrt{\frac{5}{\beta^2} + \frac{4L_a}{\beta} + 2L_a^2 - \frac{2AE\delta}{f_m}} \tag{5.9}$$

5.1.4 Equilibrium

A second relation can be derived by enforcing equilibrium. The force in the pipe in Region I plus the net force exerted along the pipe in Region II must equal the force in the pipe at the start of Region III:

$$K_a D_s + f_m(L_a - L_b) = EA \frac{du_p}{dx}(L_b) \tag{5.10}$$

where $u_p(L_b)$ is given by equation (5.6). Hence:

$$\frac{K_a D_s}{EA} + \frac{f_m(L_a - L_b)}{EA} = -\beta D_s \left[\frac{e^{\beta L_b}}{e^{\beta L_b} + e^{\beta(L-L_b)}} - \frac{e^{-\beta L_b}}{e^{-\beta L_b} + e^{-\beta(L-L_b)}} \right] \quad (5.11)$$

Note that $K_a D_s = f_m/\beta$. Rearranging and simplifying yields a relation for L_a in terms of L_b.

$$L_a = -\frac{1}{\beta} - \frac{1}{\beta} \left[\frac{e^{\beta(2L_b-L)} - e^{\beta(L-2L_b)}}{2 + e^{\beta(L-2L_b)} + e^{\beta(2L_b-L)}} \right] + L_b \quad (5.12)$$

The length L_b can now be determined by substitution of equation (5.9) into equation (5.12):

$$L_b = \frac{1}{\beta} + [-\frac{1}{\beta} - \frac{1}{\beta} v + L_b] + \sqrt{\frac{5}{\beta^2} + \frac{4L_a}{\beta} + 2L_a^2 - \frac{2AE\delta}{f_m}} \quad (5.13)$$

which reduces to

$$\frac{3}{\beta^2} + \frac{v^2}{\beta^2} - \frac{4vL_b}{\beta} + 2L_b^2 - \frac{2AE\delta}{f_m} = 0 \quad (5.14)$$

where:

$$v = \frac{e^{\beta(2L_b-L)} - e^{\beta(L-2L_b)}}{2 + e^{\beta(L-2L_b)} + e^{\beta(2L_b-L)}} \quad (5.15)$$

The secant method is applied to equation (5.13) to evaluate L_b.

5.1.5 Maximum Pipe Strain

For a Rigid Block pattern of longitudinal PGD, the maximum tensile pipe strain occurs at the head of the slide (i.e. at x=0). This strain can be evaluated from the force in the pipe

at this point. The total force is the force in the pipe at $x = x_a$, which is $K_a D_s$ from Figure 4–3, plus the friction force per unit length acting over the length L_a.

$$\epsilon = (K_a D_s + f_m L_a)/EA \tag{5.16}$$

The length L_a is determined by substituting the value of L_b given by equation 5.13 into equation 5.12.

Tables 5–Ia through 5–XXVIIa present the maximum pipe strain, ϵ, for a Rigid Block pattern of longitudinal PGD evaluated using equation 5.16. In these tables, the soil and pipe properties are the same as for Ramp PGD. That is, unit weight of soil $\gamma = 100$ pcf, coefficient of friction $\mu = 0.75$, pipe diameters, ϕ, of 12, 30 and 48 inches, wall thickness, t, of 1/4, 1/2, and 3/4 inch, and burial depths to the top of the pipe, C, of 3, 6, and 9 feet. In the tables the amount of ground movement δ ranges from 0.1 to 0.7 m, and the length L of the PGD zone ranges from 200 to 800 m. For a fixed amount of ground movement, δ, the maximum pipe strain increases with the block length, L, to a certain value and then is constant for further increases in L. Similarly, for fixed value of the length, L, the pipe strain is an increasing function of the ground displacement, δ, to a certain value and then is constant for further increases in δ. As with Ramp PGD, the pipe strain for Rigid Block PGD is an increasing function of the burial depth and a decreasing function of the pipe wall thickness. It also appears to be an increasing function of the pipe diameter ϕ.

5.2 Rigid Spring/Slider Model

The response of a buried pipeline to Rigid Block PGD is determined herein using the simplified rigid spring/slider model for the soil pipeline interface shown in Figure 3.3. Two possible configurations are shown in Figure 5–2. For both configurations the pipe strain is largest at the head and toe of the PGD zone. At the head, $x = 0$, the strain is tensile. At the toe, $x = L$, the strain is compressive but equal in magnitude to that at the head. In addition the pipe strain is zero at the center of the PGD zone, $x = L/2$. For small length, L, of the PGD zone shown in Figure 5–2(a), there is slippage at the soil pipeline interface over the whole length of the PGD zone but the maximum pipe displacement at the center of the zone is less than the ground movement δ. Since the force in the pipe by symmetry is zero at $x = L/2$, a slip zone of length $L/2$ exists before the head of the slide zone and beyond the toe of the slide zone.

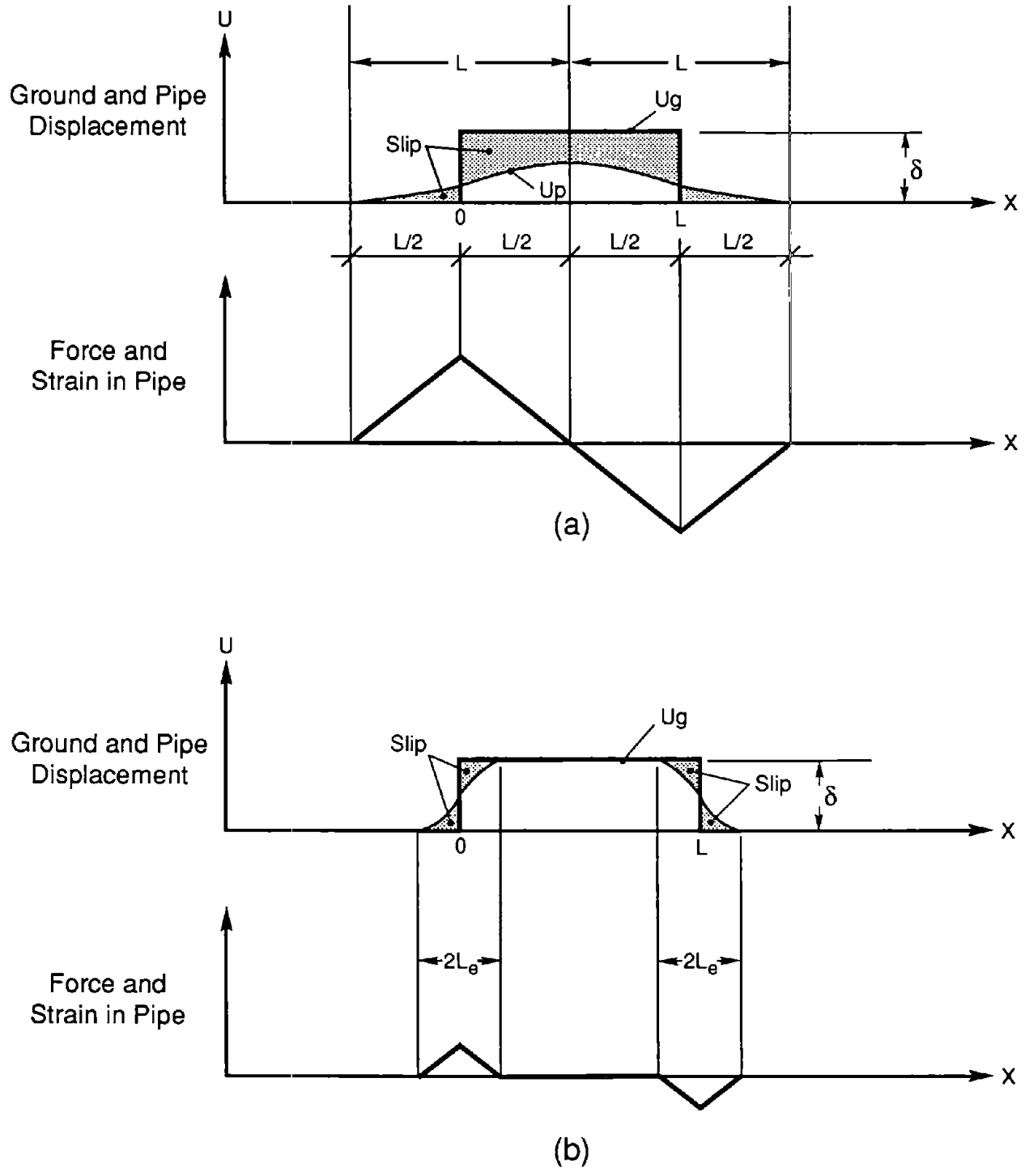

FIGURE 5-2 Simplified Model of Buried Pipe Subjected to Rigid Block PGD.

For large length L of the PGD zone shown in Figure 5–2(b), a slip zone of length L_e exists at either side of both the head and toe. However the pipe displacement matches ground displacement over a region of length $L - 2L_e$ within the PGD zone. Assuming that L is large as shown in Figure 5–2(b), an equation for L_e can be determined by enforcing continuity of the pipe. The displacement due to the stretching of the pipe over the slip region must equal the displacement of the soil, δ, since relative displacement between the soil and pipe are assumed to be zero beyond the slip region. Noting that the length L_e can not exceed L/2, we have

$$\frac{f_m(L_e^2 + L_e^2)}{2EA} = \delta \tag{5.17}$$

and

$$L_e = \sqrt{\frac{AE\delta}{f_m}} \leq L/2 \tag{5.18}$$

The maximum force in the pipe is equal to the force per unit length times L_e. Upon substitution of the constitutive equations, the maximum pipe strain, ϵ, due to Rigid Block PGD is:

$$\epsilon = \sqrt{\frac{f_m \delta}{EA}} \leq \frac{f_m L}{2EA} \tag{5.19}$$

For $L > \sqrt{4\delta EA/f_m}$, the maximum pipe strain is due to friction forces which result in a pipe displacement of δ towards the center of the PGD zone. In this case the pipe strain is a function of δ and Figure 5–2(b) applies.

For $L < \sqrt{4\delta EA/f_m}$, the maximum pipe strain is due to friction forces acting over a distance of L/2 on either side of both the head and toe of the PGD zone. In this case, the pipe strain is a function of L and Figure 5–2(a) applies.

Tables 5–Ib through 5–XXVIIb present results from equation 5.19 for maximum pipe strain using the simplified rigid spring/slider model. Results are given for the same range

of parameters used with the complete elastic spring/slider model which were presented in Table 5–Ia through 5–XXVIIa. Note that equation 5.19 explains the influence of various parameters on the maximum pipe strain which were observed previously in relation to the complete interface model. That is, the maximum pipe strain is always an increasing function of the burial depth, H, and a decreasing function of the wall thickness t.

For a fixed value of δ, the maximum pipe strain is an increasing function of the length of the PGD zone for $L \leq \sqrt{4\delta EA}/f_m$ and is a constant value of $(f_m\delta/EA)^{\frac{1}{2}}$ for larger values of L. Similarly for a fixed value of L, the maximum pipe strain is an increasing function of amount of ground movement for $\delta \leq (L/4EA)^{\frac{1}{2}}$ and is a constant value of $f_mL/2AE$ for larger values of δ. As with Ramp PGD, the maximum pipe strain using the simplified soil pipe interface model is not directly a function of the pipe diameter ϕ. However since Tables 5–I through 5–XXVII are presented in terms of the cover over the top of the pipe, C, a larger pipe diameter results in a larger burial depth $H = C + \phi/2$ and pipe strain is a function of burial depth H.

The simplified model in Figure 5–2(b) for which the maximum pipe strain is $(f_m\delta_g/EA)^{\frac{1}{2}}$, is also applicable to an idealized ground displacement pattern

$$u_g(x) = \begin{cases} 0 & x < 0 \\ \delta & x > 0 \end{cases} \tag{5.20}$$

This corresponds to the situation of zero soil strain on either side of a tensile ground crack of width δ at the head of a very long landslide as shown in Figure 5–3. It is also applicable to the corresponding compression situation of an abrupt relative displacement of δ at the toe of a very long landslide.

5.3 Comparison of Models

Tables 5–Ic through 5–XXVIIc list the percent different in the maximum pipe strain due to Rigid Block PGD evaluated using the complete elastic spring/slider model and the simplified rigid spring/slider model. Note that both models give very similar results and the simplified model is always conservative, predicting maximum pipe strains slightly higher than the complete model. In the cases examined, which correspond to what is felt to be typical conditions, the error between the models does not exceed 1.5 percent.

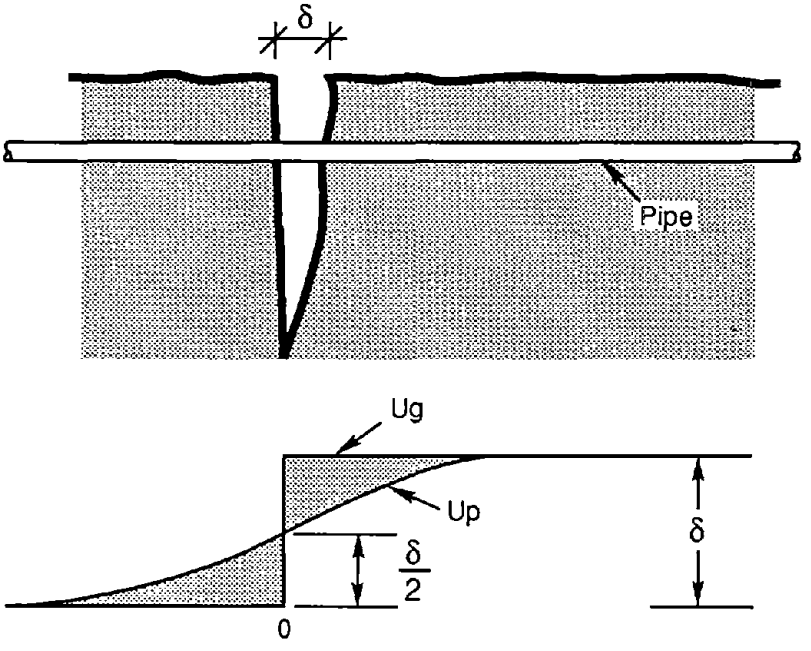

FIGURE 5-3 Simplified Model of a Buried Pipeline at a tensile ground crack of width δ

δ (m)	L(m) 200	400	600	800
0.10	0.0009632	0.0009807	0.0009807	0.0009807
0.20	0.0009632	0.0013874	0.0013874	0.0013874
0.30	0.0009632	0.0016995	0.0016995	0.0016995
0.40	0.0009632	0.0019264	0.0019625	0.0019625
0.50	0.0009632	0.0019264	0.0021942	0.0021942
0.60	0.0009632	0.0019264	0.0024037	0.0024037
0.70	0.0009632	0.0019264	0.0025963	0.0025963

TABLE 5–Ia Maximum Pipe Strain for a Rigid Block pattern of Longitudinal PGD using the Complete Soil–Pipeline Interface Model. ϕ = 12 in (30.5 cm), t = 0.25 in (6.4 mm), C = 3 ft (0.91 m)

δ (m)	L(m) 200	400	600	800
0.10	0.0009632	0.0009814	0.0009814	0.0009814
0.20	0.0009632	0.0013879	0.0013879	0.0013879
0.30	0.0009632	0.0016999	0.0016999	0.0016999
0.40	0.0009632	0.0019264	0.0019629	0.0019629
0.50	0.0009632	0.0019264	0.0021945	0.0021945
0.60	0.0009632	0.0019264	0.0024040	0.0024040
0.70	0.0009632	0.0019264	0.0025966	0.0025966

TABLE 5–Ib Maximum Pipe Strain for a Rigid Block Pattern of Longitudinal PGD Using the Simplified Model. ϕ = 12 in (30.5 cm), t = 0.25 in (6.4 mm), C = 3 ft (0.91 m)

δ (m)	L(m) 200	400	600	800
0.10	0.0000000	0.0750274	0.0750274	0.0750274
0.20	0.0000000	0.0374928	0.0374928	0.0374928
0.30	0.0000000	0.0249906	0.0249905	0.0249905
0.40	0.0000000	0.0000000	0.0187411	0.0187411
0.50	0.0000000	0.0000000	0.0148633	0.0148633
0.60	0.0000000	0.0000000	0.0123949	0.0123949
0.70	0.0000000	0.0000000	0.0106302	0.0106302

TABLE 5–Ic Percent difference in Maximum Pipe Strain between Simplified and Complete Models. ϕ = 12 in (30.5 cm), t = 0.25 in (6.4 mm), C = 3 ft (0.91 m)

δ (m)	L(m) 200	400	600	800
0.10	0.0010790	0.0010790	0.0010790	0.0010790
0.20	0.0011696	0.0015277	0.0015277	0.0015277
0.30	0.0011696	0.0018718	0.0018718	0.0018718
0.40	0.0011696	0.0021617	0.0021617	0.0021617
0.50	0.0011696	0.0023392	0.0024172	0.0024172
0.60	0.0011696	0.0023392	0.0026481	0.0026481
0.70	0.0011696	0.0023392	0.0028604	0.0028604

TABLE 5–IIa Maximum Pipe Strain for a Rigid Block Pattern of Longitudinal PGD Using the Complete Soil–Pipeline Interface Model. ϕ = 30 in (76.2 cm), t = 0.25 in (6.4 mm), C = 3 ft (0.91 m)

δ (m)	L(m) 200	400	600	800
0.10	0.0010815	0.0010815	0.0010815	0.0010815
0.20	0.0011696	0.0015294	0.0015294	0.0015294
0.30	0.0011696	0.0018732	0.0018732	0.0018732
0.40	0.0011696	0.0021630	0.0021630	0.0021630
0.50	0.0011696	0.0023392	0.0024183	0.0024183
0.60	0.0011696	0.0023392	0.0026491	0.0026491
0.70	0.0011696	0.0023392	0.0028613	0.0028613

TABLE 5–IIb Maximum Pipe Strain for a Rigid Block Pattern of Longitudinal PGD Using the Simplified Model. ϕ = 30 in (76.2 cm), t = 0.25 in (6.4 mm), C = 3 ft (0.91 m)

δ (m)	L(m) 200	400	600	800
0.10	0.2334565	0.2282779	0.2282779	0.2282779
0.20	0.0000000	0.1139465	0.1139465	0.1139465
0.30	0.0000000	0.0759216	0.0759216	0.0759216
0.40	0.0000000	0.0570809	0.0569251	0.0569251
0.50	0.0000000	0.0000000	0.0455324	0.0455324
0.60	0.0000000	0.0000000	0.0379394	0.0379394
0.70	0.0000000	0.0000000	0.0325168	0.0325168

TABLE 5–IIc Percent difference in Maximum Pipe Strain between Simplified and Complete Models. ϕ = 30 in (76.2 cm), t = 0.25 in (6.4 mm), C = 3 ft (0.91 m)

δ (m)	L(m) 200	400	600	800
0.10	0.0011680	0.0011680	0.0011680	0.0011680
0.20	0.0013760	0.0016554	0.0016554	0.0016554
0.30	0.0013760	0.0020288	0.0020288	0.0020288
0.40	0.0013760	0.0023435	0.0023435	0.0023435
0.50	0.0013760	0.0026207	0.0026207	0.0026207
0.60	0.0013760	0.0027520	0.0028713	0.0028713
0.70	0.0013760	0.0027520	0.0031016	0.0031016

TABLE 5–IIIa Maximum Pipe Strain for a Rigid Block Pattern of Longitudinal PGD Using the Complete Soil–Pipeline Interface Model. ϕ = 48 in (122 cm), t = 0.25 in (6.4 mm), C = 3 ft (0.91 m)

δ (m)	L(m) 200	400	600	800
0.10	0.0011730	0.0011730	0.0011730	0.0011730
0.20	0.0013760	0.0016589	0.0016589	0.0016589
0.30	0.0013760	0.0020317	0.0020317	0.0020317
0.40	0.0013760	0.0023461	0.0023461	0.0023461
0.50	0.0013760	0.0026230	0.0026230	0.0026230
0.60	0.0013760	0.0027520	0.0028733	0.0028733
0.70	0.0013760	0.0027520	0.0031035	0.0031035

TABLE 5–IIIb Maximum Pipe Strain for a Rigid Block Pattern of Longitudinal PGD Using the Simplified Model. ϕ = 48 in (122 cm), t = 0.25 in (6.4 mm), C = 3 ft (0.91 m)

δ (m)	L(m) 200	400	600	800
0.10	0.4335768	0.4309769	0.4309769	0.4309769
0.20	0.0000000	0.2148071	0.2148071	0.2148071
0.30	0.0000000	0.1430534	0.1430533	0.1430533
0.40	0.0000000	0.1072490	0.1072331	0.1072331
0.50	0.0000000	0.0878803	0.0857592	0.0857592
0.60	0.0000000	0.0000000	0.0714508	0.0714508
0.70	0.0000000	0.0000000	0.0612343	0.0612343

TABLE 5–IIIc Percent difference in Maximum Pipe Strain between Simplified and Complete Models. ϕ = 48 in (122 cm), t = 0.25 in (6.4 mm), C = 3 ft (0.91 m)

δ (m)	L(m) 200	400	600	800
0.10	0.0013356	0.0013356	0.0013356	0.0013356
0.20	0.0017888	0.0018901	0.0018901	0.0018901
0.30	0.0017888	0.0023155	0.0023155	0.0023155
0.40	0.0017888	0.0026740	0.0026740	0.0026740
0.50	0.0017888	0.0029898	0.0029898	0.0029898
0.60	0.0017888	0.0032753	0.0032753	0.0032753
0.70	0.0017888	0.0035378	0.0035379	0.0035379

TABLE 5–IVa Maximum Pipe Strain for a Rigid Block Pattern of Longitudinal PGD Using the Complete Soil–Pipeline Interface Model. ϕ = 12 in (30.5 cm), t = 0.25 in (6.4 mm), C = 6 ft (1.83 m)

δ (m)	L(m) 200	400	600	800
0.10	0.0013375	0.0013375	0.0013375	0.0013375
0.20	0.0017888	0.0018915	0.0018915	0.0018915
0.30	0.0017888	0.0023165	0.0023165	0.0023165
0.40	0.0017888	0.0026749	0.0026749	0.0026749
0.50	0.0017888	0.0029906	0.0029906	0.0029906
0.60	0.0017888	0.0032761	0.0032761	0.0032761
0.70	0.0017888	0.0035386	0.0035386	0.0035386

TABLE 5–IVb Maximum Pipe Strain for a Rigid Block Pattern of Longitudinal PGD Using the Simplified Model. ϕ = 12 in (30.5 cm), t = 0.25 in (6.4 mm), C = 6 ft (1.83 m)

δ (m)	L(m) 200	400	600	800
0.10	0.1394697	0.1394696	0.1394696	0.1394696
0.20	0.0000000	0.0696627	0.0696627	0.0696627
0.30	0.0000000	0.0464258	0.0464258	0.0464258
0.40	0.0000000	0.0348133	0.0348133	0.0348133
0.50	0.0000000	0.0278478	0.0278478	0.0278478
0.60	0.0000000	0.0232061	0.0232049	0.0232049
0.70	0.0000000	0.0217990	0.0198889	0.0198889

TABLE 5–IVc Percent difference in Maximum Pipe Strain between Simplified and Complete Models. ϕ = 12 in (30.5 cm), t = 0.25 in (6.4 mm), C = 6 ft (1.83 m)

δ (m)	L(m) 200	400	600	800
0.10	0.0014070	0.0014070	0.0014070	0.0014070
0.20	0.0019952	0.0019937	0.0019937	0.0019937
0.30	0.0019952	0.0024434	0.0024434	0.0024434
0.40	0.0019952	0.0028223	0.0028223	0.0028223
0.50	0.0019952	0.0031560	0.0031560	0.0031560
0.60	0.0019952	0.0034577	0.0034577	0.0034577
0.70	0.0019952	0.0037351	0.0037351	0.0037351

TABLE 5–Va Maximum Pipe Strain for a Rigid Block Pattern of Longitudinal PGD Using the Complete Soil–Pipeline Interface Model. ϕ = 30 in (76.2 cm), t = 0.25 in (6.4 mm), C = 6 ft (1.83 m)

δ (m)	L(m) 200	400	600	800
0.10	0.0014125	0.0014125	0.0014125	0.0014125
0.20	0.0019952	0.0019976	0.0019976	0.0019976
0.30	0.0019952	0.0024465	0.0024465	0.0024465
0.40	0.0019952	0.0028250	0.0028250	0.0028250
0.50	0.0019952	0.0031585	0.0031585	0.0031585
0.60	0.0019952	0.0034599	0.0034599	0.0034599
0.70	0.0019952	0.0037372	0.0037372	0.0037372

TABLE 5–Vb Maximum Pipe Strain for a Rigid Block Pattern of Longitudinal PGD Using the Simplified Model. ϕ = 30 in (76.2 cm), t = 0.25 in (6.4 mm), C = 6 ft (1.83 m)

δ (m)	L(m) 200	400	600	800
0.10	0.3903500	0.3903413	0.3903413	0.3903413
0.20	0.0000000	0.1946111	0.1946111	0.1946111
0.30	0.0000000	0.1296163	0.1296163	0.1296163
0.40	0.0000000	0.0971655	0.0971655	0.0971655
0.50	0.0000000	0.0777100	0.0777100	0.0777100
0.60	0.0000000	0.0647493	0.0647459	0.0647459
0.70	0.0000000	0.0557386	0.0554888	0.0554888

TABLE 5–Vc Percent difference in Maximum Pipe Strain between Simplified and Complete Models. ϕ = 30 in (76.2 cm), t = 0.25 in (6.4 mm), C = 6 ft (1.83 m)

δ (m)	L(m) 200	400	600	800
0.10	0.0014736	0.0014736	0.0014736	0.0014736
0.20	0.0020906	0.0020912	0.0020912	0.0020912
0.30	0.0022016	0.0025641	0.0025641	0.0025641
0.40	0.0022016	0.0029625	0.0029625	0.0029625
0.50	0.0022016	0.0033133	0.0033133	0.0033133
0.60	0.0022016	0.0036303	0.0036303	0.0036303
0.70	0.0022016	0.0039219	0.0039219	0.0039219

TABLE 5–VIa Maximum Pipe Strain for a Rigid Block Pattern of Longitudinal PGD Using the Complete Soil–Pipeline Interface Model. ϕ = 48 in (122 cm), t = 0.25 in (6.4 mm), C = 6 ft (1.83 m)

δ (m)	L(m) 200	400	600	800
0.10	0.0014838	0.0014838	0.0014838	0.0014838
0.20	0.0020984	0.0020984	0.0020984	0.0020984
0.30	0.0022016	0.0025700	0.0025700	0.0025700
0.40	0.0022016	0.0029676	0.0029676	0.0029676
0.50	0.0022016	0.0033178	0.0033178	0.0033178
0.60	0.0022016	0.0036345	0.0036345	0.0036345
0.70	0.0022016	0.0039257	0.0039257	0.0039257

TABLE 5–VIb Maximum Pipe Strain for a Rigid Block Pattern of Longitudinal PGD Using the Simplified Model. ϕ = 48 in (122 cm), t = 0.25 in (6.4 mm), C = 6 ft (1.83 m)

δ (m)	L(m) 200	400	600	800
0.10	0.6922295	0.6921823	0.6921823	0.6921823
0.20	0.3727553	0.3443454	0.3443454	0.3443454
0.30	0.0000000	0.2291761	0.2291761	0.2291761
0.40	0.0000000	0.1717367	0.1717367	0.1717367
0.50	0.0000000	0.1373197	0.1373195	0.1373195
0.60	0.0000000	0.1143984	0.1143941	0.1143941
0.70	0.0000000	0.0981334	0.0980284	0.0980284

TABLE 5–VIc Percent difference in Maximum Pipe Strain between Simplified and Complete Models. ϕ = 48 in (122 cm), t = 0.25 in (6.4 mm), C = 6 ft (1.83 m)

δ (m)	L(m) 200	400	600	800
0.10	0.0016136	0.0016136	0.0016136	0.0016136
0.20	0.0022843	0.0022843	0.0022843	0.0022843
0.30	0.0026144	0.0027987	0.0027987	0.0027987
0.40	0.0026144	0.0032322	0.0032322	0.0032322
0.50	0.0026144	0.0036140	0.0036140	0.0036140
0.60	0.0026144	0.0039593	0.0039593	0.0039593
0.7000	0.0026144	0.0042767	0.0042767	0.0042767

TABLE 5–VIIa Maximum Pipe Strain for a Rigid Block Pattern of Longitudinal PGD Using the Complete Soil–Pipeline Interface Model. ϕ = 12 in (30.5 cm), t = 0.25 in (6.4 mm), C = 9 ft (2.74 m)

δ (m)	L(m) 200	400	600	800
0.1000	0.0016169	0.0016169	0.0016169	0.0016169
0.20	0.0022867	0.0022867	0.0022867	0.0022867
0.30	0.0026144	0.0028006	0.0028006	0.0028006
0.40	0.0026144	0.0032338	0.0032338	0.0032338
0.50	0.0026144	0.0036155	0.0036155	0.0036155
0.60	0.0026144	0.0039606	0.0039606	0.0039606
0.70	0.0026144	0.0042779	0.0042779	0.0042779

TABLE 5–VIIb Maximum Pipe Strain for a Rigid Block Pattern of Longitudinal PGD Using the Simplified Model. ϕ = 12 in (30.5 cm), t = 0.25 in (6.4 mm), C = 9 ft (2.74 m)

δ (m)	L(m) 200	400	600	800
0.10	0.2040345	0.2040345	0.2040345	0.2040345
0.20	0.1019097	0.1018634	0.1018634	0.1018634
0.30	0.0000000	0.0678747	0.0678747	0.0678747
0.40	0.0000000	0.0508932	0.0508932	0.0508932
0.50	0.0000000	0.0407084	0.0407084	0.0407084
0.60	0.0000000	0.0339202	0.0339202	0.0339202
0.70	0.0000000	0.0290724	0.0290724	0.0290724

TABLE 5–VIIc Percent difference in Maximum Pipe Strain between Simplified and Complete Models. ϕ = 12 in (30.5 cm), t = 0.25 in (6.4 mm), C = 9 ft (2.74 m)

δ (m)	L(m) 200	400	600	800
0.10	0.0016703	0.0016703	0.0016703	0.0016703
0.20	0.0023687	0.0023687	0.0023687	0.0023687
0.30	0.0028208	0.0029037	0.0029037	0.0029037
0.40	0.0028208	0.0033544	0.0033544	0.0033544
0.50	0.0028208	0.0037514	0.0037514	0.0037514
0.60	0.0028208	0.0041102	0.0041102	0.0041102
0.70	0.0028208	0.0044401	0.0044401	0.0044401

TABLE 5–VIIIa Maximum Pipe Strain for a Rigid Block Pattern of Longitudinal PGD Using the Complete Soil–Pipeline Interface Model. ϕ = 30 in (76.2 cm), t = 0.25 in (6.4 mm), C = 9 ft (2.74 m)

δ (m)	L(m) 200	400	600	800
0.10	0.0016795	0.0016795	0.0016795	0.0016795
0.20	0.0023752	0.0023752	0.0023752	0.0023752
0.30	0.0028208	0.0029090	0.0029090	0.0029090
0.40	0.0028208	0.0033590	0.0033590	0.0033590
0.50	0.0028208	0.0037555	0.0037555	0.0037555
0.60	0.0028208	0.0041140	0.0041140	0.0041140
0.70	0.0028208	0.0044436	0.0044436	0.0044436

TABLE 5–VIIIb Maximum Pipe Strain for a Rigid Block Pattern of Longitudinal PGD Using the Simplified Model. ϕ = 30 in (76.2 cm), t = 0.25 in (6.4 mm), C = 9 ft (2.74 m)

δ (m)	L(m) 200	400	600	800
0.10	0.5531722	0.5531719	0.5531719	0.5531719
0.20	0.2759169	0.2754672	0.2754672	0.2754672
0.30	0.0000000	0.1833962	0.1833962	0.1833962
0.40	0.0000000	0.1374539	0.1374539	0.1374539
0.50	0.0000000	0.1099183	0.1099183	0.1099183
0.60	0.0000000	0.0915737	0.0915737	0.0915737
0.70	0.0000000	0.0784765	0.0784765	0.0784765

TABLE 5–VIIIc Percent difference in Maximum Pipe Strain between Simplified and Complete Models. ϕ = 30 in (76.2 cm), t = 0.25 in (6.4 mm), C = 9 ft (2.74 m)

δ (m)	L(m) 200	400	600	800
0.10	0.0017234	0.0017234	0.0017234	0.0017234
0.20	0.0024489	0.0024489	0.0024489	0.0024489
0.30	0.0030012	0.0030041	0.0030041	0.0030041
0.40	0.0030272	0.0034716	0.0034716	0.0034716
0.50	0.0030272	0.0038832	0.0038832	0.0038832
0.60	0.0030272	0.0042551	0.0042551	0.0042551
0.70	0.0030272	0.0045971	0.0045971	0.0045971

TABLE 5–IXa Maximum Pipe Strain for a Rigid Block Pattern of Longitudinal PGD Using the Complete Soil–Pipeline Interface Model. ϕ = 48 in (122 cm), t = 0.25 in (6.4 mm), C = 9 ft (2.74 m)

δ (m)	L(m) 200	400	600	800
0.10	0.0017399	0.0017399	0.0017399	0.0017399
0.20	0.0024606	0.0024606	0.0024606	0.0024606
0.30	0.0030136	0.0030136	0.0030136	0.0030136
0.40	0.0030272	0.0034798	0.0034798	0.0034798
0.50	0.0030272	0.0038905	0.0038905	0.0038905
0.60	0.0030272	0.0042618	0.0042618	0.0042618
0.70	0.0030272	0.0046033	0.0046033	0.0046033

TABLE 5–IXb Maximum Pipe Strain for a Rigid Block Pattern of Longitudinal PGD Using the Simplified Model. ϕ = 48 in (122 cm), t = 0.25 in (6.4 mm), C = 9 ft (2.74 m)

δ (m)	L(m) 200	400	600	800
0.10	0.9553673	0.9553620	0.9553620	0.9553620
0.20	0.4754379	0.4743744	0.4743744	0.4743744
0.30	0.4121014	0.3155168	0.3155168	0.3155168
0.40	0.0000000	0.2363628	0.2363628	0.2363628
0.50	0.0000000	0.1889583	0.1889583	0.1889583
0.60	0.0000000	0.1573920	0.1573920	0.1573920
0.70	0.0000000	0.1348627	0.1348625	0.1348625

TABLE 5–IXc Percent difference in Maximum Pipe Strain between Simplified and Complete Models. ϕ = 48 in (122 cm), t = 0.25 in (6.4 mm), C = 9 ft (2.74 m)

δ (m)	L(m) 200	400	600	800
0.10	0.0004816	0.0006935	0.0006935	0.0006935
0.20	0.0004816	0.0009632	0.0009811	0.0009811
0.30	0.0004816	0.0009632	0.0012017	0.0012017
0.40	0.0004816	0.0009632	0.0013877	0.0013877
0.50	0.0004816	0.0009632	0.0014448	0.0015515
0.60	0.0004816	0.0009632	0.0014448	0.0016997
0.70	0.0004816	0.0009632	0.0014448	0.0018359

TABLE 5–Xa Maximum Pipe Strain for a Rigid Block Pattern of Longitudinal PGD Using the Complete Soil–Pipeline Interface Model. ϕ = 12 in (30.5 cm), t = 0.50 in (12.7 mm), C = 3 ft (0.91 m)

δ (m)	L(m) 200	400	600	800
0.10	0.0004816	0.0006940	0.0006940	0.0006940
0.20	0.0004816	0.0009632	0.0009814	0.0009814
0.30	0.0004816	0.0009632	0.0012020	0.0012020
0.40	0.0004816	0.0009632	0.0013879	0.0013879
0.50	0.0004816	0.0009632	0.0014448	0.0015518
0.60	0.0004816	0.0009632	0.0014448	0.0016999
0.70	0.0004816	0.0009632	0.0014448	0.0018361

TABLE 5–Xb Maximum Pipe Strain for a Rigid Block Pattern of Longitudinal PGD Using the Simplified Model. ϕ = 12 in (30.5 cm), t = 0.50 in (12.7 mm), C = 3 ft (0.91 m)

δ (m)	L(m) 200	400	600	800
0.10	0.0000000	0.0750274	0.0750274	0.0750274
0.20	0.0000000	0.0000000	0.0374928	0.0374928
0.30	0.0000000	0.0000000	0.0249905	0.0249905
0.40	0.0000000	0.0000000	0.0188137	0.0187411
0.50	0.0000000	0.0000000	0.0000000	0.0149921
0.60	0.0000000	0.0000000	0.0000000	0.0124929
0.70	0.0000000	0.0000000	0.0000000	0.0106721

TABLE 5–Xc Percent difference in Maximum Pipe Strain between Simplified and Complete Models. ϕ = 12 in (30.5 cm), t = 0.50 in (12.7 mm), C = 3 ft (0.91 m)

δ (m)	L(m) 200	400	600	800
0.10	0.0005848	0.0007630	0.0007630	0.0007630
0.20	0.0005848	0.0010802	0.0010802	0.0010802
0.30	0.0005848	0.0011696	0.0013235	0.0013235
0.40	0.0005848	0.0011696	0.0015286	0.0015286
0.50	0.0005848	0.0011696	0.0017092	0.0017092
0.60	0.0005848	0.0011696	0.0017544	0.0018725
0.70	0.0005848	0.0011696	0.0017544	0.0020226

TABLE 5–XIa Maximum Pipe Strain for a Rigid Block Pattern of Longitudinal PGD Using the Complete Soil–Pipeline Interface Model. ϕ = 30 in (76.2 cm), t = 0.50 in (12.7 mm), C = 3 ft (0.91 m)

δ (m)	L(m) 200	400	600	800
0.10	0.0005848	0.0007647	0.0007647	0.0007647
0.20	0.0005848	0.0010815	0.0010815	0.0010815
0.30	0.0005848	0.0011696	0.0013245	0.0013245
0.40	0.0005848	0.0011696	0.0015294	0.0015294
0.50	0.0005848	0.0011696	0.0017100	0.0017100
0.60	0.0005848	0.0011696	0.0017544	0.0018732
0.70	0.0005848	0.0011696	0.0017544	0.0020233

TABLE 5–XIb Maximum Pipe Strain for a Rigid Block Pattern of Longitudinal PGD Using the Simplified Model. ϕ = 30 in (76.2 cm), t = 0.50 in (12.7 mm), C = 3 ft (0.91 m)

δ (m)	L(m) 200	400	600	800
0.10	0.0000000	0.2282778	0.2282778	0.2282778
0.2000	0.0000000	0.1149243	0.1139465	0.1139465
0.30	0.0000000	0.0000000	0.0759216	0.0759216
0.40	0.0000000	0.0000000	0.0569276	0.0569251
0.50	0.0000000	0.0000000	0.0478159	0.0455324
0.60	0.0000000	0.0000000	0.0000000	0.0379394
0.70	0.0000000	0.0000000	0.0000000	0.0325169

TABLE 5–XIc Percent difference in Maximum Pipe Strain between Simplified and Complete Models. ϕ = 30 in (76.2 cm), t = 0.50 in (12.7 mm), C = 3 ft (0.91 m)

δ (m)	L(m) 200	400	600	800
0.10	0.0006880	0.0008259	0.0008259	0.0008259
0.20	0.0006880	0.0011705	0.0011705	0.0011705
0.30	0.0006880	0.0013760	0.0014346	0.0014346
0.40	0.0006880	0.0013760	0.0016571	0.0016571
0.50	0.0006880	0.0013760	0.0018531	0.0018531
0.60	0.0006880	0.0013760	0.0020301	0.0020303
0.70	0.0006880	0.0013760	0.0020640	0.0021932

TABLE 5–XIIa Maximum Pipe Strain for a Rigid Block Pattern of Longitudinal PGD Using the Complete Soil–Pipeline Interface Model. ϕ = 48 in (122 cm), t = 0.50 in (12.7 mm), C = 3 ft (0.91 m)

δ (m)	L(m) 200	400	600	800
0.10	0.0006880	0.0008295	0.0008295	0.0008295
0.20	0.0006880	0.0011730	0.0011730	0.0011730
0.30	0.0006880	0.0013760	0.0014367	0.0014367
0.40	0.0006880	0.0013760	0.0016589	0.0016589
0.50	0.0006880	0.0013760	0.0018547	0.0018547
0.60	0.0006880	0.0013760	0.0020317	0.0020317
0.70	0.0006880	0.0013760	0.0020640	0.0021945

TABLE 5–XIIb Maximum Pipe Strain for a Rigid Block Pattern of Longitudinal PGD Using the Simplified Model. ϕ = 48 in (122 cm), t = 0.50 in (12.7 mm), C = 3 ft (0.91 m)

δ (m)	L(m) 200	400	600	800
0.10	0.0000000	0.4309768	0.4309768	0.4309768
0.20	0.0000000	0.2150886	0.2148071	0.2148071
0.30	0.0000000	0.0000000	0.1430533	0.1430533
0.40	0.0000000	0.0000000	0.1072339	0.1072331
0.50	0.0000000	0.0000000	0.0858555	0.0857592
0.60	0.0000000	0.0000000	0.0805913	0.0714508
0.70	0.0000000	0.0000000	0.0000000	0.0612343

TABLE 5–XIIc Percent difference in Maximum Pipe Strain between Simplified and Complete Models. ϕ = 48 in (122 cm), t = 0.50 in (12.7 mm), C = 3 ft (0.91 m)

δ (m)	L(m) 200	400	600	800
0.10	0.0008944	0.0009444	0.0009444	0.0009444
0.20	0.0008944	0.0013365	0.0013365	0.0013365
0.30	0.0008944	0.0016373	0.0016373	0.0016373
0.40	0.0008944	0.0017888	0.0018908	0.0018908
0.50	0.0008944	0.0017888	0.0021141	0.0021141
0.60	0.0008944	0.0017888	0.0023160	0.0023160
0.70	0.0008944	0.0017888	0.0025017	0.0025017

TABLE 5–XIIIa Maximum Pipe Strain for a Rigid Block Pattern of Longitudinal PGD Using the Complete Soil–Pipeline Interface Model. ϕ = 12 in (30.5 cm), t = 0.50 in (12.7 mm), C = 6 ft (1.83 m)

δ (m)	L(m) 200	400	600	800
0.10	0.0008944	0.0009457	0.0009457	0.0009457
0.20	0.0008944	0.0013375	0.0013375	0.0013375
0.30	0.0008944	0.0016380	0.0016380	0.0016380
0.40	0.0008944	0.0017888	0.0018915	0.0018915
0.50	0.0008944	0.0017888	0.0021147	0.0021147
0.60	0.0008944	0.0017888	0.0023165	0.0023165
0.70	0.0008944	0.0017888	0.0025022	0.0025022

TABLE 5–XIIIb Maximum Pipe Strain for a Rigid Block Pattern of Longitudinal PGD Using the Simplified Model. ϕ = 12 in (30.5 cm), t = 0.50 in (12.7 mm), C = 6 ft (1.83 m)

δ (m)	L(m) 200	400	600	800
0.10	0.0000000	0.1394696	0.1394696	0.1394696
0.20	0.0000000	0.0696627	0.0696627	0.0696627
0.30	0.0000000	0.0464549	0.0464258	0.0464258
0.40	0.0000000	0.0000000	0.0348133	0.0348133
0.50	0.0000000	0.0000000	0.0278478	0.0278478
0.6000	0.0000000	0.0000000	0.0232049	0.0232049
0.70	0.0000000	0.0000000	0.0198926	0.0198889

TABLE 5–XIIIc Percent difference in Maximum Pipe Strain between Simplified and Complete Models. ϕ = 12 in (30.5 cm), t = 0.50 in (12.7 mm), C = 6 ft (1.83 m)

δ (m)	L(m) 200	400	600	800
0.10	0.0009976	0.0009949	0.0009949	0.0009949
0.20	0.0009976	0.0014098	0.0014098	0.0014098
0.30	0.0009976	0.0017277	0.0017277	0.0017277
0.40	0.0009976	0.0019952	0.0019957	0.0019957
0.50	0.0009976	0.0019952	0.0022316	0.0022316
0.60	0.0009976	0.0019952	0.0024450	0.0024450
0.70	0.0009976	0.0019952	0.0026411	0.0026411

TABLE 5–XIVa Maximum Pipe Strain for a Rigid Block Pattern of Longitudinal PGD Using the Complete Soil–Pipeline Interface Model. ϕ = 30 in (76.2 cm), t = 0.50 in (12.7 mm), C = 6 ft (1.83 m)

δ (m)	L(m) 200	400	600	800
0.10	0.0009976	0.0009988	0.0009988	0.0009988
0.20	0.0009976	0.0014125	0.0014125	0.0014125
0.30	0.0009976	0.0017300	0.0017300	0.0017300
0.40	0.0009976	0.0019952	0.0019976	0.0019976
0.50	0.0009976	0.0019952	0.0022334	0.0022334
0.60	0.0009976	0.0019952	0.0024465	0.0024465
0.70	0.0009976	0.0019952	0.0026426	0.0026426

TABLE 5–XIVb Maximum Pipe Strain for a Rigid Block Pattern of Longitudinal PGD Using the Simplified Model. ϕ = 30 in (76.2 cm), t = 0.50 in (12.7 mm), C = 6 ft (1.83 m)

δ (m)	L(m) 200	400	600	800
0.10	0.0000000	0.3903412	0.3903412	0.3903412
0.20	0.0000000	0.1946112	0.1946111	0.1946111
0.30	0.0000000	0.1296979	0.1296163	0.1296163
0.40	0.0000000	0.0000000	0.0971655	0.0971655
0.50	0.0000000	0.0000000	0.0777100	0.0777100
0.60	0.0000000	0.0000000	0.0647459	0.0647459
0.70	0.0000000	0.0000000	0.0554939	0.0554888

TABLE 5–XIVc Percent difference in Maximum Pipe Strain between Simplified and Complete Models. ϕ = 30 in (76.2 cm), t = 0.50 in (12.7 mm), C = 6 ft (1.83 m)

δ (m)	L(m) 200	400	600	800
0.10	0.0010411	0.0010420	0.0010420	0.0010420
0.20	0.0011008	0.0014787	0.0014787	0.0014787
0.30	0.0011008	0.0018131	0.0018131	0.0018131
0.40	0.0011008	0.0020946	0.0020948	0.0020948
0.50	0.0011008	0.0022016	0.0023428	0.0023428
0.60	0.0011008	0.0022016	0.0025670	0.0025670
0.70	0.0011008	0.0022016	0.0027732	0.0027732

TABLE 5–XVa Maximum Pipe Strain for a Rigid Block Pattern of Longitudinal PGD Using the Complete Soil–Pipeline Interface Model. ϕ = 48 in (122 cm), t = 0.50 in (12.7 mm), C = 6 ft (1.83 m)

δ (m)	L(m) 200	400	600	800
0.10	0.0010492	0.0010492	0.0010492	0.0010492
0.20	0.0011008	0.0014838	0.0014838	0.0014838
0.30	0.0011008	0.0018172	0.0018172	0.0018172
0.40	0.0011008	0.0020984	0.0020984	0.0020984
0.50	0.0011008	0.0022016	0.0023461	0.0023461
0.60	0.0011008	0.0022016	0.0025700	0.0025700
0.70	0.0011008	0.0022016	0.0027759	0.0027759

TABLE 5–XVb Maximum Pipe Strain for a Rigid Block Pattern of Longitudinal PGD Using the Simplified Model. ϕ = 48 in (122 cm), t = 0.50 in (12.7 mm), C = 6 ft (1.83 m)

δ (m)	L(m) 200	400	600	800
0.10	0.7730010	0.6921820	0.6921820	0.6921820
0.20	0.0000000	0.3443461	0.3443454	0.3443454
0.30	0.0000000	0.2292902	0.2291761	0.2291761
0.40	0.0000000	0.1803782	0.1717367	0.1717367
0.50	0.0000000	0.0000000	0.1373195	0.1373195
0.60	0.0000000	0.0000000	0.1143943	0.1143941
0.70	0.0000000	0.0000000	0.0980332	0.0980284

TABLE 5–XVc Percent difference in Maximum Pipe Strain between Simplified and Complete Models. ϕ = 48 in (122 cm), t = 0.50 in (12.7 mm), C = 6 ft (1.83 m)

δ (m)	L(m) 200	400	600	800
0.10	0.0011410	C.0011410	0.0011410	0.0011410
0.20	0.0013072	C.0016153	0.0016153	0.0016153
0.3000	0.0013072	C.0019790	0.0019790	0.0019790
0.40	0.0013072	C.0022855	0.0022855	0.0022855
0.50	0.0013072	C.0025555	0.0025555	0.0025555
0.60	0.0013072	C.0026144	0.0027996	0.0027996
0.70	0.0013072	C.0026144	0.0030241	0.0030241

TABLE 5–XVIa Maximum Pipe Strain for a Rigid Block Pattern of Longitudinal PGD Using the Complete Soil–Pipeline Interface Model. ϕ = 12 in (30.5 cm); t = 0.50 in (12.7 mm), C = 9 ft (2.74 m)

δ (m)	L(m) 200	400	600	800
0.10	0.0011433	C.0011433	0.0011433	0.0011433
0.20	0.0013072	C.0016169	0.0016169	0.0016169
0.30	0.0013072	C.0019803	0.0019803	0.0019803
0.40	0.0013072	C.0022867	0.0022867	0.0022867
0.50	0.0013072	C.0025566	0.0025566	0.0025566
0.60	0.0013072	C.0026144	0.0028006	0.0028006
0.70	0.0013072	C.0026144	0.0030250	0.0030250

TABLE 5–XVIb Maximum Pipe Strain for a Rigid Block Pattern of Longitudinal PGD Using the Simplified Model. ϕ = 12 in (30.5 cm), t = 0.50 in (12.7 mm), C = 9 ft (2.74 m)

δ (m)	L(m) 200	400	600	800
0.10	0.2046232	0.2040344	0.2040344	0.2040344
0.20	0.0000000	0.1018634	0.1018634	0.1018634
0.30	0.0000000	0.0678747	0.0678747	0.0678747
0.40	0.0000000	0.0508949	0.0508932	0.0508932
0.50	0.0000000	0.0431363	0.0407084	0.0407084
0.60	0.0000000	0.0000000	0.0339202	0.0339202
0.70	0.0000000	0.0000000	0.0290724	0.0290724

TABLE 5–XVIc Percent difference in Maximum Pipe Strain between Simplified and Complete Models. ϕ = 12 in (30.5 cm), t = 0.50 in (12.7 mm), C = 9 ft (2.74 m)

δ (m)	L(m) 200	400	600	800
0.10	0.0011810	0.0011811	0.0011811	0.0011811
0.20	0.0014104	0.0016749	0.0016749	0.0016749
0.30	0.0014104	0.0020532	0.0020532	0.0020532
0.40	0.0014104	0.0023719	0.0023719	0.0023719
0.50	0.0014104	0.0026526	0.0026526	0.0026526
0.60	0.0014104	0.0028208	0.0029064	0.0029064
0.70	0.0014104	0.0028208	0.0031396	0.0031396

TABLE 5–XVIIa Maximum Pipe Strain for a Rigid Block Pattern of Longitudinal PGD Using the Complete Soil–Pipeline Interface Model. ϕ = 30 in (76.2 cm), t = 0.50 in (12.7 mm), C = 9 ft (2.74 m)

δ (m)	L(m) 200	400	600	800
0.10	0.0011876	0.0011876	0.0011876	0.0011876
0.20	0.0014104	0.0016795	0.0016795	0.0016795
0.30	0.0014104	0.0020570	0.0020570	0.0020570
0.40	0.0014104	0.0023752	0.0023752	0.0023752
0.50	0.0014104	0.0026556	0.0026556	0.0026556
0.60	0.0014104	0.0028208	0.0029090	0.0029090
0.70	0.0014104	0.0028208	0.0031421	0.0031421

TABLE 5–XVIIb Maximum Pipe Strain for a Rigid Block Pattern of Longitudinal PGD Using the Simplified Model. ϕ = 30 in (76.2 cm), t = 0.50 in (12.7 mm), C = 9 ft (2.74 m)

δ (m)	L(m) 200	400	600	800
0.10	0.5570564	0.5531717	0.5531717	0.5531717
0.20	0.0000000	0.2754671	0.2754671	0.2754671
0.30	0.0000000	0.1833964	0.1833962	0.1833962
0.40	0.0000000	0.1374817	0.1374539	0.1374539
0.50	0.0000000	0.1118939	0.1099183	0.1099183
0.60	0.0000000	0.0000000	0.0915737	0.0915737
0.70	0.0000000	0.0000000	0.0784765	0.0784765

TABLE 5–XVIIc Percent difference in Maximum Pipe Strain between Simplified and Complete Models. ϕ = 30 in (76.2 cm), t = 0.50 in (12.7 mm), C = 9 ft (2.74 m)

δ (m)	L(m) 200	400	600	800
0.10	0.0012185	0.0012186	0.0012186	0.0012186
0.20	0.0015136	0.0017317	0.0017317	0.0017317
0.30	0.0015136	0.0021242	0.0021242	0.0021242
0.40	0.0015136	0.0024548	0.0024548	0.0024548
0.50	0.0015136	0.0027458	0.0027458	0.0027458
0.60	0.0015136	0.0030074	0.0030088	0.0030088
0.70	0.0015136	0.0030272	0.0032506	0.0032506

TABLE 5–XVIIIa Maximum Pipe Strain for a Rigid Block Pattern of Longitudinal PGD Using the Complete Soil–Pipeline Interface Model. ϕ = 48 in (122 cm), t = 0.50 in (12.7 mm), C = 9 ft (2.74 m)

δ (m)	L(m) 200	400	600	800
0.1000	0.0012303	0.0012303	0.0012303	0.0012303
0.20	0.0015136	0.0017399	0.0017399	0.0017399
0.30	0.0015136	0.0021309	0.0021309	0.0021309
0.40	0.0015136	0.0024606	0.0024606	0.0024606
0.50	0.0015136	0.0027510	0.0027510	0.0027510
0.60	0.0015136	0.0030136	0.0030136	0.0030136
0.70	0.0015136	0.0030272	0.0032550	0.0032550

TABLE 5–XVIIIb Maximum Pipe Strain for a Rigid Block Pattern of Longitudinal PGD Using the Simplified Model. ϕ = 48 in (122 cm), t = 0.50 in (12.7 mm), C = 9 ft (2.74 m)

δ (m)	L(m) 200	400	600	800
0.10	0.9637064	0.9553614	0.9553614	0.9553614
0.20	0.0000000	0.4743743	0.4743743	0.4743743
0.30	0.0000000	0.3155187	0.3155167	0.3155167
0.40	0.0000000	0.2364378	0.2363628	0.2363628
0.50	0.0000000	0.1908155	0.1889583	0.1889583
0.60	0.0000000	0.2041652	0.1573920	0.1573920
0.70	0.0000000	0.0000000	0.1348625	0.1348625

TABLE 5–XVIIIc Percent difference in Maximum Pipe Strain between Simplified and Complete Models. ϕ = 48 in (122 cm), t = 0.50 in (12.7 mm), C = 9 ft (2.74 m)

δ (m)	L(m) 200	400	600	800
0.10	0.0003211	0.0005662	0.0005662	0.0005662
0.20	0.0003211	0.0006421	0.0008010	0.0008010
0.30	0.0003211	0.0006421	0.0009632	0.0009812
0.40	0.0003211	0.0006421	0.0009632	0.0011330
0.50	0.0003211	0.0006421	0.0009632	0.0012668
0.60	0.0003211	0.0006421	0.0009632	0.0012843
0.70	0.0003211	0.0006421	0.0009632	0.0012843

TABLE 5–XIXa Maximum Pipe Strain for a Rigid Block Pattern of Longitudinal PGD Using the Complete Soil–Pipeline Interface Model. ϕ = 12 in (30.5 cm), t = 0.75 in (19.1 mm), C = 3 ft (0.91 m)

δ (m)	L(m) 200	400	600	800
0.10	0.0003211	0.0005666	0.0005666	0.0005666
0.20	0.0003211	0.0006421	0.0008013	0.0008013
0.30	0.0003211	0.0006421	0.0009632	0.0009814
0.40	0.0003211	0.0006421	0.0009632	0.0011333
0.50	0.0003211	0.0006421	0.0009632	0.0012670
0.60	0.0003211	0.0006421	0.0009632	0.0012843
0.70	0.0003211	0.0006421	0.0009632	0.0012843

TABLE 5–XIXb Maximum Pipe Strain for a Rigid Block Pattern of Longitudinal PGD Using the Simplified Model. ϕ = 12 in (30.5 cm), t = 0.75 in (19.1 mm), C = 3 ft (0.91 m)

δ (m)	L(m) 200	400	600	800
0.10	0.0000000	0.0750476	0.0750274	0.0750274
0.20	0.0000000	0.0000000	0.0374928	0.0374928
0.30	0.0000000	0.0000000	0.0000000	0.0249905
0.40	0.0000000	0.0000000	0.0000000	0.0187411
0.50	0.0000000	0.0000000	0.0000000	0.0158697
0.60	0.0000000	0.0000000	0.0000000	0.0000000
0.70	0.0000000	0.0000000	0.0000000	0.0000000

TABLE 5–XIXc Percent difference in Maximum Pipe Strain between Simplified and Complete Models. ϕ = 12 in (30.5 cm), t = 0.75 in (19.1 mm), C = 3 ft (0.91 m)

δ (m)	L(m) 200	400	600	800
0.10	0.0003899	0.0006230	0.0006230	0.0006230
0.20	0.0003899	0.0007797	0.0008820	0.0008820
0.30	0.0003899	0.0007797	0.0010807	0.0010807
0.40	0.0003899	0.0007797	0.0011696	0.0012481
0.50	0.0003899	0.0007797	0.0011696	0.0013955
0.60	0.0003899	0.0007797	0.0011696	0.0015288
0.70	0.0003899	0.0007797	0.0011696	0.0015595

TABLE 5–XXa Maximum Pipe Strain for a Rigid Block Pattern of Longitudinal PGD Using the Complete Soil–Pipeline Interface Model. ϕ = 30 in (76.2 cm), t = 0.75 in (19.1 mm), C = 3 ft (0.91 m)

δ (m)	L(m) 200	400	600	800
0.10	0.0003899	0.0006244	0.0006244	0.0006244
0.20	0.0003899	0.0007797	0.0008830	0.0008830
0.30	0.0003899	0.0007797	0.0010815	0.0010815
0.40	0.0003899	0.0007797	0.0011696	0.0012488
0.50	0.0003899	0.0007797	0.0011696	0.0013962
0.6000	0.0003899	0.0007797	0.0011696	0.0015294
0.70	0.0003899	0.0007797	0.0011696	0.0015595

TABLE 5–XXb Maximum Pipe Strain for a Rigid Block Pattern of Longitudinal PGD Using the Simplified Model. ϕ = 30 in (76.2 cm), t = 0.75 in (19.1 mm), C = 3 ft (0.91 m)

δ (m)	L(m) 200	400	600	800
0.10	0.0000000	0.2283151	0.2282778	0.2282778
0.20	0.0000000	0.0000000	0.1139466	0.1139465
0.30	0.0000000	0.0000000	0.0763248	0.0759216
0.40	0.0000000	0.0000000	0.0000000	0.0569251
0.50	0.0000000	0.0000000	0.0000000	0.0455375
0.60	0.0000000	0.0000000	0.0000000	0.0405085
0.70	0.0000000	0.0000000	0.0000000	0.0000000

TABLE 5–XXc Percent difference in Maximum Pipe Strain between Simplified and Complete Models. ϕ = 30 in (76.2 cm), t = 0.75 in (19.1 mm), C = 3 ft (0.91 m)

δ (m)	L(m) 200	400	600	800
0.10	0.0004587	0.0006743	0.0006743	0.0006743
0.20	0.0004587	0.0009173	0.0009557	0.0009557
0.30	0.0004587	0.0009173	0.0011714	0.0011714
0.40	0.0004587	0.0009173	0.0013528	0.0013530
0.50	0.0004587	0.0009173	0.0013760	0.0015131
0.60	0.0004587	0.0009173	0.0013760	0.0016577
0.70	0.0004587	0.0009173	0.0013760	0.0017907

TABLE 5–XXIa Maximum Pipe Strain for a Rigid Block Pattern of Longitudinal PGD Using the Complete Soil–Pipeline Interface Model. ϕ = 48 in (122 cm), t = 0.75 in (19.1 mm), C = 3 ft (0.91 m)

δ (m)	L(m) 200	400	600	800
0.10	0.0004587	0.0006772	0.0006772	0.0006772
0.20	0.0004587	0.0009173	0.0009578	0.0009578
0.30	0.0004587	0.0009173	0.0011730	0.0011730
0.40	0.0004587	0.0009173	0.0013545	0.0013545
0.50	0.0004587	0.0009173	0.0013760	0.0015144
0.60	0.0004587	0.0009173	0.0013760	0.0016589
0.70	0.0004587	0.0009173	0.0013760	0.0017918

TABLE 5–XXIb Maximum Pipe Strain for a Rigid Block Pattern of Longitudinal PGD Using the Simplified Model. ϕ = 48 in (122 cm), t = 0.75 in (19.1 mm), C = 3 ft (0.91 m)

δ (m)	L(m) 200	400	600	800
0.10	0.0000000	0.4310298	0.4309767	0.4309767
0.20	0.0000000	0.0000000	0.2148072	0.2148071
0.30	0.0000000	0.0000000	0.1431108	0.1430533
0.40	0.0000000	0.0000000	0.1234686	0.1072331
0.50	0.0000000	0.0000000	0.0000000	0.0857600
0.60	0.0000000	0.0000000	0.0000000	0.0715197
0.70	0.0000000	0.0000000	0.0000000	0.0656157

TABLE 5–XXIc Percent difference in Maximum Pipe Strain between Simplified and Complete Models. ϕ = 48 in (122 cm), t = 0.75 in (19.1 mm), C = 3 ft (0.91 m)

δ (m)	L(m) 200	400	600	800
0.10	0.0005963	0.0007711	0.0007711	0.0007711
0.20	0.0005963	0.0010913	0.0010913	0.0010913
0.30	0.0005963	0.0011925	0.0013368	0.0013368
0.40	0.0005963	0.0011925	0.0015438	0.0015438
0.50	0.0005963	0.0011925	0.0017262	0.0017262
0.60	0.0005963	0.0011925	0.0017888	0.0018910
0.70	0.0005963	0.0011925	0.0017888	0.0020426

TABLE 5–XXIIa Maximum Pipe Strain for a Rigid Block Pattern of Longitudinal PGD Using the Complete Soil–Pipeline Interface Model. ϕ = 12 in (30.5 cm), t = 0.75 in (19.1 mm), C = 6 ft (1.83 m)

δ (m)	L(m) 200	400	600	800
0.10	0.0005963	0.0007722	0.0007722	0.0007722
0.20	0.0005963	0.0010920	0.0010920	0.0010920
0.30	0.0005963	0.0011925	0.0013375	0.0013375
0.40	0.0005963	0.0011925	0.0015444	0.0015444
0.50	0.0005963	0.0011925	0.0017267	0.0017267
0.60	0.0005963	0.0011925	0.0017888	0.0018915
0.70	0.0005963	0.0011925	0.0017888	0.0020430

TABLE 5–XXIIb Maximum Pipe Strain for a Rigid Block Pattern of Longitudinal PGD Using the Simplified Model. ϕ = 12 in (30.5 cm), t = 0.75 in (19.1 mm), C = 6 ft (1.83 m)

δ (m)	L(m) 200	400	600	800
0.10	0.0000000	0.1394696	0.1394696	0.1394696
0.2000	0.0000000	0.0697152	0.0696627	0.0696627
0.30	0.0000000	0.0000000	0.0464258	0.0464258
0.40	0.0000000	0.0000000	0.0348134	0.0348133
0.50	0.0000000	0.0000000	0.0281888	0.0278478
0.60	0.0000000	0.0000000	0.0000000	0.0232049
0.70	0.0000000	0.0000000	0.0000000	0.0198889

TABLE 5–XXIIc Percent difference in Maximum Pipe Strain between Simplified and Complete Models. ϕ = 12 in (30.5 cm), t = 0.75 in (19.1 mm), C = 6 ft (1.83 m)

δ (m)	L(m) 200	400	600	800
0.10	0.0006651	0.0008123	0.0008123	0.0008123
0.20	0.0006651	0.0011511	0.0011511	0.0011511
0.30	0.0006651	0.0013301	0.0014107	0.0014107
0.40	0.0006651	0.0013301	0.0016294	0.0016294
0.50	0.0006651	0.0013301	0.0018221	0.0018221
0.60	0.0006651	0.0013301	0.0019952	0.0019963
0.70	0.0006651	0.0013301	0.0019952	0.0021565

TABLE 5–XXIIIa Maximum Pipe Strain for a Rigid Block Pattern of Longitudinal PGD Using the Complete Soil–Pipeline Interface Model. ϕ = 30 in (76.2 cm), t = 0.75 in (19.1 mm), C = 6 ft (1.83 m)

δ (m)	L(m) 200	400	600	800
0.10	0.0006651	0.0008155	0.0008155	0.0008155
0.20	0.0006651	0.0011533	0.0011533	0.0011533
0.30	0.0006651	0.0013301	0.0014125	0.0014125
0.40	0.0006651	0.0013301	0.0016310	0.0016310
0.50	0.0006651	0.0013301	0.0018235	0.0018235
0.60	0.0006651	0.0013301	0.0019952	0.0019976
0.70	0.0006651	0.0013301	0.0019952	0.0021577

TABLE 5–XXIIIb Maximum Pipe Strain for a Rigid Block Pattern of Longitudinal PGD Using the Simplified Model. ϕ = 30 in (76.2 cm), t = 0.75 in (19.1 mm), C = 6 ft (1.83 m)

δ (m)	L(m) 200	400	600	800
0.10	0.0000000	0.3903412	0.3903411	0.3903411
0.20	0.0000000	0.1949784	0.1946111	0.1946111
0.30	0.0000000	0.0000000	0.1296163	0.1296163
0.40	0.0000000	0.0000000	0.0971666	0.0971655
0.50	0.0000000	0.0000000	0.0778696	0.0777100
0.60	0.0000000	0.0000000	0.0000000	0.0647459
0.70	0.0000000	0.0000000	0.0000000	0.0554888

TABLE 5–XXIIIc Percent difference in Maximum Pipe Strain between Simplified and Complete Models. ϕ = 30 in (76.2 cm), t = 0.75 in (19.1 mm), C = 6 ft (1.83 m)

δ (m)	L(m) 200	400	600	800
0.10	0.0007339	0.0008508	0.0008508	0.0008508
0.20	0.0007339	0.0012073	0.0012073	0.0012073
0.30	0.0007339	0.0014677	0.0014804	0.0014804
0.40	0.0007339	0.0014677	0.0017104	0.0017104
0.50	0.0007339	0.0014677	0.0019129	0.0019129
0.60	0.0007339	0.0014677	0.0020959	0.0020960
0.70	0.0007339	0.0014677	0.0022016	0.0022643

TABLE 5–XXIVa Maximum Pipe Strain for a Rigid Block Pattern of Longitudinal PGD Using the Complete Soil–Pipeline Interface Model. ϕ = 48 in (122 cm), t = 0.75 in (19.1 mm), C = 6 ft (1.83 m)

δ (m)	L(m) 200	400	600	800
0.10	0.0007339	0.0008567	0.0008567	0.0008567
0.20	0.0007339	0.0012115	0.0012115	0.0012115
0.30	0.0007339	0.0014677	0.0014838	0.0014838
0.40	0.0007339	0.0014677	0.0017133	0.0017133
0.50	0.0007339	0.0014677	0.0019155	0.0019155
0.60	0.0007339	0.0014677	0.0020984	0.0020984
0.70	0.0007339	0.0014677	0.0022016	0.0022665

TABLE 5–XXIVb Maximum Pipe Strain for a Rigid Block Pattern of Longitudinal PGD Using the Simplified Model. ϕ = 48 in (122 cm), t = 0.75 in (19.1 mm), C = 6 ft (1.83 m)

δ (m)	L(m) 200	400	600	800
0.10	0.0000000	0.6921828	0.6921819	0.6921819
0.20	0.0000000	0.3448828	0.3443454	0.3443454
0.30	0.0000000	0.0000000	0.2291761	0.2291760
0.40	0.0000000	0.0000000	0.1717393	0.1717367
0.50	0.0000000	0.0000000	0.1374388	0.1373195
0.60	0.0000000	0.0000000	0.1182981	0.1143941
0.70	0.0000000	0.0000000	0.0000000	0.0980284

TABLE 5–XXIVc Percent difference in Maximum Pipe Strain between Simplified and Complete Models. ϕ = 48 in (122 cm), t = 0.75 in (19.1 mm), C = 6 ft (1.83 m)

δ (m)	L(m) 200	400	600	800
0.10	0.0008715	0.0009316	0.0009316	0.0009316
0.20	0.0008715	0.0013189	0.0013189	0.0013189
0.30	0.0008715	0.0016158	0.0016158	0.0016158
0.40	0.0008715	0.0017429	0.0018661	0.0018661
0.50	0.0008715	0.0017429	0.0020866	0.0020866
0.60	0.0008715	0.0017429	0.0022859	0.0022859
0.70	0.0008715	0.0017429	0.0024691	0.0024692

TABLE 5–XXVa Maximum Pipe Strain for a Rigid Block Pattern of Longitudinal PGD Using the Complete Soil–Pipeline Interface Model. ϕ = 12 in (30.5 cm), t = 0.75 in (19.1 mm), C = 9 ft (2.74 m)

δ (m)	L(m) 200	400	600	800
0.10	0.0008715	0.0009335	0.0009335	0.0009335
0.20	0.0008715	0.0013202	0.0013202	0.0013202
0.30	0.0008715	0.0016169	0.0016169	0.0016169
0.40	0.0008715	0.0017429	0.0018670	0.0018670
0.50	0.0008715	0.0017429	0.0020874	0.0020874
0.60	0.0008715	0.0017429	0.0022867	0.0022867
0.70	0.0008715	0.0017429	0.0024699	0.0024699

TABLE 5–XXVb Maximum Pipe Strain for a Rigid Block Pattern of Longitudinal PGD Using the Simplified Model. ϕ = 12 in (30.5 cm), t = 0.75 in (19.1 mm), C = 9 ft (2.74 m)

δ (m)	L(m) 200	400	600	800
0.10	0.0000000	0.2040344	0.2040344	0.2040344
0.20	0.0000000	0.1018634	0.1018634	0.1018634
0.30	0.0000000	0.0682110	0.0678747	0.0678747
0.40	0.0000000	0.0000000	0.0508932	0.0508932
0.50	0.0000000	0.0000000	0.0407084	0.0407084
0.60	0.0000000	0.0000000	0.0339204	0.0339202
0.70	0.0000000	0.0000000	0.0291722	0.0290724

TABLE 5–XXVc Percent difference in Maximum Pipe Strain between Simplified and Complete Models. ϕ = 12 in (30.5 cm), t = 0.75 in (19.1 mm), C = 9 ft (2.74 m)

δ (m)	L(m) 200	400	600	800
0.10	0.0009403	0.0009643	0.0009643	0.0009643
0.20	0.0009403	0.0013676	0.0013676	0.0013676
0.30	0.0009403	0.0016764	0.0016764	0.0016764
0.40	0.0009403	0.0018805	0.0019367	0.0019367
0.50	0.0009403	0.0018805	0.0021659	0.0021659
0.60	0.0009403	0.0018805	0.0023730	0.0023730
0.70	0.0009403	0.0018805	0.0025635	0.0025635

TABLE 5–XXVIa Maximum Pipe Strain for a Rigid Block Pattern of Longitudinal PGD Using the Complete Soil–Pipeline Interface Model. ϕ = 30 in (76.2 cm), t = 0.75 in (19.1 mm), C = 9 ft (2.74 m)

δ (m)	L(m) 200	400	600	800
0.10	0.0009403	0.0009697	0.0009697	0.0009697
0.20	0.0009403	0.0013713	0.0013713	0.0013713
0.30	0.0009403	0.0016795	0.0016795	0.0016795
0.40	0.0009403	0.0018805	0.0019393	0.0019393
0.50	0.0009403	0.0018805	0.0021683	0.0021683
0.60	0.0009403	0.0018805	0.0023752	0.0023752
0.70	0.0009403	0.0018805	0.0025655	0.0025655

TABLE 5–XXVIb Maximum Pipe Strain for a Rigid Block Pattern of Longitudinal PGD Using the Simplified Model. ϕ = 30 in (76.2 cm), t = 0.75 in (19.1 mm), C = 9 ft (2.74 m)

δ (m)	L(m) 200	400	600	800
0.10	0.0000000	0.5531716	0.5531716	0.5531716
0.20	0.0000000	0.2754703	0.2754671	0.2754671
0.30	0.0000000	0.1843005	0.1833962	0.1833962
0.40	0.0000000	0.0000000	0.1374539	0.1374539
0.50	0.0000000	0.0000000	0.1099184	0.1099183
0.60	0.0000000	0.0000000	0.0915774	0.0915737
0.70	0.0000000	0.0000000	0.0786115	0.0784765

TABLE 5–XXVIc Percent difference in Maximum Pipe Strain between Simplified and Complete Models. ϕ = 30 in (76.2 cm), t = 0.75 in (19.1 mm), C = 9 ft (2.74 m)

δ (m)	L(m) 200	400	600	800
0.10	0.0009922	0.0009950	0.0009950	0.0009950
0.20	0.0010091	0.0014139	0.0014139	0.0014139
0.30	0.0010091	0.0017344	0.0017344	0.0017344
0.40	0.0010091	0.0020029	0.0020043	0.0020043
0.50	0.0010091	0.0020181	0.0022419	0.0022419
0.60	0.0010091	0.0020181	0.0024567	0.0024567
0.70	0.0010091	0.0020181	0.0026541	0.0026541

TABLE 5–XXVIIa Maximum Pipe Strain for a Rigid Block Pattern of Longitudinal PGD Using the Complete Soil–Pipeline Interface Model. ϕ = 48 in (122 cm), t = 0.75 in (19.1 mm), C = 9 ft (2.74 m)

δ (m)	L(m) 200	400	600	800
0.10	0.0010045	0.0010045	0.0010045	0.0010045
0.20	0.0010091	0.0014206	0.0014206	0.0014206
0.30	0.0010091	0.0017399	0.0017399	0.0017399
0.40	0.0010091	0.0020090	0.0020090	0.0020090
0.50	0.0010091	0.0020181	0.0022462	0.0022462
0.60	0.0010091	0.0020181	0.0024606	0.0024606
0.70	0.0010091	0.0020181	0.0026577	0.0026577

TABLE 5–XXVIIb Maximum Pipe Strain for a Rigid Block Pattern of Longitudinal PGD Using the Simplified Model. ϕ = 48 in (122 cm), t = 0.75 in (19.1 mm), C = 9 ft (2.74 m)

δ (m)	L(m) 200	400	600	800
0.10	1.2395555	0.9556748	0.9556747	0.9556747
0.20	0.0000000	0.4743957	0.4743743	0.4743743
0.30	0.0000000	0.3169429	0.3155167	0.3155167
0.40	0.0000000	0.3081560	0.2363628	0.2363628
0.50	0.0000000	0.0000000	0.1889589	0.1889583
0.60	0.0000000	0.0000000	0.1574030	0.1573920
0.70	0.0000000	0.0000000	0.1350279	0.1348625

TABLE 5–XXVIIc Percent difference in Maximum Pipe Strain between Simplified and Complete Models. ϕ = 48 in (122 cm), t = 0.75 in (19.1 mm), C = 9 ft (2.74 m)

SECTION 6
RAMP/STEP PGD

The axial strain induced in a continuous buried steel pipeline due to a Ramp/Step pattern of longitudinal PGD is determined in this section. As with the other idealized PGD patterns, the burial depth of the pipeline is assumed to be constant in and around the PGD zone and any vertical component of PGD (i.e. subsidence and heaving) is neglected. As shown in Table 3–I the value of D_s, the relative displacement for slippage at the soil pipeline interface, is quite small and as a result the simplified interface model yields accurate results for the idealized PGD patterns investigated in Sections 4 and 5. In this section the simplified model for the soil pipeline interface, that is the rigid spring–slider model shown in Figure 3–3, is used.

As mentioned previously, the idealized Ramp/Step pattern shown in Figure 2–13 could result from a lateral spread near a free face such as a river bank. It would be an appropriate model for the postulated soil displacement pattern shown in Figure 2–10(c) and might be appropriate for the observed PGD patterns shown on the right hand side of Figure 2–6(c), as well as in Figures 2–7(c) and 2–7(o).

As shown in Figure 2–13, a coordinate system is established at the head of the lateral spread zone which has a length L. The soil strains on either side of the zone are zero. Since the Ramp/Step pattern is most likely to occur at a free face, the soil movement would probably be towards the free face resulting in tensile soil strain within the lateral spread zone. Herein, the tensile soil strain is assumed to have constant value of α.

6.1. Possible Configurations

There are two possible configurations for pipeline response to Ramp/Step PGD using the simplified rigid spring–slider model. The first configuration is shown in Figure 6–1 and corresponds to the case where the maximum tensile strain in the pipe is less than the ground strain α. The second configuration is shown in Figure 6–2 where the tensile strain in the pipe is equal to the ground strain, α, over a length L_2. Both configurations are considered herein.

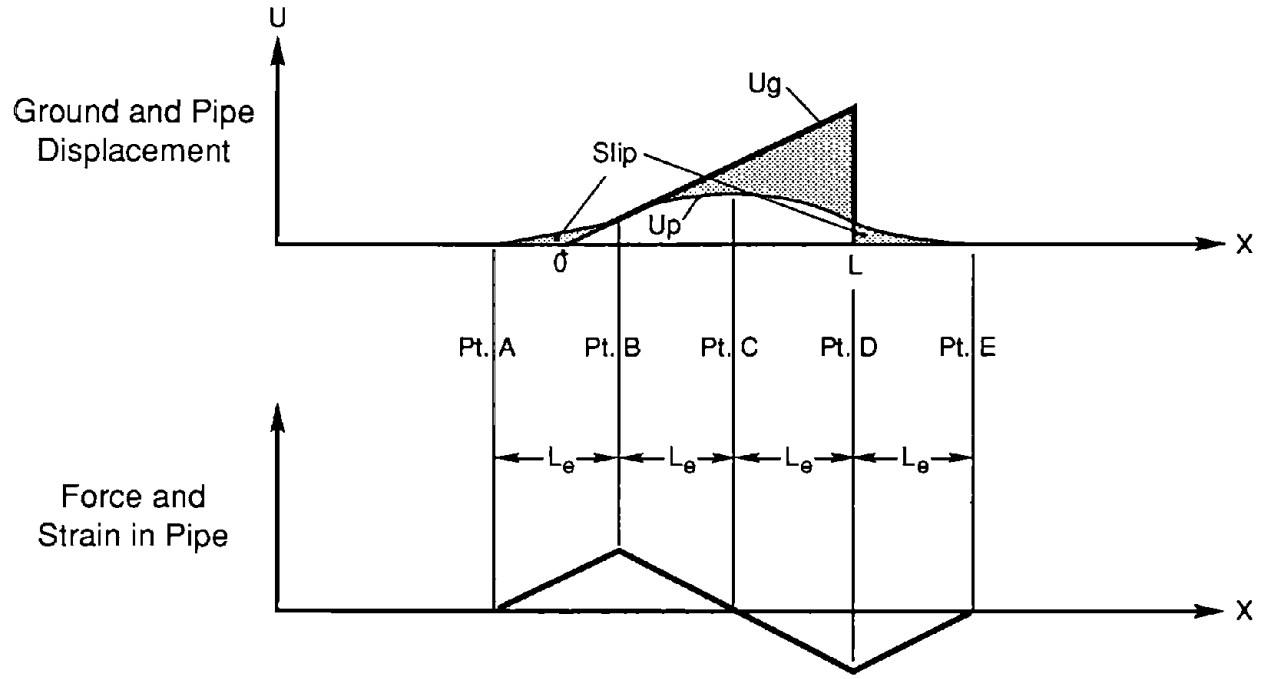

FIGURE 6-1 Simplified Model for Ramp/Step PGD with pipe strain less than ground strain.

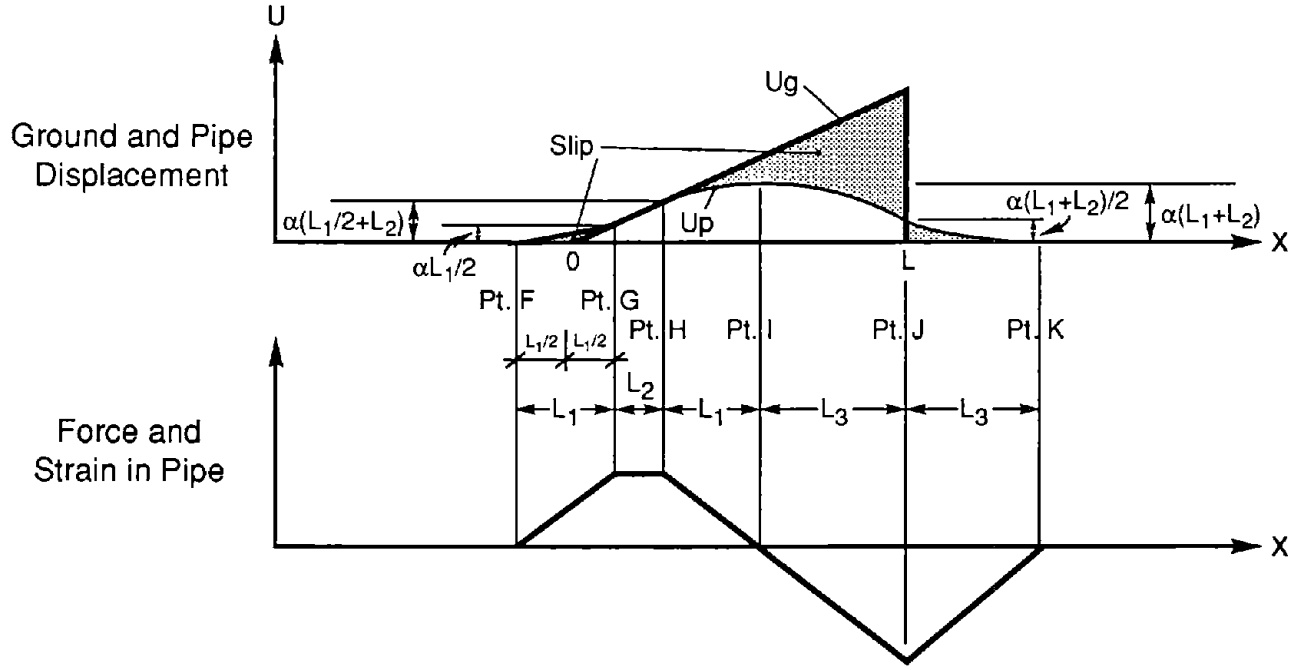

FIGURE 6-2 Simplified Model for Ramp/Step PGD with tensile pipe strain equal to ground strain.

6.2. Tensile Pipe Strain Less Than α

Figure 6.1 shows the case where the pipe strain is less than α. The pipe strain is zero at points A, C and E. The maximum tensile force in the pipe occurs at point B where the pipe displacement matches the ground displacement. The maximum axial displacement of the pipe occurs at point C. The pipe forces to the right of point C, are symmetric about point D. The maximum compressive force in the pipe equal in magnitude to the maximum tensile force, occurs at Point D (i.e., at the free face step). Since the slippage force per unit length is a constant, the separation distances between points A through E is also a constant, L_e. The length L_e can be determined by recalling that the pipe displacement equals the ground displacement at point B. That is

$$U_p(B) = U_g(B) = \alpha(L-2L_e) \tag{6.1}$$

This pipe displacement at point B is due to a force per unit length f_m acting over a length L_e, that is

$$U_p(B) = \int_0^{L_e} \frac{f_m s}{EA}\, ds = \frac{f_m L_e^2}{2EA} \tag{6.2}$$

Equations 6.1 and 6.2 can be solved for the length L_e

$$L_e = \frac{\sqrt{4\alpha^2 + 2f_m \alpha L/EA} - 2\alpha}{f_m/EA} \tag{6.3}$$

which, of course, is always a positive quantity. The maximum pipe strain, tension at point B and compression at point D is then

$$\epsilon = f_m L_e/AE = \sqrt{4\alpha^2 + 2f_m \alpha L/EA} - 2\alpha \tag{6.4}$$

The configuration in Figure 6–1 holds if the maximum pipe strain is less than the ground strain α. Setting $\epsilon < \alpha$ in equation 6.4 yields $L < 5\alpha EA/2f_m$. Hence the configuration in Figure 6–1 is applicable if $L < 5\alpha EA/2f_m$.

6.3 Tensile Pipe Strain Equals α

For an idealized Ramp/Step pattern of longitudinal PGD, the configuration in Figure 6.2 holds if $L > 5\alpha EA/2f_m$. The pipe strain is zero at points F, I and K. The tensile pipe strain equals α over a length L_2 between points G and H, when the pipe displacement matches exactly the assumed ground displacement. The maximum compressive strain in the pipe occurs at point J.

As mentioned above, the force in the pipe at point F is zero. Since the slippage force per unit length between points F and G is a constant, the force in the pipe is a linear function of distance and the pipe axial displacement is a parabolic function of distance between points F and G. Since the pipe strain matches the ground strain at point G, the point of zero ground strain bisects the line segment between F and G as shown in Figure 6.3.

The force in the pipe is zero at point I, and the force per unit length between H and I (decreasing) equals that between F and G (increasing). Hence the distance between H and I must equal L_1. Similarly, the distance between points I and J matches the distance between points J and K. This distance is denoted herein as L_3.

The axial displacement of the pipe equals $\alpha L_1/2$ at point G and $\alpha(L_1/2 + L_2)$ at point H. Since the pipe displacement is zero at point F and the force in the pipe between F and I is symmetric about the midpoint of segment FI, the pipe displacement at point I is $\alpha(L_1 + L_2)$. Similarly, the axial displacement of the pipe at point J equals $\alpha(L_1 + L_2)/2$.

For the configuration in Figure 6–2, the maximum tensile pipe strain is α. The maximum compressive pipe strain is determined herein by enforcing continuity. Recall that the pipe displacement at point G equals the assumed ground displacement at that point

$$U_p(G) = U_g(G) = \frac{\alpha L_1}{2} \tag{6.5}$$

The pipe displacement at this point is due to a force per unit length f_m acting over a distance of L_1, hence

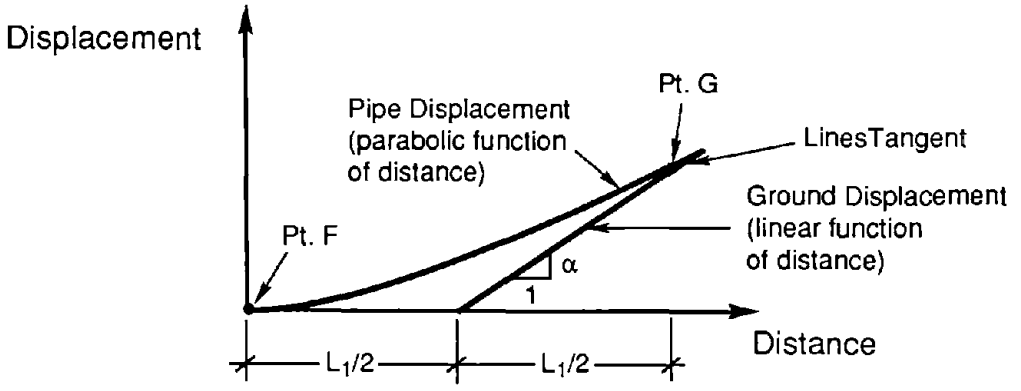

FIGURE 6-3 Diagram showing point of zero ground strain bisecting line segment between F and G.

$$U_p(G) = \int_0^{L_1} \frac{f_m s}{EA} ds = \frac{f_m L_1^2}{2EA} \tag{6.6}$$

Hence, from equations 6.5 and 6.6, we have

$$L_1 = \frac{\alpha EA}{f_m} \tag{6.7}$$

The pipe displacement at point J must equal the pipe displacement at point H plus the stretching and/or compression over the distance from H to J.

$$U_p(H) + \int_H^J \frac{f(s)}{EA} ds = U_p(J) \tag{6.8}$$

or

$$\alpha\left(\frac{L_1}{2} + L_2\right) + \int_0^{L_1+L_3} \left[\frac{L_1 f_m}{EA} - \frac{f_m s}{EA}\right] ds = \frac{\alpha}{2}(L_1 + L_2) \tag{6.9}$$

which reduces to

$$L_2 = \frac{f_m}{\alpha EA}[L_3^2 - L_1^2] \tag{6.10}$$

Finally, note that the total length of the lateral spread zone L is

$$L = \frac{3L_1}{2} + L_2 + L_3 \tag{6.11}$$

Combining equations (6.7), (6.10) and (6.11) results in the following expression for the length L_3

$$L_3 = \frac{\sqrt{\frac{4 f_m L}{\alpha EA} - 1} - 1}{\frac{2 f_m}{\alpha EA}} \tag{6.12}$$

The maximum compressive strain in the pipe, which occurs at point J, is simply

$$\epsilon = f_m L_3/EA = \frac{\alpha}{2}\left[\sqrt{\frac{4f_m L}{\alpha EA} - 1} - 1\right] \tag{6.13}$$

For $L > 5\alpha EA/2f_m$ which applies to the situation in Figure 6–2, the maximum compressive strain in the pipe, by equation (6.13), is larger than the tensile ground strain α.

6.4 Maximum Pipe Strain

Tables 6–I through 6–XXVII present the maximum compressive pipe strain for an idealized Ramp/Step pattern of longitudinal PGD. Results are calculated using equation (6.4) for $L < 5\alpha EA/2f_m$, and using equation (6.13) for $L > 5\alpha EA/2f_m$.

As with the tables in Sections 4 and 5, the unit weight of the soil, γ, is taken as 100 pcf and the coefficient of friction of the soil pipeline interface, μ, is taken as 0.75. Results are presented for pipe diameters, ϕ, of 12, 30 and 48 inches, pipe wall thicknesses, t, of 1/4, 1/2 and 3/4 inches and for 3, 6 and 9 feet of soil cover, C, over the the top of the pipe.

The range of values for the ground strain, α, and the length of the lateral spread zone L are the same as those used for the Ramp pattern in Section 4. That is, α and L are based upon the work of Suzuki and Masuda [8].

For a fixed value of the ground strain, α, pipe strain is an increasing function of the length of the lateral spread zone L. For a fixed value of L, the pipe strain is an increasing function of α. For fixed α and L, pipe strain is an increasing function of the burial depth H, or C, and a decreasing function of the wall thickness t. For a fixed burial depth to the pipe centerline H, the pipe strain is not a function of the pipe diameter ϕ. This results from the fact that both the slippage force, f_m, and the pipe cross–sectional area, A, are proportional to the pipe diameter, ϕ

α	L(m) 25	50	100	150	200
0.0025	0.0001190	0.0002353	0.0004604	0.0006766	0.0008849
0.0033	0.0001193	0.0002366	0.0004654	0.0006870	0.0009022
0.0050	0.0001197	0.0002380	0.0004705	0.0006980	0.0009208
0.0100	0.0001200	0.0002394	0.0004759	0.0007098	0.0009411
0.0200	0.0001202	0.0002401	0.0004787	0.0007160	0.0009519

TABLE 6–I Maximum Compressive Pipe Strain for a Ramp/Step Pattern of Longitudinal PGD using the Simplified Soil–Pipeline Interface Model. ϕ = 12 in (30.5 cm), t = 0.25 in (6.4 mm), C = 3 ft (0.91 m)

α	L(m) 25	50	100	150	200
0.0025	0.0001441	0.0002843	0.0005541	0.0008114	0.0010577
0.0033	0.0001446	0.0002863	0.0005612	0.0008260	0.0010818
0.0050	0.0001451	0.0002882	0.0005686	0.0008418	0.0011082
0.0100	0.0001457	0.0002903	0.0005765	0.0008588	0.0011373
0.0200	0.0001459	0.0002913	0.0005806	0.0008678	0.0011530

TABLE 6–II Maximum Compressive Pipe Strain for a Ramp/Step Pattern of Longitudinal PGD using the Simplified Soil–Pipeline Interface Model. ϕ = 30 in (76.2 cm), t = 0.25 in (6.4 mm), C = 3 ft (0.91 m)

α	L(m) 25	50	100	150	200
0.0025	0.0001691	0.0003329	0.0006462	0.0009431	0.0012258
0.0033	0.0001698	0.0003356	0.0006557	0.0009625	0.0012574
0.0050	0.0001705	0.0003383	0.0006658	0.0009836	0.0012925
0.0100	0.0001713	0.0003411	0.0006766	0.0010067	0.0013317
0.0200	0.0001716	0.0003425	0.0006822	0.0010190	0.0013531

TABLE 6–III Maximum Compressive Pipe Strain for a Ramp/Step Pattern of Longitudinal PGD using the Simplified Soil–Pipeline Interface Model. ϕ = 48 in (122 cm), t = 0.25 in (6.4 mm), C = 3 ft (0.91 m)

α	L(m) 25	50	100	150	200
0.0025	0.0002188	0.0004288	0.0008261	0.0011981	0.0015489
0.0033	0.0002200	0.0004331	0.0008413	0.0012284	0.0015974
0.0050	0.0002212	0.0004376	0.0008576	0.0012620	0.0016523
0.0100	0.0002224	0.0004423	0.0008752	0.0012994	0.0017152
0.0200	0.0002230	0.0004447	0.0008846	0.0013198	0.0017505

TABLE 6–IV Maximum Compressive Pipe Strain for a Ramp/Step Pattern of Longitudinal PGD using the Simplified Soil–Pipeline Interface Model. ϕ = 12 in (30.5 cm), t = 0.25 in (6.4 mm), C = 6 ft (1.83 m)

α	L(m) 25	50	100	150	200
0.0025	0.0002435	0.0004761	0.0009140	0.0013217	0.0017046
0.0033	0.0002449	0.0004814	0.0009324	0.0013581	0.0017623
0.0050	0.0002464	0.0004869	0.0009523	0.0013986	0.0018281
0.0100	0.0002479	0.0004927	0.0009739	0.0014443	0.0019045
0.0200	0.0002486	0.0004957	0.0009855	0.0014694	0.0019478

TABLE 6–V Maximum Compressive Pipe Strain for a Ramp/Step Pattern of Longitudinal PGD using the Simplified Soil–Pipeline Interface Model. ϕ = 30 in (76.2 cm), t = 0.25 in (6.4 mm), C = 6 ft (1.83 m)

α	L(m) 25	50	100	150	200
0.0025	0.0002680	0.0005230	0.0010007	0.0014430	0.0018568
0.0033	0.0002697	0.0005294	0.0010224	0.0014857	0.0019240
0.0050	0.0002715	0.0005360	0.0010461	0.0015336	0.0020013
0.0100	0.0002733	0.0005430	0.0010721	0.0015881	0.0020922
0.0200	0.0002743	0.0005467	0.0010861	0.0016185	0.0021441

TABLE 6–VI Maximum Compressive Pipe Strain for a Ramp/Step Pattern of Longitudinal PGD using the Simplified Soil–Pipeline Interface Model. ϕ = 48 in (122 cm), t = 0.25 in (6.4 mm), C = 6 ft (1.83 m)

α	L(m) 25	50	100	150	200
0.0025	0.0003168	0.0006157	0.0011702	0.0016789	0.0021515
0.0033	0.0003192	0.0006244	0.0011993	0.0017350	0.0022386
0.0050	0.0003216	0.0006335	0.0012314	0.0017990	0.0023405
0.0100	0.0003242	0.0006433	0.0012671	0.0018731	0.0024628
0.0200	0.0003255	0.0006483	0.0012865	0.0019150	0.0025341

TABLE 6–VII Maximum Compressive Pipe Strain for a Ramp/Step Pattern of Longitudinal PGD using the Simplified Soil–Pipeline Interface Model. ϕ = 12 in (30.5 cm), t = 0.25 in (6.4 mm), C = 9 ft (2.74 m)

α	L(m) 25	50	100	150	200
0.0025	0.0003410	0.0006614	0.0012533	0.0017938	0.0022944
0.0033	0.0003437	0.0006714	0.0012863	0.0018570	0.0023918
0.0050	0.0003466	0.0006819	0.0013229	0.0019295	0.0025066
0.0100	0.0003495	0.0006932	0.0013639	0.0020142	0.0026458
0.0200	0.0003511	0.0006991	0.0013864	0.0020624	0.0027278

TABLE 6–VIII Maximum Compressive Pipe Strain for a Ramp/Step Pattern of Longitudinal PGD using the Simplified Soil–Pipeline Interface Model. ϕ = 30 in (76.2 cm), t = 0.25 in (6.4 mm), C = 9 ft (2.74 m)

α	L(m) 25	50	100	150	200
0.0025	0.0003651	0.0007068	0.0013353	0.0019068	0.0024345
0.0033	0.0003682	0.0007181	0.0013723	0.0019772	0.0025424
0.0050	0.0003715	0.0007301	0.0014137	0.0020585	0.0026706
0.0100	0.0003749	0.0007430	0.0014603	0.0021544	0.0028273
0.0200	0.0003766	0.0007498	0.0014860	0.0022094	0.0029206

TABLE 6–IX Maximum Compressive Pipe Strain for a Ramp/Step Pattern of Longitudinal PGD using the Simplified Soil–Pipeline Interface Model. ϕ = 48 in (122 cm), t = 0.25 in (6.4 mm), C = 9 ft (2.74 m)

α	L(m) 25	50	100	150	200
0.0025	0.0000598	0.0001190	0.0002353	0.0003490	0.0004604
0.0033	0.0000599	0.0001193	0.0002366	0.0003519	0.0004654
0.0050	0.0000600	0.0001197	0.0002380	0.0003549	0.0004705
0.0100	0.0000601	0.0001200	0.0002394	0.0003580	0.0004759
0.0200	0.0000602	0.0001202	0.0002401	0.0003596	0.0004787

TABLE 6–X Maximum Compressive Pipe Strain for a Ramp/Step Pattern of Longitudinal PGD using the Simplified Soil–Pipeline Interface Model. ϕ = 12 in (30.5 cm), t = 0.50 in (12.7 mm), C = 3 ft (0.91 m)

α	L(m) 25	50	100	150	200
0.0025	0.0000726	0.0001441	0.0002843	0.0004209	0.0005541
0.0033	0.0000727	0.0001446	0.0002863	0.0004250	0.0005612
0.0050	0.0000728	0.0001451	0.0002882	0.0004294	0.0005686
0.0100	0.0000730	0.0001457	0.0002903	0.0004339	0.0005765
0.0200	0.0000730	0.0001459	0.0002913	0.0004362	0.0005806

TABLE 6–XI Maximum Compressive Pipe Strain for a Ramp/Step Pattern of Longitudinal PGD using the Simplified Soil–Pipeline Interface Model. ϕ = 30 in (76.2 cm), t = 0.50 in (12.7 mm), C = 3 ft (0.91 m)

α	L(m) 25	50	100	150	200
0.0025	0.0000853	0.0001691	0.0003329	0.0004918	0.0006462
0.0033	0.0000855	0.0001698	0.0003356	0.0004974	0.0006557
0.0050	0.0000856	0.0001705	0.0003383	0.0005033	0.0006658
0.0100	0.0000858	0.0001713	0.0003411	0.0005095	0.0006766
0.0200	0.0000859	0.0001716	0.0003425	0.0005127	0.0006822

TABLE 6–XII Maximum Compressive Pipe Strain for a Ramp/Step Pattern of Longitudinal PGD using the Simplified Soil–Pipeline Interface Model. ϕ = 48 in (122 cm), t = 0.50 in (12.7 mm), C = 3 ft (0.91 m)

α	L(m) 25	50	100	150	200
0.0025	0.0001106	0.0002188	0.0004288	0.0006310	0.0008261
0.0033	0.0001109	0.0002200	0.0004331	0.0006401	0.0008413
0.0050	0.0001112	0.0002212	0.0004376	0.0006497	0.0008576
0.0100	0.0001115	0.0002224	0.0004423	0.0006599	0.0008752
0.0200	0.0001116	0.0002230	0.0004447	0.0006653	0.0008846

TABLE 6–XIII Maximum Compressive Pipe Strain for a Ramp/Step Pattern of Longitudinal PGD using the Simplified Soil–Pipeline Interface Model. ϕ = 12 in (30.5 cm), t = 0.50 in (12.7 mm), C = 6 ft (1.83 m)

α	L(m) 25	50	100	150	200
0.0025	0.0001232	0.0002435	0.0004761	0.0006993	0.0009140
0.0033	0.0001236	0.0002449	0.0004814	0.0007104	0.0009324
0.0050	0.0001239	0.0002464	0.0004869	0.0007221	0.0009523
0.0100	0.0001243	0.0002479	0.0004927	0.0007347	0.0009739
0.0200	0.0001245	0.0002486	0.0004957	0.0007413	0.0009855

TABLE 6–XIV Maximum Compressive Pipe Strain for a Ramp/Step Pattern of Longitudinal PGD using the Simplified Soil–Pipeline Interface Model. ϕ = 30 in (76.2 cm), t = 0.50 in (12.7 mm), C = 6 ft (1.83 m)

α	L(m) 25	50	100	150	200
0.0025	0.0001358	0.0002680	0.0005230	0.0007668	0.0010007
0.0033	0.0001362	0.0002697	0.0005294	0.0007800	0.0010224
0.0050	0.0001367	0.0002715	0.0005360	0.0007941	0.0010461
0.0100	0.0001371	0.0002733	0.0005430	0.0008092	0.0010721
0.0200	0.0001374	0.0002743	0.0005467	0.0008172	0.0010861

TABLE 6–XV Maximum Compressive Pipe Strain for a Ramp/Step Pattern of Longitudinal PGD using the Simplified Soil–Pipeline Interface Model. ϕ = 48 in (122 cm), t = 0.50 in (12.7 mm), C = 6 ft (1.83 m)

α	L(m) 25	50	100	150	200
0.0025	0.0001608	0.0003168	0.0006157	0.0008995	0.0011702
0.0033	0.0001614	0.0003192	0.0006244	0.0009173	0.0011993
0.0050	0.0001621	0.0003216	0.0006335	0.0009365	0.0012314
0.0100	0.0001627	0.0003242	0.0006433	0.0009575	0.0012671
0.0200	0.0001631	0.0003255	0.0006483	0.0009687	0.0012865

TABLE 6–XVI Maximum Compressive Pipe Strain for a Ramp/Step Pattern of Longitudinal PGD using the Simplified Soil–Pipeline Interface Model. ϕ = 12 in (30.5 cm), t = 0.50 in (12.7 mm), C = 9 ft (2.74 m)

α	L(m) 25	50	100	150	200
0.0025	0.0001733	0.0003410	0.0006614	0.0009647	0.0012533
0.0033	0.0001740	0.0003437	0.0006714	0.0009850	0.0012863
0.0050	0.0001748	0.0003466	0.0006819	0.0010071	0.0013229
0.0100	0.0001755	0.0003495	0.0006932	0.0010312	0.0013639
0.0200	0.0001759	0.0003511	0.0006991	0.0010442	0.0013864

TABLE 6–XVII Maximum Compressive Pipe Strain for a Ramp/Step Pattern of Longitudinal PGD using the Simplified Soil–Pipeline Interface Model. ϕ = 30 in (76.2 cm), t = 0.50 in (12.7 mm), C = 9 ft (2.74 m)

α	L(m) 25	50	100	150	200
0.0025	0.0001857	0.0003651	0.0007068	0.0010293	0.0013353
0.0033	0.0001866	0.0003682	0.0007181	0.0010522	0.0013723
0.0050	0.0001874	0.0003715	0.0007301	0.0010772	0.0014137
0.0100	0.0001883	0.0003749	0.0007430	0.0011047	0.0014603
0.0200	0.0001888	0.0003766	0.0007498	0.0011195	0.0014860

TABLE 6–XVIII Maximum Compressive Pipe Strain for a Ramp/Step Pattern of Longitudinal PGD using the Simplified Soil–Pipeline Interface Model. ϕ = 48 in (122 cm), t = 0.50 in (12.7 mm), C = 9 ft (2.74 m)

α	L(m) 25	50	100	150	200
0.0025	0.0000400	0.0000796	0.0001580	0.0002353	0.0003114
0.0033	0.0000400	0.0000798	0.0001586	0.0002366	0.0003137
0.0050	0.0000401	0.0000799	0.0001593	0.0002380	0.0003161
0.0100	0.0000401	0.0000801	0.0001599	0.0002394	0.0003185
0.0200	0.0000401	0.0000802	0.0001602	0.0002401	0.0003198

TABLE 6–XIX Maximum Compressive Pipe Strain for a Ramp/Step Pattern of Longitudinal PGD using the Simplified Soil–Pipeline Interface Model. ϕ = 12 in (30.5 cm), t = 0.75 in (19.1 mm), C = 3 ft (0.91 m)

α	L(m) 25	50	100	150	200
0.0025	0.0000485	0.0000965	0.0001913	0.0002843	0.0003757
0.0033	0.0000486	0.0000968	0.0001922	0.0002863	0.0003791
0.0050	0.0000486	0.0000970	0.0001931	0.0002882	0.0003825
0.0100	0.0000487	0.0000972	0.0001940	0.0002903	0.0003861
0.0200	0.0000487	0.0000973	0.0001945	0.0002913	0.0003880

TABLE 6–XX Maximum Compressive Pipe Strain for a Ramp/Step Pattern of Longitudinal PGD using the Simplified Soil–Pipeline Interface Model. ϕ = 30 in (76.2 cm), t = 0.75 in (19.1 mm), C = 3 ft (0.91 m)

α	L(m) 25	50	100	150	200
0.0025	0.0000570	0.0001134	0.0002243	0.0003329	0.0004394
0.0033	0.0000571	0.0001137	0.0002255	0.0003356	0.0004439
0.0050	0.0000572	0.0001140	0.0002268	0.0003383	0.0004486
0.0100	0.0000573	0.0001143	0.0002280	0.0003411	0.0004535
0.0200	0.0000573	0.0001145	0.0002287	0.0003425	0.0004561

TABLE 6–XXI Maximum Compressive Pipe Strain for a Ramp/Step Pattern of Longitudinal PGD using the Simplified Soil–Pipeline Interface Model. ϕ = 48 in (122 cm), t = 0.75 in (19.1 mm), C = 3 ft (0.91 m)

α	L(m) 25	50	100	150	200
0.0025	0.0000740	0.0001469	0.0002897	0.0004288	0.0005644
0.0033	0.0000741	0.0001474	0.0002917	0.0004331	0.0005717
0.0050	0.0000743	0.0001480	0.0002938	0.0004376	0.0005795
0.0100	0.0000744	0.0001485	0.0002959	0.0004423	0.0005876
0.0200	0.0000745	0.0001488	0.0002970	0.0004447	0.0005919

TABLE 6–XXII Maximum Compressive Pipe Strain for a Ramp/Step Pattern of Longitudinal PGD using the Simplified Soil–Pipeline Interface Model. ϕ = 12 in (30.5 cm), t = 0.75 in (19.1 mm), C = 6 ft (1.83 m)

α	L(m) 25	50	100	150	200
0.0025	0.0000825	0.0001636	0.0003222	0.0004761	0.0006259
0.0033	0.0000826	0.0001642	0.0003246	0.0004814	0.0006348
0.0050	0.0000828	0.0001649	0.0003272	0.0004869	0.0006443
0.0100	0.0000830	0.0001656	0.0003298	0.0004927	0.0006544
0.0200	0.0000830	0.0001659	0.0003312	0.0004957	0.0006596

TABLE 6–XXIII Maximum Compressive Pipe Strain for a Ramp/Step Pattern of Longitudinal PGD using the Simplified Soil–Pipeline Interface Model. ϕ = 30 in (76.2 cm), t = 0.75 in (19.1 mm), C = 6 ft (1.83 m)

α	L(m) 25	50	100	150	200
0.0025	0.0000909	0.0001802	0.0003544	0.0005230	0.0006867
0.0033	0.0000911	0.0001810	0.0003574	0.0005294	0.0006974
0.0050	0.0000913	0.0001818	0.0003604	0.0005360	0.0007087
0.0100	0.0000915	0.0001826	0.0003636	0.0005430	0.0007209
0.0200	0.0000916	0.0001830	0.0003653	0.0005467	0.0007273

TABLE 6–XXIV Maximum Compressive Pipe Strain for a Ramp/Step Pattern of Longitudinal PGD using the Simplified Soil–Pipeline Interface Model. ϕ = 48 in (122 cm), t = 0.75 in (19.1 mm), C = 6 ft (1.83 m)

α	L(m) 25	50	100	150	200
0.0025	0.0001078	0.0002133	0.0004182	0.0006157	0.0008064
0.0033	0.0001081	0.0002144	0.0004224	0.0006244	0.0008209
0.0050	0.0001083	0.0002155	0.0004266	0.0006335	0.0008365
0.0100	0.0001086	0.0002167	0.0004311	0.0006433	0.0008533
0.0200	0.0001088	0.0002173	0.0004334	0.0006483	0.0008622

TABLE 6–XXV Maximum Compressive Pipe Strain for a Ramp/Step Pattern of Longitudinal PGD using the Simplified Soil–Pipeline Interface Model. ϕ = 12 in (30.5 cm), t = 0.75 in (19.1 mm), C = 9 ft (2.74 m)

α	L(m) 25	50	100	150	200
0.0025	0.0001162	0.0002298	0.0004499	0.0006614	0.0008654
0.0033	0.0001165	0.0002311	0.0004546	0.0006714	0.0008819
0.0050	0.0001169	0.0002324	0.0004596	0.0006819	0.0008998
0.0100	0.0001172	0.0002337	0.0004647	0.0006932	0.0009191
0.0200	0.0001174	0.0002344	0.0004674	0.0006991	0.0009295

TABLE 6–XXVI Maximum Compressive Pipe Strain for a Ramp/Step Pattern of Longitudinal PGD using the Simplified Soil–Pipeline Interface Model. ϕ = 30 in (76.2 cm), t = 0.75 in (19.1 mm), C = 9 ft (2.74 m)

α	L(m) 25	50	100	150	200
0.0025	0.0001246	0.0002462	0.0004814	0.0007068	0.0009237
0.0033	0.0001250	0.0002477	0.0004868	0.0007181	0.0009424
0.0050	0.0001253	0.0002492	0.0004924	0.0007301	0.0009627
0.0100	0.0001257	0.0002507	0.0004983	0.0007430	0.0009848
0.0200	0.0001259	0.0002515	0.0005014	0.0007498	0.0009966

TABLE 6–XXVII Maximum Compressive Pipe Strain for a Ramp/Step Pattern of Longitudinal PGD using the Simplified Soil–Pipeline Interface Model. ϕ = 48 in (122 cm), t = 0.75 in (19.1 mm), C = 9 ft (2.74 m)

SECTION 7
RIDGE PGD

The axial strain induced in a continuous steel pipeline due to a Ridge pattern of longitudinal PGD is determined in this section. As with the other idealized PGD patterns, the burial depth of the pipeline is assumed to be constant in and around the PGD zone and any vertical component of PGD (i.e. subsidence and heaving) is neglected. As shown in Table 3.1 the value of D_s, the relative displacement for slippage at the soil pipeline interface, is quite small and as a result the simplified interface model yields accurate results for the idealized PGD patterns investigated in Sections 4 and 5. As in Section 6, the simplified model for the soil pipeline interface, that is the rigid spring–slider model shown in Figure 3–3, is used herein to evaluate pipe strains.

As mentioned previously, the idealized Ridge pattern shown in Figure 2–14 may be an appropriate model for the observed PGD patterns to the left of the Bandai Bridge in Figure 2–6(c), in Figures 2–7(b) and on the south side of the Yoshino Creek in Figure 2–8.

As shown in Figure 2--14, a coordinate system is established at the head of the lateral spread zone which has a length L. The soil strains on either side of the zone are zero. Within the lateral spread zone, there is uniform tensile ground strain, α, to the left of the ridge and uniform compressive ground strain, α, to the right of the ridge.

7.1. Possible Configurations

There are two possible configurations for pipeline response to Ridge PGD using the simplified rigid spring–slider model. The first configuration is shown in Figure 7–1 and corresponds to the case where the maximum strain in the pipe is less than the ground strain α. The second configuration is shown in Figure 7–2 where the strain in the pipe is equal to the ground strain α over a limited distance on each side of the ridge. Both configurations are considered herein.

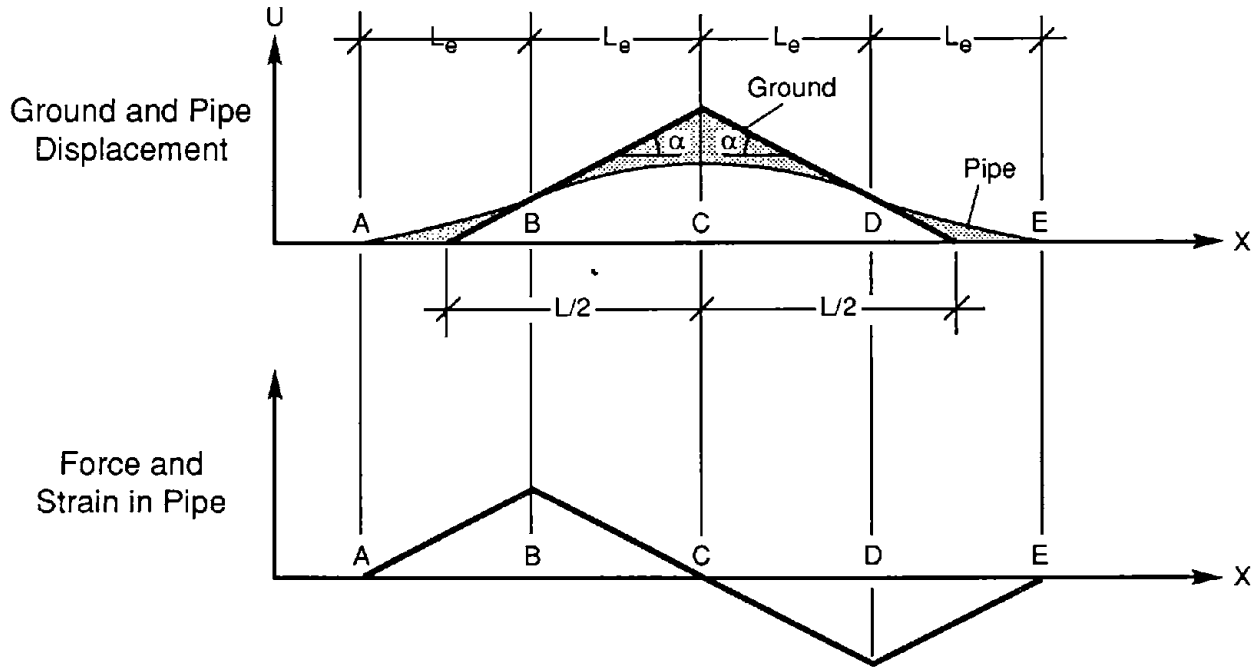

FIGURE 7-1 Simplified Model for Ridge PGD with pipe strain less than ground strain.

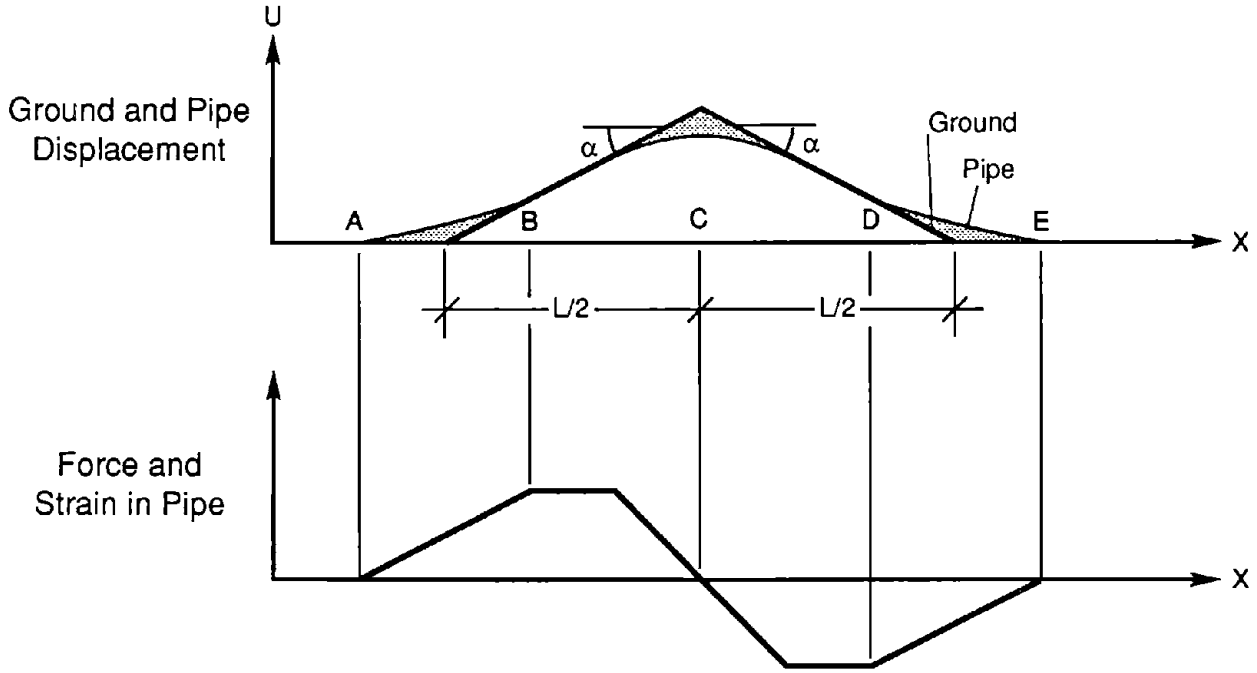

FIGURE 7-2 Simplified Model for Ridge PGD with maximum pipe strain equal to ground strain.

7.2. Tensile Pipe Strain Less Than α

Figure 7.1 shows the case where the pipe strain is less than α. The pipe strain is zero at points A, C and E. The maximum tensile and compressive strains in the pipe occur at points B and D respectively. The pipe displacement matches the ground displacement at these points. The maximum axial displacement of the pipe occurs directly under the ridge, at point C. To the left and right of point C, the pipe force is symmetric about points B and D respectively. Since the slippage force per unit length is a constant, the separation distances between points A through E is also a constant L_e. The length L_e can be determined by recalling that the pipe displacement equals the ground displacement at point B.

$$U_p(B) = U_g(B) = \alpha(\frac{L}{2} - L_e) \tag{7.1}$$

This pipe displacement at point B is due to a force per unit length f_m acting over a length L_e,

$$U_p(B) = \int_0^{L_e} \frac{f_m s}{EA} ds = \frac{f_m L_e^2}{2EA} \tag{7.2}$$

Equations 7.1 and 7.2 can be solved for the length L_e

$$L_e = \frac{\sqrt{\alpha^2 + f_m L \alpha/EA} - \alpha}{f_m/EA} \tag{7.3}$$

which, of course, is always a positive quantity. The maximum pipe strain, tension at point B and compression at point D is then

$$\epsilon = f_m L_e/AE = \sqrt{\alpha^2 + f_m L \alpha/EA} - \alpha \tag{7.4}$$

The configuration in Figure 7–1 holds if the maximum pipe strain is less than the ground strain α. Setting $\epsilon < \alpha$ in equation 7.4 yields $L < 3\alpha EA/f_m$. That is, the configuration in Figure 7–1 is applicable if $L < 3\alpha EA/f_m$.

7.3 Tensile Pipe Strain Equals α

For an idealized Ridge pattern of longitudinal PGD, the configuration in Figure 7–2 holds if $L > 3\alpha EA/f_m$. For this case, the maximum tensile pipe strain equals the ground strain α over a limited distance somewhere to the left of point C while the maximum compressive pipe strain equals the ground strain, α, over a limited distance somewhere to the right of point C.

7.4 Maximum Pipe Strain

Tables 7–I through 7–XXVII present the maximum pipe strain for an idealized Ridge pattern of longitudinal PGD. Results are calculated using equation (7.4) for $L < 3\alpha EA/f_m$. For $L > 3\alpha EA/f_m$ the maximum pipe strain equals the ground strain α.

As with the tables in Sections 4 through 6, the unit weight of the soil, γ, is taken as 100 pcf and the coefficient of friction at the soil pipeline interface, μ, is taken as 0.75. Results are presented for pipe diameters, ϕ, of 12, 30 and 48 inches, pipe wall thicknesses, t, of 1/4, 1/2 and 3/4 inches and for 3, 6 and 9 feet of soil cover, C, over the the top of the pipe.

The range of values for the ground strain, α, and the length of the lateral spread zone, L, are the same as those used for the Ramp pattern in Section 4 and the Ramp/Step pattern in Section 6.

For a fixed value of the ground strain α, pipe strain is an increasing function of the length of the lateral spread zone for $L \leq 3\alpha EA/f_m$. For lengths beyond that value the pipe strain is a constant. For a fixed value of L, the pipe strain is an increasing function of the burial depth, H or C, and a decreasing function of the pipe wall thickness t. For a fixed burial depth to the pipe centerline, H, the pipe strain is not a function of the pipe diameter ϕ. This results from both f_m and A being proportional to the pipe diameter ϕ.

α	L(m) 25	50	100	150	200
0.0025	0.0001176	0.0002302	0.0004424	0.0006404	0.0008266
0.0033	0.0001183	0.0002327	0.0004511	0.0006575	0.0008538
0.0050	0.0001190	0.0002353	0.0004604	0.0006766	0.0008849
0.0100	0.0001197	0.0002380	0.0004705	0.0006980	0.0009208
0.0200	0.0001200	0.0002394	0.0004759	0.0007098	0.0009411

TABLE 7–I Maximum Pipe Strain for a Ridge Pattern of Longitudinal PGD Using the Simplified Soil–Pipeline Interface Model.
ϕ = 12 in (30.5 cm), t = 0.25 in (6.4 mm), C = 3 ft (0.91 m)

α	L(m) 25	50	100	150	200
0.0025	0.0001422	0.0002770	0.0005289	0.0007613	0.0009782
0.0033	0.0001431	0.0002806	0.0005409	0.0007848	0.0010150
0.0050	0.0001441	0.0002843	0.0005541	0.0008114	0.0010577
0.0100	0.0001451	0.0002882	0.0005686	0.0008418	0.0011082
0.0200	0.0001457	0.0002903	0.0005765	0.0008588	0.0011373

TABLE 7–II Maximum Pipe Strain for a Ridge Pattern of Longitudinal PGD Using the Simplified Soil–Pipeline Interface Model.
ϕ = 30 in (76.2 cm), t = 0.25 in (6.4 mm), C = 3 ft (0.91 m)

α	L(m) 25	50	100	150	200
0.0025	0.0001665	0.0003231	0.0006129	0.0008779	0.0011235
0.0033	0.0001678	0.0003279	0.0006287	0.0009083	0.0011705
0.0050	0.0001691	0.0003329	0.0006462	0.0009431	0.0012258
0.0100	0.0001705	0.0003383	0.0006658	0.0009836	0.0012925
0.0200	0.0001713	0.0003411	0.0006766	0.0010067	0.0013317

TABLE 7–III Maximum Pipe Strain for a Ridge Pattern of Longitudinal PGD Using the Simplified Soil–Pipeline Interface Model.
ϕ = 48 in (122 cm), t = 0.25 in (6.4 mm), C = 3 ft (0.91 m)

α	L(m) 25	50	100	150	200
0.0025	0.0002144	0.0004131	0.0007744	0.0010997	0.0013979
0.0033	0.0002166	0.0004207	0.0007987	0.0011450	0.0014663
0.0050	0.0002188	0.0004288	0.0008261	0.0011981	0.0015489
0.0100	0.0002212	0.0004376	0.0008576	0.0012620	0.0016523
0.0200	0.0002224	0.0004423	0.0008752	0.0012994	0.0017152

TABLE 7–IV Maximum Pipe Strain for a Ridge Pattern of Longitudinal PGD Using the Simplified Soil–Pipeline Interface Model.
ϕ = 12 in (30.5 cm), t = 0.25 in (6.4 mm), C = 6 ft (1.83 m)

α	L(m) 25	50	100	150	200
0.0025	0.0002381	0.0004570	0.0008523	0.0012057	0.0015281
0.0033	0.0002407	0.0004662	0.0008811	0.0012587	0.0016076
0.0050	0.0002435	0.0004761	0.0009140	0.0013217	0.0017046
0.0100	0.0002464	0.0004869	0.0009523	0.0013986	0.0018281
0.0200	0.0002479	0.0004927	0.0009739	0.0014443	0.0019045

TABLE 7–V Maximum Pipe Strain for a Ridge Pattern of Longitudinal PGD Using the Simplified Soil–Pipeline Interface Model.
ϕ = 30 in (76.2 cm), t = 0.25 in (6.4 mm), C = 6 ft (1.83 m)

α	L(m) 25	50	100	150	200
0.0025	0.0002615	0.0005003	0.0009284	0.0013087	0.0016543
0.0033	0.0002647	0.0005112	0.0009620	0.0013698	0.0017449
0.0050	0.0002680	0.0005230	0.0010007	0.0014430	0.0018568
0.0100	0.0002715	0.0005360	0.0010461	0.0015336	0.0020013
0.0200	0.0002733	0.0005430	0.0010721	0.0015881	0.0020922

TABLE 7–VI Maximum Pipe Strain for a Ridge Pattern of Longitudinal PGD Using the Simplified Soil–Pipeline Interface Model.
ϕ = 48 in (122 cm), t = 0.25 in (6.4 mm), C = 6 ft (1.83 m)

α	L(m) 25	50	100	150	200
0.0025	0.0003078	0.0005851	0.0010757	0.0015067	0.0018957
0.0033	0.0003122	0.0005997	0.0011193	0.0015843	0.0020090
0.0050	0.0003168	0.0006157	0.0011702	0.0016789	0.0021515
0.0100	0.0003216	0.0006335	0.0012314	0.0017990	0.0023405
0.0200	0.0003242	0.0006433	0.0012671	0.0018731	0.0024628

TABLE 7–VII Maximum Pipe Strain for a Ridge Pattern of Longitudinal PGD Using the Simplified Soil–Pipeline Interface Model.
ϕ = 12 in (30.5 cm), t = 0.25 in (6.4 mm), C = 9 ft (2.74 m)

α	L(m) 25	50	100	150	200
0.0025	0.0003307	0.0006267	0.0011472	0.0016022	0.0020115
0.0033	0.0003357	0.0006432	0.0011959	0.0016881	0.0021363
0.0050	0.0003410	0.0006614	0.0012533	0.0017938	0.0022944
0.0100	0.0003466	0.0006819	0.0013229	0.0019295	0.0025066
0.0200	0.0003495	0.0006932	0.0013639	0.0020142	0.0026458

TABLE 7–VIII Maximum Pipe Strain for a Ridge Pattern of Longitudinal PGD Using the Simplified Soil–Pipeline Interface Model.
ϕ = 30 in (76.2 cm), t = 0.25 in (6.4 mm), C = 9 ft (2.74 m)

α	L(m) 25	50	100	150	200
0.0025	0.0003534	0.0006676	0.0012173	0.0016955	0.0021245
0.0033	0.0003591	0.0006862	0.0012712	0.0017899	0.0022606
0.0050	0.0003651	0.0007068	0.0013353	0.0019068	0.0024345
0.0100	0.0003715	0.0007301	0.0014137	0.0020585	0.0026706
0.0200	0.0003749	0.0007430	0.0014603	0.0021544	0.0028273

TABLE 7–IX Maximum Pipe Strain for a Ridge Pattern of Longitudinal PGD Using the Simplified Soil–Pipeline Interface Model.
ϕ = 48 in (122 cm), t = 0.25 in (6.4 mm), C = 9 ft (2.74 m)

α	L(m) 25	50	100	150	200
0.0025	0.0000595	0.0001176	0.0002302	0.0003383	0.0004424
0.0033	0.0000597	0.0001183	0.0002327	0.0003435	0.0004511
0.0050	0.0000598	0.0001190	0.0002353	0.0003490	0.0004604
0.0100	0.0000600	0.0001197	0.0002380	0.0003549	0.0004705
0.0200	0.0000601	0.0001200	0.0002394	0.0003580	0.0004759

TABLE 7–X Maximum Pipe Strain for a Ridge Pattern of Longitudinal PGD Using the Simplified Soil–Pipeline Interface Model.
ϕ = 12 in (30.5 cm), t = 0.50 in (12.7 mm), C = 3 ft (0.91 m)

α	L(m) 25	50	100	150	200
0.0025	0.0000721	0.0001422	0.0002770	0.0004057	0.0005289
0.0033	0.0000723	0.0001431	0.0002806	0.0004130	0.0005409
0.0050	0.0000726	0.0001441	0.0002843	0.0004209	0.0005541
0.0100	0.0000728	0.0001451	0.0002882	0.0004294	0.0005686
0.0200	0.0000730	0.0001457	0.0002903	0.0004339	0.0005765

TABLE 7–XI Maximum Pipe Strain for a Ridge Pattern of Longitudinal PGD Using the Simplified Soil–Pipeline Interface Model.
ϕ = 30 in (76.2 cm), t = 0.50 in (12.7 mm), C = 3 ft (0.91 m)

α	L(m) 25	50	100	150	200
0.0025	0.0000846	0.0001665	0.0003231	0.0004715	0.0006129
0.0033	0.0000849	0.0001678	0.0003279	0.0004813	0.0006287
0.0050	0.0000853	0.0001691	0.0003329	0.0004918	0.0006462
0.0100	0.0000856	0.0001705	0.0003383	0.0005033	0.0006658
0.0200	0.0000858	0.0001713	0.0003411	0.0005095	0.0006766

TABLE 7–XII Maximum Pipe Strain for a Ridge Pattern of Longitudinal PGD Using the Simplified Soil–Pipeline Interface Model.
ϕ = 48 in (122 cm), t = 0.50 in (12.7 mm), C = 3 ft (0.91 m)

α	L(m) 25	50	100	150	200
0.0025	0.0001094	0.0002144	0.0004131	0.0005990	0.0007744
0.0033	0.0001100	0.0002166	0.0004207	0.0006142	0.0007987
0.0050	0.0001106	0.0002188	0.0004288	0.0006310	0.0008261
0.0100	0.0001112	0.0002212	0.0004376	0.0006497	0.0008576
0.0200	0.0001115	0.0002224	0.0004423	0.0006599	0.0008752

TABLE 7–XIII Maximum Pipe Strain for a Ridge Pattern of Longitudinal PGD Using the Simplified Soil–Pipeline Interface Model.
ϕ = 12 in (30.5 cm), t = 0.50 in (12.7 mm), C = 6 ft (1.83 m)

α	L(m) 25	50	100	150	200
0.0025	0.0001217	0.0002381	0.0004570	0.0006609	0.0008523
0.0033	0.0001225	0.0002407	0.0004662	0.0006790	0.0008811
0.0050	0.0001232	0.0002435	0.0004761	0.0006993	0.0009140
0.0100	0.0001239	0.0002464	0.0004869	0.0007221	0.0009523
0.0200	0.0001243	0.0002479	0.0004927	0.0007347	0.0009739

TABLE 7–XIV Maximum Pipe Strain for a Ridge Pattern of Longitudinal PGD Using the Simplified Soil–Pipeline Interface Model.
ϕ = 30 in (76.2 cm), t = 0.50 in (12.7 mm), C = 6 ft (1.83 m)

α	L(m) 25	50	100	150	200
0.0025	0.0001340	0.0002615	0.0005003	0.0007215	0.0009284
0.0033	0.0001349	0.0002647	0.0005112	0.0007428	0.0009620
0.0050	0.0001358	0.0002680	0.0005230	0.0007668	0.0010007
0.0100	0.0001367	0.0002715	0.0005360	0.0007941	0.0010461
0.0200	0.0001371	0.0002733	0.0005430	0.0008092	0.0010721

TABLE 7–XV Maximum Pipe Strain for a Ridge Pattern of Longitudinal PGD Using the Simplified Soil–Pipeline Interface Model.
ϕ = 48 in (122 cm), t = 0.50 in (12.7 mm), C = 6 ft (1.83 m)

α	L(m) 25	50	100	150	200
0.0025	0.0001584	0.0003078	0.0005851	0.0008395	0.0010757
0.0033	0.0001596	0.0003122	0.0005997	0.0008675	0.0011193
0.0050	0.0001608	0.0003168	0.0006157	0.0008995	0.0011702
0.0100	0.0001621	0.0003216	0.0006335	0.0009365	0.0012314
0.0200	0.0001627	0.0003242	0.0006433	0.0009575	0.0012671

TABLE 7–XVI Maximum Pipe Strain for a Ridge Pattern of Longitudinal PGD Using the Simplified Soil–Pipeline Interface Model.
ϕ = 12 in (30.5 cm), t = 0.50 in (12.7 mm), C = 9 ft (2.74 m)

α	L(m) 25	50	100	150	200
0.0025	0.0001705	0.0003307	0.0006267	0.0008969	0.0011472
0.0033	0.0001719	0.0003357	0.0006432	0.0009285	0.0011959
0.0050	0.0001733	0.0003410	0.0006614	0.0009647	0.0012533
0.0100	0.0001748	0.0003466	0.0006819	0.0010071	0.0013229
0.0200	0.0001755	0.0003495	0.0006932	0.0010312	0.0013639

TABLE 7–XVII Maximum Pipe Strain for a Ridge Pattern of Longitudinal PGD Using the Simplified Soil–Pipeline Interface Model.
ϕ = 30 in (76.2 cm), t = 0.50 in (12.7 mm), C = 9 ft (2.74 m)

α	L(m) 25	50	100	150	200
0.0025	0.0001825	0.0003534	0.0006676	0.0009534	0.0012173
0.0033	0.0001841	0.0003591	0.0006862	0.0009886	0.0012712
0.0050	0.0001857	0.0003651	0.0007068	0.0010293	0.0013353
0.0100	0.0001874	0.0003715	0.0007301	0.0010772	0.0014137
0.0200	0.0001883	0.0003749	0.0007430	0.0011047	0.0014603

TABLE 7–XVIII Maximum Pipe Strain for a Ridge Pattern of Longitudinal PGD Using the Simplified Soil–Pipeline Interface Model.
ϕ = 48 in (122 cm), t = 0.50 in (12.7 mm), C = 9 ft (2.74 m)

α	L(m) 25	50	100	150	200
0.0025	0.0000398	0.0000790	0.0001557	0.0002302	0.0003027
0.0033	0.0000399	0.0000793	0.0001568	0.0002327	0.0003069
0.0050	0.0000400	0.0000796	0.0001580	0.0002353	0.0003114
0.0100	0.0000401	0.0000799	0.0001593	0.0002380	0.0003161
0.0200	0.0000401	0.0000801	0.0001599	0.0002394	0.0003185

TABLE 7–XIX Maximum Pipe Strain for a Ridge Pattern of Longitudinal PGD Using the Simplified Soil–Pipeline Interface Model.
ϕ = 12 in (30.5 cm), t = 0.75 in (19.1 mm), C = 3 ft (0.91 m)

α	L(m) 25	50	100	150	200
0.0025	0.0000483	0.0000956	0.0001879	0.0002770	0.0003634
0.0033	0.0000484	0.0000961	0.0001895	0.0002806	0.0003694
0.0050	0.0000485	0.0000965	0.0001913	0.0002843	0.0003757
0.0100	0.0000486	0.0000970	0.0001931	0.0002882	0.0003825
0.0200	0.0000487	0.0000972	0.0001940	0.0002903	0.0003861

TABLE 7–XX Maximum Pipe Strain for a Ridge Pattern of Longitudinal PGD Using the Simplified Soil–Pipeline Interface Model.
ϕ = 30 in (76.2 cm), t = 0.75 in (19.1 mm), C = 3 ft (0.91 m)

α	L(m) 25	50	100	150	200
0.0025	0.0000567	0.0001122	0.0002197	0.0003231	0.0004229
0.0033	0.0000568	0.0001128	0.0002219	0.0003279	0.0004308
0.0050	0.0000570	0.0001134	0.0002243	0.0003329	0.0004394
0.0100	0.0000572	0.0001140	0.0002268	0.0003383	0.0004486
0.0200	0.0000573	0.0001143	0.0002280	0.0003411	0.0004535

TABLE 7–XXI Maximum Pipe Strain for a Ridge Pattern of Longitudinal PGD Using the Simplified Soil–Pipeline Interface Model.
ϕ = 48 in (122 cm), t = 0.75 in (19.1 mm), C = 3 ft (0.91 m)

α	L(m) 25	50	100	150	200
0.0025	0.0000735	0.0001449	0.0002822	0.0004131	0.0005383
0.0033	0.0000737	0.0001459	0.0002859	0.0004207	0.0005508
0.0050	0.0000740	0.0001469	0.0002897	0.0004288	0.0005644
0.0100	0.0000743	0.0001480	0.0002938	0.0004376	0.0005795
0.0200	0.0000744	0.0001485	0.0002959	0.0004423	0.0005876

TABLE 7–XXII Maximum Pipe Strain for a Ridge Pattern of Longitudinal PGD Using the Simplified Soil–Pipeline Interface Model.
ϕ = 12 in (30.5 cm), t = 0.75 in (19.1 mm), C = 6 ft (1.83 m)

α	L(m) 25	50	100	150	200
0.0025	0.0000818	0.0001611	0.0003129	0.0004570	0.0005944
0.0033	0.0000821	0.0001623	0.0003174	0.0004662	0.0006094
0.0050	0.0000825	0.0001636	0.0003222	0.0004761	0.0006259
0.0100	0.0000828	0.0001649	0.0003272	0.0004869	0.0006443
0.0200	0.0000830	0.0001656	0.0003298	0.0004927	0.0006544

TABLE 7–XXIII Maximum Pipe Strain for a Ridge Pattern of Longitudinal PGD Using the Simplified Soil–Pipeline Interface Model.
ϕ = 30 in (76.2 cm), t = 0.75 in (19.1 mm), C = 6 ft (1.83 m)

α	L(m) 25	50	100	150	200
0.0025	0.0000901	0.0001772	0.0003434	0.0005003	0.0006495
0.0033	0.0000905	0.0001787	0.0003487	0.0005112	0.0006671
0.0050	0.0000909	0.0001802	0.0003544	0.0005230	0.0006867
0.0100	0.0000913	0.0001818	0.0003604	0.0005360	0.0007087
0.0200	0.0000915	0.0001826	0.0003636	0.0005430	0.0007209

TABLE 7–XXIV Maximum Pipe Strain for a Ridge Pattern of Longitudinal PGD Using the Simplified Soil–Pipeline Interface Model.
ϕ = 48 in (122 cm), t = 0.75 in (19.1 mm), C = 6 ft (1.83 m)

α	L(m) 25	50	100	150	200
0.0025	0.0001067	0.0002091	0.0004032	0.0005851	0.0007569
0.0033	0.0001072	0.0002112	0.0004105	0.0005997	0.0007802
0.0050	0.0001078	0.0002133	0.0004182	0.0006157	0.0008064
0.0100	0.0001083	0.0002155	0.0004266	0.0006335	0.0008365
0.0200	0.0001086	0.0002167	0.0004311	0.0006433	0.0008533

TABLE 7–XXV Maximum Pipe Strain for a Ridge Pattern of Longitudinal PGD Using the Simplified Soil–Pipeline Interface Model.
ϕ = 12 in (30.5 cm), t = 0.75 in (19.1 mm), C = 9 ft (2.74 m)

α	L(m) 25	50	100	150	200
0.0025	0.0001149	0.0002249	0.0004327	0.0006267	0.0008093
0.0033	0.0001155	0.0002273	0.0004410	0.0006432	0.0008355
0.0050	0.0001162	0.0002298	0.0004499	0.0006614	0.0008654
0.0100	0.0001169	0.0002324	0.0004596	0.0006819	0.0008998
0.0200	0.0001172	0.0002337	0.0004647	0.0006932	0.0009191

TABLE 7–XXVI Maximum Pipe Strain for a Ridge Pattern of Longitudinal PGD Using the Simplified Soil–Pipeline Interface Model.
ϕ = 30 in (76.2 cm), t = 0.75 in (19.1 mm), C = 9 ft (2.74 m)

α	L(m) 25	50	100	150	200
0.0025	0.0001231	0.0002407	0.0004619	0.0006676	0.0008609
0.0033	0.0001238	0.0002434	0.0004712	0.0006862	0.0008902
0.0050	0.0001246	0.0002462	0.0004814	0.0007068	0.0009237
0.0100	0.0001253	0.0002492	0.0004924	0.0007301	0.0009627
0.0200	0.0001257	0.0002507	0.0004983	0.0007430	0.0009848

TABLE 7–XXVII Maximum Pipe Strain for a Ridge Pattern of Longitudinal PGD Using the Simplified Soil–Pipeline Interface Model.
ϕ = 48 in (122 cm), t = 0.75 in (19.1 mm), C = 9 ft (2.74 m)

SECTION 8
COMPARISON OF PATTERNS

In the preceding sections, the response of a buried steel pipeline to four idealized patterns of longitudinal PGD was determined. In this section, the pipe strains induced by the four patterns will be compared.

8.1 Normalized Pipe Strain

To facilitate the comparison of pipe strain, we define an embedment length, L_{em}, as the length over which the constant slippage force f_m must act to induce a pipe strain ϵ equal to the ground strain α.

$$\epsilon = \alpha = \frac{f_m L_{em}}{AE} \tag{8.1}$$

or

$$L_{em} = \frac{\alpha EA}{f_m} \tag{8.2}$$

Table 8–I lists L_{em} in meters for various values of the ground strain, α, the pipe wall thickness, t, and the burial depth to the centerline of the pipe H. In Table 8–I the unit weight of the soil, γ, is taken as 100 pcf and the coefficient of friction at the soil pipe interface ranges from 0.45 to 0.75. Note that since both the slippage force, f_m, and the pipe cross–sectional area, A, are proportional to the pipe diameter, ϕ, the embedment length L_{em} is independent of pipe diameter.

For a Ramp pattern of longitudinal PGD, the pipe strain using the simplified interface model is given by Equation (4.26). Utilizing the embedment length, L_{em}, given by Equation (8.2) yields

$$\epsilon = \begin{cases} \alpha\sqrt{L/L_{em}} & L < L_{em} \\ \alpha & L > L_{em} \end{cases} \tag{8.3}$$

For the Rigid Block pattern of longitudinal PGD, the pipe strain using the simplified model is given by Equation (5.18). Defining an "equivalent" ground strain for this pattern as

$$\alpha = \delta/L \tag{8.4}$$

we get

$$\epsilon = \begin{cases} \dfrac{\alpha L}{2L_{em}} & L < 4\,L_{em} \\ \alpha\sqrt{L/L_{em}} & L > 4\,L_{em} \end{cases} \tag{8.4}$$

For a Ramp/Step pattern of longitudinal PGD, the pipe strain using the simplified model is given by Equation (6.4) for $L < 5\alpha EA/2f_m$ and by Equation (6.13) for $L > 5\alpha EA/2f_m$. Introducing the embedment length L_{em}, we get

$$\epsilon = \begin{cases} \alpha\left[\sqrt{4 + 2L/L_{em}} - 2\right] & L < 2.5L_{em} \\ \dfrac{\alpha}{2}\left[\sqrt{\dfrac{4L}{L_{em}} - 1} - 1\right] & L > 2.5L_{em} \end{cases} \tag{8.5}$$

For the Ridge pattern, the pipe strain is given by Equation (7.4) for $L < 3\alpha EA/f_m$ and is simply α for $L > 3\alpha EA/f_m$. Utilizing the embedment length, L_{em}, we get

$$\epsilon = \begin{cases} \alpha\left[\sqrt{1 + L/L_{em}} - 1\right] & L < 3L_{em} \\ \alpha & L > 3L_{em} \end{cases} \tag{8.6}$$

The pipe strain, ϵ, for each PGD pattern, normalized by the ground strain, α, is plotted in Figure 8–1 as a function of the normalized length of the lateral spread zone, L/L_{em}. For both the Ramp and Ridge patterns of longitudinal PGD, the pipe strain is always less than or equal to the pipe strain α. However for the Rigid Block and Ramp/Step patterns, the pipe strain is larger than the ground strain for $L > 2L_{em}$ and $L > 2.5L_{em}$ respectively. For a given value of the ground strain, α, the Ramp pattern of longitudinal PGD leads to the largest pipe strains for $L < 2L_{em}$, while the Rigid Block pattern leads to the largest pipe strains for $L > 2L_{em}$.

8.2 Example Calculation

Figure 8–1 and Table 8–I can be used to estimate pipe strain induced by any of the four patterns of longitudinal PGD considered. As an example, we consider a pipeline subject to the Ramp/Step pattern of longitudinal PGD shown in Figure 2–10(c). That is, the length of the lateral spread zone L = 390 m and the ground strain $\alpha = 7.5/210 = 0.036$. The burial depth to the pipe centerline, H, is taken as 6 ft, the unit weight of the soil is taken as 100 pcf, the pipe wall thickness is 1/4 inch and the coefficient of friction at the soil pipeline interface is 0.75 which from Equation (3.2) corresponds to an angle of shearing resistance $\theta = 40°$.

From Equation (8.2) or extrapolating from Table 8–1 the embedment length for the pipe, L_{em}, is 2120 m. Hence the normalized length of the lateral spread zone $L/L_{em} = 390/2120 = 0.184$ and from Figure 8–1 the normalized pipe strain for Ramp/Step PGD $\epsilon/\alpha \simeq 0.09$. Hence the strain in the pipe induced by this pattern of longitudinal PGD is 0.00324.

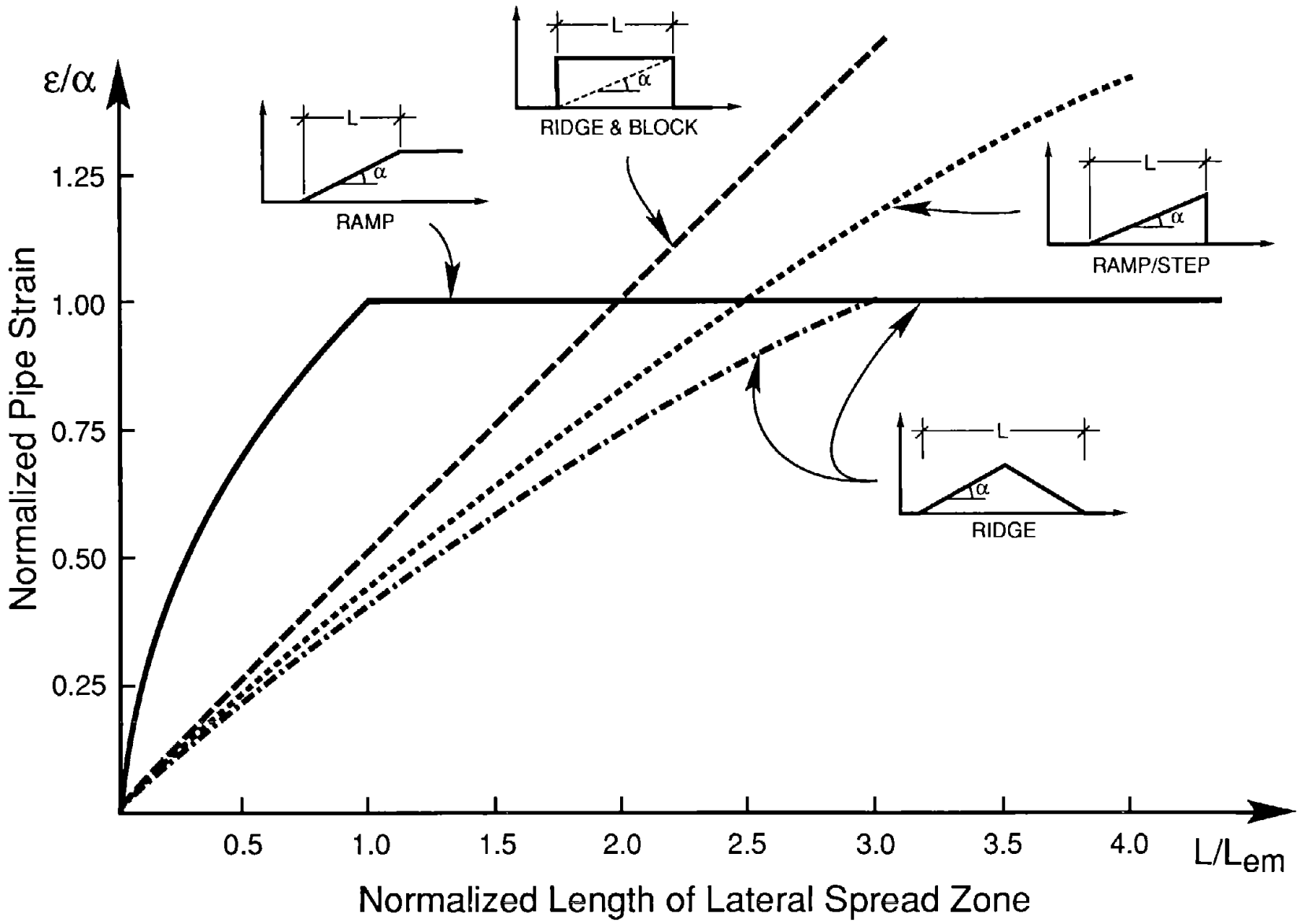

FIGURE 8-1 Normalized Pipe Strain as function of Normalized Length of the Lateral Spread zone for four idealized patterns of Longitudinal PGD.

α	H = 3 ft (0.91 m) t=1/4" (6.4mm)	t=1/2" (12.7mm)	t=3/4" (19.1mm)	H = 6 ft (1.83 m) t=1/4" (6.4mm)	t=1/2" (12.7mm)	t=3/4" (19.1mm)	H = 9 ft (2.74 m) t=1/4" (6.4mm)	t=1/2" (12.7mm)	t=3/4" (19.1mm)
0.002	236	471	707	118	236	353	78.5	157	236
0.005	589	1178	1767	294	589	883	196	393	589
0.010	1178	7356	3533	588	1178	1767	393	785	1178
0.020	2356	4711	7066	1177	2356	3533	785	1570	2356
0.030	3533	7066	10600	1767	3533	5300	1178	2356	3533

(a) $\mu = 0.75$

α	H = 3 ft (0.91 m) t=1/4" (6.4mm)	t=1/2" (12.7mm)	t=3/4" (19.1mm)	H = 6 ft (1.83 m) t=1/4" (6.4mm)	t=1/2" (12.7mm)	t=3/4" (19.1mm)	H = 9 ft (2.74 m) t=1/4" (6.4mm)	t=1/2" (12.7mm)	t=3/4" (19.1mm)
0.002	294	588	883	147	294	442	98.1	196	294
0.005	736	1472	2208	368	736	1104	245	491	736
0.010	1472	2944	4417	736	1472	2208	491	981	1472
0.020	2944	5889	8833	1472	2944	4417	981	1963	2944
0.030	4417	8833	13250	2208	4417	6625	1472	2944	4416

(b) $\mu = 0.60$

α	H = 3 ft (0.91 m) t=1/4" (6.4mm)	t=1/2" (12.7mm)	t=3/4" (19.1mm)	H = 6 ft (1.83 m) t=1/4" (6.4mm)	t=1/2" (12.7mm)	t=3/4" (19.1mm)	H = 9 ft (2.74 m) t=1/4" (6.4mm)	t=1/2" (12.7mm)	t=3/4" (19.1mm)
0.002	392	785	1178	196	392	589	131	262	393
0.005	981	1963	2944	491	981	1472	327	654	981
0.010	1963	3926	5889	981	1963	2944	654	1308	1963
0.020	3926	7852	11778	1963	3926	5889	1308	2617	3926
0.030	5889	11778	17667	2944	5889	8833	1963	3926	5889

(c) $\mu = 0.45$

TABLE 8–I Embedment Length L_{em}, in meters, as a function of ground strain α, for a unit weight of soil equal to 100 pcf and various values of the burial depth H to pipe centerline, pipe wall thickness t, and coefficient of friction μ.

SECTION 9
SUMMARY AND RECOMMENDATIONS

9.1 Summary

The response of an elastic buried steel pipeline to four idealized patterns of longitudinal PGD were determined herein. The four patterns of horizontal ground movement considered (i.e. Ramp, Rigid Block, Ramp/Step and Ridge) are idealizations of ground movement patterns observed after earthquakes in Japan. Vertical components of PGD resulting from subsidence or heaving are neglected and the horizontal PGD is assumed parallel to the pipeline axis. In addition, the burial depth of the pipeline in and around the PGD zone is assumed to be constant.

Two models for the force–deformation relationship in the axial direction at the soil pipeline interface are considered. The complete model shown in Figure 3–2 consists of a linear elastic soil spring in series with a slider. The simplified model shown in Figure 3–3 consists of simply a slider. The stiffness of the soil spring and the force per unit length for the slider were developed using information available in the technical literature. The relative axial displacement at the soil pipeline interface corresponding to slippage, D_s, (i.e. relative displacement beyond which the slider is effective) is shown in Table 3–I to be an increasing function of the pipe diameter, ϕ, the burial depth to the top of the pipe, C, and the coefficient of friction at the soil pipe interface, μ. However, for what is felt to be a reasonable range for the parameter of interest, D_s is less than 0.075 inches.

For the Ramp pattern and the Rigid Block pattern, the maximum pipe strain was evaluated using both the complete elastic spring/slider model for the soil pipe interface as well as the simplified rigid spring/slider model. Tables 4–I(c) through 4–XXVII(c) for the Ramp pattern and Tables 5–I(c) through 5–XXVII(c) for the Rigid Block pattern show that the simplified interface model gives results which are no more than 4% larger than the complete interface model. This is likely due to the fact that the ground displacement magnitudes considered are quite large compared to D_s.

The simplified interface model is used to evaluate the maximum pipe strain for both the Ramp/Step pattern and the Ridge pattern of longitudinal PGD. The maximum pipe strain ϵ, for all four patterns normalized by the ground strain, α, is plotted as a function of the normalized length of the PGD zone in Figure 8–1. The length of the PGD zone is

normalized by the embedment length, L_{em}, which is defined as the length over which the constant slippage force f_m must act to induce a pipe strain equal to the ground strain α. As shown in Table 8–I, the embedment distance L_{em} is an increasing function of the ground strain, α, and the pipe wall thickness t. It is a decreasing function of the coefficient of friction at the soil pipe interface, μ, and the burial depth to the pipe centerline H.

For both the Ramp and Ridge patterns of longitudinal PGD, the pipe strain is an increasing function of the length of the PGD zone for $L < L_{em}$ and $L < 3L_{em}$ respectively and equal to the ground strain beyond. However for the Rigid Block and Ramp/Step patterns, the pipe strain is larger than the ground strain for $L > 2L_{em}$ and $L > 2.5L_{em}$ respectively. For a fixed value of the ground strain α, the Ramp patterns leads to larger pipe strains for $L < 2L_{em}$, while the Rigid Block pattern leads to the largest pipe strain for $L > 2L_{em}$.

9.2 Recommendations

For the design of new pipelines, areas susceptible to PGD due to landslides or liquefaction induced lateral spreading should be avoided if possible. However, if right–of–way considerations require that the pipeline route cross an area of potential PGD, the following actions would reduce the level of buried pipe strain, induced by horizontal PGD, by increasing the embedment length, L_{em}.

- increase the pipe wall thickness.
- use the smallest allowable soil cover over the top of the pipe.
- backfill the pipeline trench with lighter weight soils having a low angle of shearing resistance.

If design calculations suggest that the above listed actions still result in an unacceptable level of pipe stress, consideration should be given to the following:

- soil replacement or soil improvement through dynamic compaction, stone columns, etc. to avoid liquefaction all together.
- if economically possible, support the pipeline on battered piles which penetrate down to a firm bearing layer.
- install block valves, possibly remote controlled or automatic shutoff, at each side of the potential PGD zone.

SECTION 10
REFERENCES

[1] O'Rourke, M.J. and Ayala, G., "Seismic Damage to Pipeline: Case Study", Journal of Transportation Engineering, American Society of Civil Engineers, Vol. 116, No. 2, March/April 1990.

[2] O'Rourke, T. and Tawfik, M., "Effects of Lateral Spreading on Buried Pipelines During the 1971 San Fernando Earthquake", Earthquake Behavior and Safety of Oil and Gas Storage Facilities, Buried Pipelines and Equipment, PVP–Vol. 77, American Society of Mechanical Engineers, New York, NY, 1983, pp. 124–132.

[3] Finn, L, "Permanent Deformations in Ground and Earth Structures During Earthquakes", Proc. Ninth World Conference on Earthquake Engineering, Tokyo–Kyoto, Japan, 1988, Vol. VIII, pp. VIII–201 to VIII–212.

[4] Hamada, M., Yasuda, S., Isoyama, R., and Emoto, K., "Study of Liquefaction Induced Permanent Ground Displacements", Assoc. for the Development of Earthquake Prediction, Japan, 1986, p. 87.

[5] Youd, T., and Perkins, D., "Mapping of Liquefaction Severity Index", J. Geotechnical Engineering, ASCE, Vol. 113, No. 11, Nov. 1987, pp. 1374–1392.

[6] Baziar, M., "Engineering Evaluation of Permanent Ground Deformation Due to Seismically–Induced Liquefaction", dissertation for Ph.D. in Civil Engineering, Rensselaer Polytechnic Institute, August 1991, p. 297.

[7] Towhata, I., Tokida, K., Tamari, Y., Matsumoto, H., and Yamada, K., "Prediction of Permanent Lateral Displacment of Liquefied Ground by Means of Variational Principle," Technical Report NCEER–91–0001, Proc. 3rd Japan–U.S. Workshop on Earthquake Resistant Design of Lifeline Facilities and Countermeasures for Soil Liquefaction, San Francisco, CA, pp. 237–251.

[8] Suzuki, N., and Masuda, N., "Idealization of Permanent Ground Movement and Strain Estimation of Buried Pipes", Technical Report NCEER–91–0001, Proc. 3rd Japan–U.S. Workshop on Earthquake Resistant Design of Lifeline Facilities and Countermeasures for Soil Liquefaction, San Francisco, CA, pp. 455–469.

[9] Hamada, M., Yasuda, S., Isoyama, R., and Emoto, K., "Study of Liquefaction Induced Permanent Ground Displacements", Association for the Development of Earthquake Prediction, Japan, November 1986, p. 87.

[10] Hamada, M., Wakamatsu, K., and Yasuda,S., "Liquefaction–Induced Ground Displacement During the 1948 Fukui Earthquake", Technical Report NCEER–89–0032, Proc. 2nd U.S.–Japan Workshop on Liquefaction, Large Ground Deformation and their Effects on Lifelines, December 1989, pp. 6–15.

[11] Yasuda, S., Hamada, M., Wakamatsu, K. and Morimoto, I., "Liquefaction Induced Permanent Ground Displacements in Niigata City", Technical Report NCEER–89–0032, Proceedings of the 2nd U.S.–Japan Workshop on Liquefaction, Large Ground Deformation and Their Effects on Lifelines, December 1989, pp. 67–81.

[12] Committee on Gas and Liquid Fuel Lifelines, "Guidelines for the Seismic Design of Oil and Gas Pipeline Systems", Technical Council on Lifeline Earthquake Engineering, ASCE, 1984, pp. 473.

[13] Colton, J.D., Chang, P.H.P., Lindberg, H.E. and Abrahamson, G.R., Project PYU–1434, "Measurement of Dynamic Soil–Pipe Axial Interaction for Full–Scale Buried Pipelines under Field Conditions", SRI International, Menlo Park, California, November 1981.

[14] Kulhawy, F.H. and Peterson, M.S., "Behavior of Sand–Concrete Interfaces", Proceedings of the Sixth Pan American Conference on Soil Mechanics and Foundation Engineering, Lima, Peru, Vol. 2, 1979.

[15] Brumund, W.F. and Leonard, G.A., "Experimental Study of Static and Dynamic Friction Between Sand and Typical Construction Materials", Journal of Testing and Evaluation, Vol. 1, No. 2, March 1973, pp. 162–165.

[16] Perloff, W.P. and Baron, W., "Soil Mechanics: Principles and Applications", John Wiley & Sons, 1976, pp. 745.

[17] O'Rourke, T.D., Grigoriu, M.D. and Khater, M.M., "Seismic Response of Buried Pipelines", Pressure Vessels and Piping Technology, A Decade of Progress, Edited by C. Sundararajan, ASME, New York, NY, 1985, pp. 281–323.

[18] Novak, M., Nogami, T. and Abdul–Ella, F., "Dynamic Soil Reaction for Plane Strain Case", Journal of the Engineering Mechanics Division, ASCE, Vol. 104, No. EM4, 1978, pp. 953–959.

[19] O'Leary, P. and Datta, S., "Dynamics of Buried Pipelines", International Journal of Soil Dynamics and Earthquake Engineering, Vol. 4, No. 3, 1985, pp. 151–159.

[20] Shibata, A., Miwa, M., Nakano, M., and Fujihashi, K., "Site Observation of Telephone Tunnel During Earthquakes", Development in Geotechnical Engineering 45 – Structures and Stochastic Methods, Edited by A. Cakmak, Elsevier, Amsterdam, 1987.

[21] Kubota Ltd, "Earthquake–Proof Design of Buried Pipelines", Tokyo, Japan, 1981.

[22] O'Rourke, M.J. and Wang, L.R., "Earthquake Response of Buried Pipelines", Proceedings of the ASCE Conference on Earthquake Engineering and Soil Dynamics, Pasadena, California, June 1978.

[23] ElHmadi, K. and O'Rourke, M., "Soil Springs for Buried Pipeline Axial Motion," J. Geotechnical Engineering, ASCE, Vol. 114, 1988, pp. 1335–1339.

[24] ElHmadi, K., and O'Rourke, M., "Seismic Wave Propagation Effects on Straight Jointed Buried Pipelines", Rept. No. NCEER–89–0022, National Center for Earthquake Engineering Research, State University of New York at Buffalo, 1989.

[25] Holloway, D.M., "The Mechanics of Pile–Soil Interaction in Cohesionless Soils", Ph.D. Thesis, Duke University, Durham, North Carolina, 1975.

NATIONAL CENTER FOR EARTHQUAKE ENGINEERING RESEARCH
LIST OF TECHNICAL REPORTS

The National Center for Earthquake Engineering Research (NCEER) publishes technical reports on a variety of subjects related to earthquake engineering written by authors funded through NCEER. These reports are available from both NCEER's Publications Department and the National Technical Information Service (NTIS). Requests for reports should be directed to the Publications Department, National Center for Earthquake Engineering Research, State University of New York at Buffalo, Red Jacket Quadrangle, Buffalo, New York 14261. Reports can also be requested through NTIS, 5285 Port Royal Road, Springfield, Virginia 22161. NTIS accession numbers are shown in parenthesis, if available.

NCEER-87-0001 "First-Year Program in Research, Education and Technology Transfer," 3/5/87, (PB88-134275/AS).

NCEER-87-0002 "Experimental Evaluation of Instantaneous Optimal Algorithms for Structural Control," by R.C. Lin, T.T. Soong and A.M. Reinhorn, 4/20/87, (PB88-134341/AS).

NCEER-87-0003 "Experimentation Using the Earthquake Simulation Facilities at University at Buffalo," by A.M. Reinhorn and R.L. Ketter, to be published.

NCEER-87-0004 "The System Characteristics and Performance of a Shaking Table," by J.S. Hwang, K.C. Chang and G.C. Lee, 6/1/87, (PB88-134259/AS). This report is available only through NTIS (see address given above).

NCEER-87-0005 "A Finite Element Formulation for Nonlinear Viscoplastic Material Using a Q Model," by O. Gyebi and G. Dasgupta, 11/2/87, (PB88-213764/AS).

NCEER-87-0006 "Symbolic Manipulation Program (SMP) - Algebraic Codes for Two and Three Dimensional Finite Element Formulations," by X. Lee and G. Dasgupta, 11/9/87, (PB88-219522/AS).

NCEER-87-0007 "Instantaneous Optimal Control Laws for Tall Buildings Under Seismic Excitations," by J.N. Yang, A. Akbarpour and P. Ghaemmaghami, 6/10/87, (PB88-134333/AS).

NCEER-87-0008 "IDARC: Inelastic Damage Analysis of Reinforced Concrete Frame - Shear-Wall Structures," by Y.J. Park, A.M. Reinhorn and S.K. Kunnath, 7/20/87, (PB88-134325/AS).

NCEER-87-0009 "Liquefaction Potential for New York State: A Preliminary Report on Sites in Manhattan and Buffalo," by M. Budhu, V. Vijayakumar, R.F. Giese and L. Baumgras, 8/31/87, (PB88-163704/AS). This report is available only through NTIS (see address given above).

NCEER-87-0010 "Vertical and Torsional Vibration of Foundations in Inhomogeneous Media," by A.S. Veletsos and K.W. Dotson, 6/1/87, (PB88-134291/AS).

NCEER-87-0011 "Seismic Probabilistic Risk Assessment and Seismic Margins Studies for Nuclear Power Plants," by Howard H.M. Hwang, 6/15/87, (PB88-134267/AS).

NCEER-87-0012 "Parametric Studies of Frequency Response of Secondary Systems Under Ground-Acceleration Excitations," by Y. Yong and Y.K. Lin, 6/10/87, (PB88-134309/AS).

NCEER-87-0013 "Frequency Response of Secondary Systems Under Seismic Excitation," by J.A. HoLung, J. Cai and Y.K. Lin, 7/31/87, (PB88-134317/AS).

NCEER-87-0014 "Modelling Earthquake Ground Motions in Seismically Active Regions Using Parametric Time Series Methods," by G.W. Ellis and A.S. Cakmak, 8/25/87, (PB88-134283/AS).

NCEER-87-0015 "Detection and Assessment of Seismic Structural Damage," by E. DiPasquale and A.S. Cakmak, 8/25/87, (PB88-163712/AS).

NCEER-87-0016 "Pipeline Experiment at Parkfield, California," by J. Isenberg and E. Richardson, 9/15/87, (PB88-163720/AS). This report is available only through NTIS (see address given above).

NCEER-87-0017 "Digital Simulation of Seismic Ground Motion," by M. Shinozuka, G. Deodatis and T. Harada, 8/31/87, (PB88-155197/AS). This report is available only through NTIS (see address given above).

NCEER-87-0018 "Practical Considerations for Structural Control: System Uncertainty, System Time Delay and Truncation of Small Control Forces," J.N. Yang and A. Akbarpour, 8/10/87, (PB88-163738/AS).

NCEER-87-0019 "Modal Analysis of Nonclassically Damped Structural Systems Using Canonical Transformation," by J.N. Yang, S. Sarkani and F.X. Long, 9/27/87, (PB88-187851/AS).

NCEER-87-0020 "A Nonstationary Solution in Random Vibration Theory," by J.R. Red-Horse and P.D. Spanos, 11/3/87, (PB88-163746/AS).

NCEER-87-0021 "Horizontal Impedances for Radially Inhomogeneous Viscoelastic Soil Layers," by A.S. Veletsos and K.W. Dotson, 10/15/87, (PB88-150859/AS).

NCEER-87-0022 "Seismic Damage Assessment of Reinforced Concrete Members," by Y.S. Chung, C. Meyer and M. Shinozuka, 10/9/87, (PB88-150867/AS). This report is available only through NTIS (see address given above).

NCEER-87-0023 "Active Structural Control in Civil Engineering," by T.T. Soong, 11/11/87, (PB88-187778/AS).

NCEER-87-0024 "Vertical and Torsional Impedances for Radially Inhomogeneous Viscoelastic Soil Layers," by K.W. Dotson and A.S. Veletsos, 12/87, (PB88-187786/AS).

NCEER-87-0025 "Proceedings from the Symposium on Seismic Hazards, Ground Motions, Soil-Liquefaction and Engineering Practice in Eastern North America," October 20-22, 1987, edited by K.H. Jacob, 12/87, (PB88-188115/AS).

NCEER-87-0026 "Report on the Whittier-Narrows, California, Earthquake of October 1, 1987," by J. Pantelic and A. Reinhorn, 11/87, (PB88-187752/AS). This report is available only through NTIS (see address given above).

NCEER-87-0027 "Design of a Modular Program for Transient Nonlinear Analysis of Large 3-D Building Structures," by S. Srivastav and J.F. Abel, 12/30/87, (PB88-187950/AS).

NCEER-87-0028 "Second-Year Program in Research, Education and Technology Transfer," 3/8/88, (PB88-219480/AS).

NCEER-88-0001 "Workshop on Seismic Computer Analysis and Design of Buildings With Interactive Graphics," by W. McGuire, J.F. Abel and C.H. Conley, 1/18/88, (PB88-187760/AS).

NCEER-88-0002 "Optimal Control of Nonlinear Flexible Structures," by J.N. Yang, F.X. Long and D. Wong, 1/22/88, (PB88-213772/AS).

NCEER-88-0003 "Substructuring Techniques in the Time Domain for Primary-Secondary Structural Systems," by G.D. Manolis and G. Juhn, 2/10/88, (PB88-213780/AS).

NCEER-88-0004 "Iterative Seismic Analysis of Primary-Secondary Systems," by A. Singhal, L.D. Lutes and P.D. Spanos, 2/23/88, (PB88-213798/AS).

NCEER-88-0005 "Stochastic Finite Element Expansion for Random Media," by P.D. Spanos and R. Ghanem, 3/14/88, (PB88-213806/AS).

NCEER-88-0006 "Combining Structural Optimization and Structural Control," by F.Y. Cheng and C.P. Pantelides, 1/10/88, (PB88-213814/AS).

NCEER-88-0007 "Seismic Performance Assessment of Code-Designed Structures," by H.H-M. Hwang, J-W. Jaw and H-J. Shau, 3/20/88, (PB88-219423/AS).

NCEER-88-0008 "Reliability Analysis of Code-Designed Structures Under Natural Hazards," by H.H-M. Hwang, H. Ushiba and M. Shinozuka, 2/29/88, (PB88-229471/AS).

NCEER-88-0009 "Seismic Fragility Analysis of Shear Wall Structures," by J-W Jaw and H.H-M. Hwang, 4/30/88. (PB89-102867/AS).

NCEER-88-0010 "Base Isolation of a Multi-Story Building Under a Harmonic Ground Motion - A Comparison of Performances of Various Systems," by F-G Fan, G. Ahmadi and I.G. Tadjbakhsh. 5/18/88, (PB89-122238/AS).

NCEER-88-0011 "Seismic Floor Response Spectra for a Combined System by Green's Functions," by F.M. Lavelle, L.A. Bergman and P.D. Spanos, 5/1/88, (PB89-102875/AS).

NCEER-88-0012 "A New Solution Technique for Randomly Excited Hysteretic Structures," by G.Q. Cai and Y.K. Lin, 5/16/88, (PB89-102883/AS).

NCEER-88-0013 "A Study of Radiation Damping and Soil-Structure Interaction Effects in the Centrifuge," by K. Weissman, supervised by J.H. Prevost, 5/24/88, (PB89-144703/AS).

NCEER-88-0014 "Parameter Identification and Implementation of a Kinematic Plasticity Model for Frictional Soils," by J.H. Prevost and D.V. Griffiths, to be published.

NCEER-88-0015 "Two- and Three- Dimensional Dynamic Finite Element Analyses of the Long Valley Dam," by D.V. Griffiths and J.H. Prevost, 6/17/88, (PB89-144711/AS).

NCEER-88-0016 "Damage Assessment of Reinforced Concrete Structures in Eastern United States," by A.M. Reinhorn, M.J. Seidel, S.K. Kunnath and Y.J. Park, 6/15/88, (PB89-122220/AS).

NCEER-88-0017 "Dynamic Compliance of Vertically Loaded Strip Foundations in Multilayered Viscoelastic Soils," by S. Ahmad and A.S.M. Israil, 6/17/88, (PB89-102891/AS).

NCEER-88-0018 "An Experimental Study of Seismic Structural Response With Added Viscoelastic Dampers," by R.C. Lin, Z. Liang, T.T. Soong and R.H. Zhang, 6/30/88, (PB89-122212/AS). This report is available only through NTIS (see address given above).

NCEER-88-0019 "Experimental Investigation of Primary - Secondary System Interaction," by G.D. Manolis, G. Juhn and A.M. Reinhorn, 5/27/88, (PB89-122204/AS).

NCEER-88-0020 "A Response Spectrum Approach For Analysis of Nonclassically Damped Structures," by J.N. Yang, S. Sarkani and F.X. Long, 4/22/88, (PB89-102909/AS).

NCEER-88-0021 "Seismic Interaction of Structures and Soils: Stochastic Approach," by A.S. Veletsos and A.M. Prasad, 7/21/88, (PB89-122196/AS).

NCEER-88-0022 "Identification of the Serviceability Limit State and Detection of Seismic Structural Damage," by E. DiPasquale and A.S. Cakmak, 6/15/88, (PB89-122188/AS). This report is available only through NTIS (see address given above).

NCEER-88-0023 "Multi-Hazard Risk Analysis: Case of a Simple Offshore Structure," by B.K. Bhartia and E.H. Vanmarcke, 7/21/88, (PB89-145213/AS).

NCEER-88-0024 "Automated Seismic Design of Reinforced Concrete Buildings," by Y.S. Chung, C. Meyer and M. Shinozuka, 7/5/88, (PB89-122170/AS). This report is available only through NTIS (see address given above).

NCEER-88-0025 "Experimental Study of Active Control of MDOF Structures Under Seismic Excitations," by L.L. Chung, R.C. Lin, T.T. Soong and A.M. Reinhorn, 7/10/88, (PB89-122600/AS).

NCEER-88-0026 "Earthquake Simulation Tests of a Low-Rise Metal Structure," by J.S. Hwang, K.C. Chang, G.C. Lee and R.L. Ketter, 8/1/88, (PB89-102917/AS).

NCEER-88-0027 "Systems Study of Urban Response and Reconstruction Due to Catastrophic Earthquakes," by F. Kozin and H.K. Zhou, 9/22/88, (PB90-162348/AS).

NCEER-88-0028 "Seismic Fragility Analysis of Plane Frame Structures," by H.H-M. Hwang and Y.K. Low, 7/31/88, (PB89-131445/AS).

NCEER-88-0029 "Response Analysis of Stochastic Structures," by A. Kardara, C. Bucher and M. Shinozuka, 9/22/88, (PB89-174429/AS).

NCEER-88-0030 "Nonnormal Accelerations Due to Yielding in a Primary Structure," by D.C.K. Chen and L.D. Lutes, 9/19/88, (PB89-131437/AS).

NCEER-88-0031 "Design Approaches for Soil-Structure Interaction," by A.S. Veletsos, A.M. Prasad and Y. Tang, 12/30/88, (PB89-174437/AS). This report is available only through NTIS (see address given above).

NCEER-88-0032 "A Re-evaluation of Design Spectra for Seismic Damage Control," by C.J. Turkstra and A.G. Tallin, 11/7/88, (PB89-145221/AS).

NCEER-88-0033 "The Behavior and Design of Noncontact Lap Splices Subjected to Repeated Inelastic Tensile Loading," by V.E. Sagan, P. Gergely and R.N. White, 12/8/88, (PB89-163737/AS).

NCEER-88-0034 "Seismic Response of Pile Foundations," by S.M. Mamoon, P.K. Banerjee and S. Ahmad, 11/1/88, (PB89-145239/AS).

NCEER-88-0035 "Modeling of R/C Building Structures With Flexible Floor Diaphragms (IDARC2)," by A.M. Reinhorn, S.K. Kunnath and N. Panahshahi, 9/7/88, (PB89-207153/AS).

NCEER-88-0036 "Solution of the Dam-Reservoir Interaction Problem Using a Combination of FEM, BEM with Particular Integrals, Modal Analysis, and Substructuring," by C-S. Tsai, G.C. Lee and R.L. Ketter, 12/31/88, (PB89-207146/AS).

NCEER-88-0037 "Optimal Placement of Actuators for Structural Control," by F.Y. Cheng and C.P. Pantelides, 8/15/88, (PB89-162846/AS).

NCEER-88-0038 "Teflon Bearings in Aseismic Base Isolation: Experimental Studies and Mathematical Modeling," by A. Mokha, M.C. Constantinou and A.M. Reinhorn, 12/5/88, (PB89-218457/AS). This report is available only through NTIS (see address given above).

NCEER-88-0039 "Seismic Behavior of Flat Slab High-Rise Buildings in the New York City Area," by P. Weidlinger and M. Ettouney, 10/15/88, (PB90-145681/AS).

NCEER-88-0040 "Evaluation of the Earthquake Resistance of Existing Buildings in New York City," by P. Weidlinger and M. Ettouney, 10/15/88, to be published.

NCEER-88-0041 "Small-Scale Modeling Techniques for Reinforced Concrete Structures Subjected to Seismic Loads," by W. Kim, A. El-Attar and R.N. White, 11/22/88, (PB89-189625/AS).

NCEER-88-0042 "Modeling Strong Ground Motion from Multiple Event Earthquakes," by G.W. Ellis and A.S. Cakmak, 10/15/88, (PB89-174445/AS).

NCEER-88-0043 "Nonstationary Models of Seismic Ground Acceleration," by M. Grigoriu, S.E. Ruiz and E. Rosenblueth, 7/15/88, (PB89-189617/AS).

NCEER-88-0044 "SARCF User's Guide: Seismic Analysis of Reinforced Concrete Frames," by Y.S. Chung, C. Meyer and M. Shinozuka, 11/9/88, (PB89-174452/AS).

NCEER-88-0045 "First Expert Panel Meeting on Disaster Research and Planning," edited by J. Pantelic and J. Stoyle, 9/15/88, (PB89-174460/AS).

NCEER-88-0046 "Preliminary Studies of the Effect of Degrading Infill Walls on the Nonlinear Seismic Response of Steel Frames," by C.Z. Chrysostomou, P. Gergely and J.F. Abel, 12/19/88, (PB89-208383/AS).

NCEER-88-0047 "Reinforced Concrete Frame Component Testing Facility - Design, Construction, Instrumentation and Operation," by S.P. Pessiki, C. Conley, T. Bond, P. Gergely and R.N. White, 12/16/88, (PB89-174478/AS).

NCEER-89-0001 "Effects of Protective Cushion and Soil Compliancy on the Response of Equipment Within a Seismically Excited Building," by J.A. HoLung, 2/16/89, (PB89-207179/AS).

NCEER-89-0002 "Statistical Evaluation of Response Modification Factors for Reinforced Concrete Structures," by H.H-M. Hwang and J-W. Jaw, 2/17/89, (PB89-207187/AS).

NCEER-89-0003 "Hysteretic Columns Under Random Excitation," by G-Q. Cai and Y.K. Lin, 1/9/89, (PB89-196513/AS).

NCEER-89-0004 "Experimental Study of 'Elephant Foot Bulge' Instability of Thin-Walled Metal Tanks," by Z-H. Jia and R.L. Ketter, 2/22/89, (PB89-207195/AS).

NCEER-89-0005 "Experiment on Performance of Buried Pipelines Across San Andreas Fault," by J. Isenberg, E. Richardson and T.D. O'Rourke, 3/10/89, (PB89-218440/AS).

NCEER-89-0006 "A Knowledge-Based Approach to Structural Design of Earthquake-Resistant Buildings," by M. Subramani, P. Gergely, C.H. Conley, J.F. Abel and A.H. Zaghw, 1/15/89, (PB89-218465/AS).

NCEER-89-0007 "Liquefaction Hazards and Their Effects on Buried Pipelines," by T.D. O'Rourke and P.A. Lane, 2/1/89, (PB89-218481).

NCEER-89-0008 "Fundamentals of System Identification in Structural Dynamics," by H. Imai, C-B. Yun, O. Maruyama and M. Shinozuka, 1/26/89, (PB89-207211/AS).

NCEER-89-0009 "Effects of the 1985 Michoacan Earthquake on Water Systems and Other Buried Lifelines in Mexico," by A.G. Ayala and M.J. O'Rourke, 3/8/89, (PB89-207229/AS).

NCEER-89-R010 "NCEER Bibliography of Earthquake Education Materials," by K.E.K. Ross, Second Revision, 9/1/89, (PB90-125352/AS).

NCEER-89-0011 "Inelastic Three-Dimensional Response Analysis of Reinforced Concrete Building Structures (IDARC-3D), Part I - Modeling," by S.K. Kunnath and A.M. Reinhorn, 4/17/89, (PB90-114612/AS).

NCEER-89-0012 "Recommended Modifications to ATC-14," by C.D. Poland and J.O. Malley, 4/12/89, (PB90-108648/AS).

NCEER-89-0013 "Repair and Strengthening of Beam-to-Column Connections Subjected to Earthquake Loading," by M. Corazao and A.J. Durrani, 2/28/89, (PB90-109885/AS).

NCEER-89-0014 "Program EXKAL2 for Identification of Structural Dynamic Systems," by O. Maruyama, C-B. Yun, M. Hoshiya and M. Shinozuka, 5/19/89, (PB90-109877/AS).

NCEER-89-0015 "Response of Frames With Bolted Semi-Rigid Connections, Part I - Experimental Study and Analytical Predictions," by P.J. DiCorso, A.M. Reinhorn, J.R. Dickerson, J.B. Radziminski and W.L. Harper, 6/1/89, to be published.

NCEER-89-0016 "ARMA Monte Carlo Simulation in Probabilistic Structural Analysis," by P.D. Spanos and M.P. Mignolet, 7/10/89, (PB90-109893/AS).

NCEER-89-P017 "Preliminary Proceedings from the Conference on Disaster Preparedness - The Place of Earthquake Education in Our Schools," Edited by K.E.K. Ross, 6/23/89.

NCEER-89-0017 "Proceedings from the Conference on Disaster Preparedness - The Place of Earthquake Education in Our Schools," Edited by K.E.K. Ross, 12/31/89, (PB90-207895). This report is available only through NTIS (see address given above).

NCEER-89-0018 "Multidimensional Models of Hysteretic Material Behavior for Vibration Analysis of Shape Memory Energy Absorbing Devices, by E.J. Graesser and F.A. Cozzarelli, 6/7/89, (PB90-164146/AS).

NCEER-89-0019 "Nonlinear Dynamic Analysis of Three-Dimensional Base Isolated Structures (3D-BASIS)," by S. Nagarajaiah, A.M. Reinhorn and M.C. Constantinou, 8/3/89, (PB90-161936/AS). This report is available only through NTIS (see address given above).

NCEER-89-0020 "Structural Control Considering Time-Rate of Control Forces and Control Rate Constraints," by F.Y. Cheng and C.P. Pantelides, 8/3/89, (PB90-120445/AS).

NCEER-89-0021 "Subsurface Conditions of Memphis and Shelby County," by K.W. Ng, T-S. Chang and H-H.M. Hwang, 7/26/89, (PB90-120437/AS).

NCEER-89-0022 "Seismic Wave Propagation Effects on Straight Jointed Buried Pipelines," by K. Elhmadi and M.J. O'Rourke, 8/24/89, (PB90-162322/AS).

NCEER-89-0023 "Workshop on Serviceability Analysis of Water Delivery Systems," edited by M. Grigoriu, 3/6/89, (PB90-127424/AS).

NCEER-89-0024 "Shaking Table Study of a 1/5 Scale Steel Frame Composed of Tapered Members," by K.C. Chang, J.S. Hwang and G.C. Lee, 9/18/89, (PB90-160169/AS).

NCEER-89-0025 "DYNA1D: A Computer Program for Nonlinear Seismic Site Response Analysis - Technical Documentation," by Jean H. Prevost, 9/14/89, (PB90-161944/AS). This report is available only through NTIS (see address given above).

NCEER-89-0026 "1:4 Scale Model Studies of Active Tendon Systems and Active Mass Dampers for Aseismic Protection," by A.M. Reinhorn, T.T. Soong, R.C. Lin, Y.P. Yang, Y. Fukao, H. Abe and M. Nakai, 9/15/89, (PB90-173246/AS).

NCEER-89-0027 "Scattering of Waves by Inclusions in a Nonhomogeneous Elastic Half Space Solved by Boundary Element Methods," by P.K. Hadley, A. Askar and A.S. Cakmak, 6/15/89, (PB90-145699/AS).

NCEER-89-0028 "Statistical Evaluation of Deflection Amplification Factors for Reinforced Concrete Structures," by H.H.M. Hwang, J-W. Jaw and A.L. Ch'ng, 8/31/89, (PB90-164633/AS).

NCEER-89-0029 "Bedrock Accelerations in Memphis Area Due to Large New Madrid Earthquakes," by H.H.M. Hwang, C.H.S. Chen and G. Yu, 11/7/89, (PB90-162330/AS).

NCEER-89-0030 "Seismic Behavior and Response Sensitivity of Secondary Structural Systems," by Y.Q. Chen and T.T. Soong, 10/23/89, (PB90-164658/AS).

NCEER-89-0031 "Random Vibration and Reliability Analysis of Primary-Secondary Structural Systems," by Y. Ibrahim, M. Grigoriu and T.T. Soong, 11/10/89, (PB90-161951/AS).

NCEER-89-0032 "Proceedings from the Second U.S. - Japan Workshop on Liquefaction, Large Ground Deformation and Their Effects on Lifelines, September 26-29, 1989," Edited by T.D. O'Rourke and M. Hamada, 12/1/89, (PB90-209388/AS).

NCEER-89-0033 "Deterministic Model for Seismic Damage Evaluation of Reinforced Concrete Structures," by J.M. Bracci, A.M. Reinhorn, J.B. Mander and S.K. Kunnath, 9/27/89.

NCEER-89-0034 "On the Relation Between Local and Global Damage Indices," by E. DiPasquale and A.S. Cakmak, 8/15/89, (PB90-173865).

NCEER-89-0035 "Cyclic Undrained Behavior of Nonplastic and Low Plasticity Silts," by A.J. Walker and H.E. Stewart, 7/26/89, (PB90-183518/AS).

NCEER-89-0036 "Liquefaction Potential of Surficial Deposits in the City of Buffalo, New York," by M. Budhu, R. Giese and L. Baumgrass, 1/17/89, (PB90-208455/AS).

NCEER-89-0037 "A Deterministic Assessment of Effects of Ground Motion Incoherence," by A.S. Veletsos and Y. Tang, 7/15/89, (PB90-164294/AS).

NCEER-89-0038 "Workshop on Ground Motion Parameters for Seismic Hazard Mapping," July 17-18, 1989, edited by R.V. Whitman, 12/1/89, (PB90-173923/AS).

NCEER-89-0039 "Seismic Effects on Elevated Transit Lines of the New York City Transit Authority," by C.J. Costantino, C.A. Miller and E. Heymsfield, 12/26/89, (PB90-207887/AS).

NCEER-89-0040 "Centrifugal Modeling of Dynamic Soil-Structure Interaction," by K. Weissman, Supervised by J.H. Prevost, 5/10/89, (PB90-207879/AS).

NCEER-89-0041 "Linearized Identification of Buildings With Cores for Seismic Vulnerability Assessment," by I-K. Ho and A.E. Aktan, 11/1/89, (PB90-251943/AS).

NCEER-90-0001 "Geotechnical and Lifeline Aspects of the October 17, 1989 Loma Prieta Earthquake in San Francisco," by T.D. O'Rourke, H.E. Stewart, F.T. Blackburn and T.S. Dickerman, 1/90, (PB90-208596/AS).

NCEER-90-0002 "Nonnormal Secondary Response Due to Yielding in a Primary Structure," by D.C.K. Chen and L.D. Lutes, 2/28/90, (PB90-251976/AS).

NCEER-90-0003 "Earthquake Education Materials for Grades K-12," by K.E.K. Ross, 4/16/90, (PB91-113415/AS).

NCEER-90-0004 "Catalog of Strong Motion Stations in Eastern North America," by R.W. Busby, 4/3/90, (PB90-251984)/AS.

NCEER-90-0005 "NCEER Strong-Motion Data Base: A User Manuel for the GeoBase Release (Version 1.0 for the Sun3)," by P. Friberg and K. Jacob, 3/31/90 (PB90-258062/AS).

NCEER-90-0006 "Seismic Hazard Along a Crude Oil Pipeline in the Event of an 1811-1812 Type New Madrid Earthquake," by H.H.M. Hwang and C-H.S. Chen, 4/16/90(PB90-258054).

NCEER-90-0007 "Site-Specific Response Spectra for Memphis Sheahan Pumping Station," by H.H.M. Hwang and C.S. Lee, 5/15/90, (PB91-108811/AS).

NCEER-90-0008 "Pilot Study on Seismic Vulnerability of Crude Oil Transmission Systems," by T. Ariman, R. Dobry, M. Grigoriu, F. Kozin, M. O'Rourke, T. O'Rourke and M. Shinozuka, 5/25/90, (PB91-108837/AS).

NCEER-90-0009 "A Program to Generate Site Dependent Time Histories: EQGEN," by G.W. Ellis, M. Srinivasan and A.S. Cakmak, 1/30/90, (PB91-108829/AS).

NCEER-90-0010 "Active Isolation for Seismic Protection of Operating Rooms," by M.E. Talbott, Supervised by M. Shinozuka, 6/8/9, (PB91-110205/AS).

NCEER-90-0011 "Program LINEARID for Identification of Linear Structural Dynamic Systems," by C-B. Yun and M. Shinozuka, 6/25/90, (PB91-110312/AS).

NCEER-90-0012 "Two-Dimensional Two-Phase Elasto-Plastic Seismic Response of Earth Dams," by A.N. Yiagos, Supervised by J.H. Prevost, 6/20/90, (PB91-110197/AS).

NCEER-90-0013 "Secondary Systems in Base-Isolated Structures: Experimental Investigation, Stochastic Response and Stochastic Sensitivity," by G.D. Manolis, G. Juhn, M.C. Constantinou and A.M. Reinhorn, 7/1/90, (PB91-110320/AS).

NCEER-90-0014 "Seismic Behavior of Lightly-Reinforced Concrete Column and Beam-Column Joint Details," by S.P. Pessiki, C.H. Conley, P. Gergely and R.N. White, 8/22/90, (PB91-108795/AS).

NCEER-90-0015 "Two Hybrid Control Systems for Building Structures Under Strong Earthquakes," by J.N. Yang and A. Danielians, 6/29/90, (PB91-125393/AS).

NCEER-90-0016 "Instantaneous Optimal Control with Acceleration and Velocity Feedback," by J.N. Yang and Z. Li, 6/29/90, (PB91-125401/AS).

NCEER-90-0017 "Reconnaissance Report on the Northern Iran Earthquake of June 21, 1990," by M. Mehrain, 10/4/90, (PB91-125377/AS).

NCEER-90-0018 "Evaluation of Liquefaction Potential in Memphis and Shelby County," by T.S. Chang, P.S. Tang, C.S. Lee and H. Hwang, 8/10/90, (PB91-125427/AS).

NCEER-90-0019 "Experimental and Analytical Study of a Combined Sliding Disc Bearing and Helical Steel Spring Isolation System," by M.C. Constantinou, A.S. Mokha and A.M. Reinhorn, 10/4/90, (PB91-125385/AS).

NCEER-90-0020 "Experimental Study and Analytical Prediction of Earthquake Response of a Sliding Isolation System with a Spherical Surface," by A.S. Mokha, M.C. Constantinou and A.M. Reinhorn, 10/11/90, (PB91-125419/AS).

NCEER-90-0021 "Dynamic Interaction Factors for Floating Pile Groups," by G. Gazetas, K. Fan, A. Kaynia and E. Kausel, 9/10/90, (PB91-170381/AS).

NCEER-90-0022 "Evaluation of Seismic Damage Indices for Reinforced Concrete Structures," by S. Rodriguez-Gomez and A.S. Cakmak, 9/30/90, PB91-171322/AS).

NCEER-90-0023 "Study of Site Response at a Selected Memphis Site," by H. Desai, S. Ahmad, E.S. Gazetas and M.R. Oh, 10/11/90, (PB91-196857/AS).

NCEER-90-0024 "A User's Guide to Strongmo: Version 1.0 of NCEER's Strong-Motion Data Access Tool for PCs and Terminals," by P.A. Friberg and C.A.T. Susch, 11/15/90, (PB91-171272/AS).

NCEER-90-0025 "A Three-Dimensional Analytical Study of Spatial Variability of Seismic Ground Motions," by L-L. Hong and A.H.-S. Ang, 10/30/90, (PB91-170399/AS).

NCEER-90-0026 "MUMOID User's Guide - A Program for the Identification of Modal Parameters," by S. Rodriguez-Gomez and E. DiPasquale, 9/30/90, (PB91-171298/AS).

NCEER-90-0027 "SARCF-II User's Guide - Seismic Analysis of Reinforced Concrete Frames," by S. Rodriguez-Gomez, Y.S. Chung and C. Meyer, 9/30/90, (PB91-171280/AS).

NCEER-90-0028 "Viscous Dampers: Testing, Modeling and Application in Vibration and Seismic Isolation," by N. Makris and M.C. Constantinou, 12/20/90 (PB91-190561/AS).

NCEER-90-0029 "Soil Effects on Earthquake Ground Motions in the Memphis Area," by H. Hwang, C.S. Lee, K.W. Ng and T.S. Chang, 8/2/90, (PB91-190751/AS).

NCEER-91-0001 "Proceedings from the Third Japan-U.S. Workshop on Earthquake Resistant Design of Lifeline Facilities and Countermeasures for Soil Liquefaction, December 17-19, 1990," edited by T.D. O'Rourke and M. Hamada, 2/1/91, (PB91-179259/AS).

NCEER-91-0002 "Physical Space Solutions of Non-Proportionally Damped Systems," by M. Tong, Z. Liang and G.C. Lee, 1/15/91, (PB91-179242/AS).

NCEER-91-0003 "Seismic Response of Single Piles and Pile Groups," by K. Fan and G. Gazetas, 1/10/91, (PB92-174994/AS).

NCEER-91-0004 "Damping of Structures: Part 1 - Theory of Complex Damping," by Z. Liang and G. Lee, 10/10/91.

NCEER-91-0005 "3D-BASIS - Nonlinear Dynamic Analysis of Three Dimensional Base Isolated Structures: Part II," by S. Nagarajaiah, A.M. Reinhorn and M.C. Constantinou, 2/28/91, (PB91-190553/AS).

NCEER-91-0006 "A Multidimensional Hysteretic Model for Plasticity Deforming Metals in Energy Absorbing Devices," by E.J. Graesser and F.A. Cozzarelli, 4/9/91.

NCEER-91-0007 "A Framework for Customizable Knowledge-Based Expert Systems with an Application to a KBES for Evaluating the Seismic Resistance of Existing Buildings," by E.G. Ibarra-Anaya and S.J. Fenves, 4/9/91, (PB91-210930/AS).

NCEER-91-0008 "Nonlinear Analysis of Steel Frames with Semi-Rigid Connections Using the Capacity Spectrum Method," by G.G. Deierlein, S-H. Hsieh, Y-J. Shen and J.F. Abel, 7/2/91, (PB92-113828/AS).

NCEER-91-0009 "Earthquake Education Materials for Grades K-12," by K.E.K. Ross, 4/30/91, (PB91-212142/AS).

NCEER-91-0010 "Phase Wave Velocities and Displacement Phase Differences in a Harmonically Oscillating Pile," by N. Makris and G. Gazetas, 7/8/91, (PB92-108356/AS).

NCEER-91-0011 "Dynamic Characteristics of a Full-Sized Five-Story Steel Structure and a 2/5 Model," by K.C. Chang, G.C. Yao, G.C. Lee, D.S. Hao and Y.C. Yeh," to be published.

NCEER-91-0012 "Seismic Response of a 2/5 Scale Steel Structure with Added Viscoelastic Dampers," by K.C. Chang, T.T. Soong, S-T. Oh and M.L. Lai, 5/17/91 (PB92-110816/AS).

NCEER-91-0013 "Earthquake Response of Retaining Walls; Full-Scale Testing and Computational Modeling," by S. Alampalli and A-W.M. Elgamal, 6/20/91, to be published.

NCEER-91-0014 "3D-BASIS-M: Nonlinear Dynamic Analysis of Multiple Building Base Isolated Structures," by P.C. Tsopelas, S. Nagarajaiah, M.C. Constantinou and A.M. Reinhorn, 5/28/91, (PB92-113885/AS).

NCEER-91-0015 "Evaluation of SEAOC Design Requirements for Sliding Isolated Structures," by D. Theodossiou and M.C. Constantinou, 6/10/91, (PB92-114602/AS).

NCEER-91-0016 "Closed-Loop Modal Testing of a 27-Story Reinforced Concrete Flat Plate-Core Building," by H.R. Somaprasad, T. Toksoy, H. Yoshiyuki and A.E. Aktan, 7/15/91, (PB92-129980/AS).

NCEER-91-0017 "Shake Table Test of a 1/6 Scale Two-Story Lightly Reinforced Concrete Building," by A.G. El-Attar, R.N. White and P. Gergely, 2/28/91.

NCEER-91-0018 "Shake Table Test of a 1/8 Scale Three-Story Lightly Reinforced Concrete Building," by A.G. El-Attar, R.N. White and P. Gergely, 2/28/91.

NCEER-91-0019 "Transfer Functions for Rigid Rectangular Foundations," by A.S. Veletsos, A.M. Prasad and W.H. Wu, 7/31/91, to be published.

NCEER-91-0020 "Hybrid Control of Seismic-Excited Nonlinear and Inelastic Structural Systems," by J.N. Yang, Z. Li and A. Danielians, 8/1/91.

NCEER-91-0021 "The NCEER-91 Earthquake Catalog: Improved Intensity-Based Magnitudes and Recurrence Relations for U.S. Earthquakes East of New Madrid," by L. Seeber and J.G. Armbruster, 8/28/91, (PB92-176742/AS).

NCEER-91-0022 "Proceedings from the Implementation of Earthquake Planning and Education in Schools: The Need for Change - The Roles of the Changemakers," by K.E.K. Ross and F. Winslow, 7/23/91, (PB92-129998/AS).

NCEER-91-0023 "A Study of Reliability-Based Criteria for Seismic Design of Reinforced Concrete Frame Buildings," by H.H.M. Hwang and H-M. Hsu, 8/10/91.

NCEER-91-0024 "Experimental Verification of a Number of Structural System Identification Algorithms," by R.G. Ghanem, H. Gavin and M. Shinozuka, 9/18/91, (PB92-176577/AS).

NCEER-91-0025 "Probabilistic Evaluation of Liquefaction Potential," by H.H.M. Hwang and C.S. Lee," 11/25/91.

NCEER-91-0026 "Instantaneous Optimal Control for Linear, Nonlinear and Hysteretic Structures - Stable Controllers," by J.N. Yang and Z. Li, 11/15/91, (PB92-163807/AS).

NCEER-91-0027 "Experimental and Theoretical Study of a Sliding Isolation System for Bridges," by M.C. Constantinou, A. Kartoum, A.M. Reinhorn and P. Bradford, 11/15/91, (PB92-176973/AS).

NCEER-92-0001 "Case Studies of Liquefaction and Lifeline Performance During Past Earthquakes, Volume 1: Japanese Case Studies," Edited by M. Hamada and T. O'Rourke, 2/17/92.

NCEER-92-0002 "Case Studies of Liquefaction and Lifeline Performance During Past Earthquakes, Volume 2: United States Case Studies," Edited by T. O'Rourke and M. Hamada, 2/17/92.

NCEER-92-0003 "Issues in Earthquake Education," Edited by K. Ross, 2/3/92.

NCEER-92-0004 "Proceedings from the First U.S. - Japan Workshop on Earthquake Protective Systems for Bridges," 2/4/92, to be published.

NCEER-92-0005 "Seismic Ground Motion from a Haskell-Type Source in a Multiple-Layered Half-Space," A.P. Theoharis, G. Deodatis and M. Shinozuka, 1/2/92, to be published.

NCEER-92-0006 "Proceedings from the Site Effects Workshop," Edited by R. Whitman, 2/29/92.

NCEER-92-0007 "Engineering Evaluation of Permanent Ground Deformations Due to Seismically-Induced Liquefaction," by M.H. Baziar, R. Dobry and A-W.M. Elgamal, 3/24/92.

NCEER-92-0008 "A Procedure for the Seismic Evaluation of Buildings in the Central and Eastern United States," by C.D. Poland and J.O. Malley, 4/2/92.

NCEER-92-0009 "Experimental and Analytical Study of a Hybrid Isolation System Using Friction Controllable Sliding Bearings," by Q. Feng, S. Fujii and M. Shinozuka, 2/15/92, to be published.

NCEER-92-0010 "Seismic Resistance of Slab-Column Connections in Existing Non-Ductile Flat-Plate Buildings," by A.J. Durrani and Y. Du, 5/18/92.

NCEER-92-0011 "The Hysteretic and Dynamic Behavior of Brick Masonry Walls Upgraded by Ferrocement Coatings Under Cyclic Loading and Strong Simulated Ground Motion," by H. Lee and S.P. Prawel, 5/11/92, to be published.

NCEER-92-0012 "Study of Wire Rope Systems for Seismic Protection of Equipment in Buildings," by G.F. Demetriades, M.C. Constantinou and A.M. Reinhorn, 5/20/92.

NCEER-92-0013 "Shape Memory Structural Dampers: Material Properties, Design and Seismic Testing," by P.R. Witting and F.A. Cozzarelli, 5/26/92.

NCEER-92-0014 "Longitudinal Permanent Ground Deforformation Effects on Buried Continuous Pipelines," by M.J. O'Rourke, and C. Nordberg, 6/15/92.